UNIVERSITY OF DELAWARE

Numerical studies of turbulent collision of cloud particles

Lian-Ping Wang

Department of Mechanical Engineering
University of Delaware
lwang@udel.edu

International School on
Fluctuations and turbulence in the microphysics and dynamics of clouds
Porquerolles, France, September 2-10, 2010

Acknowledgments:
Dr. Wojtek Grabowski (NCAR)
Dr. Y. Zhou, Dr. O. Ayala, Dr. Y. Xue, Dr. B. Rosa, Mr. H. Gao, Mr. H. Parashani, ……
U.S. National Science Foundation**,** U.S. National Center for Atmospheric Research

Outline

- The application: collision-coalescence of cloud droplets
- Simulation of small-scale air turbulence
- Point-particle based simulation
    - Geometric collision
    - Parameterization of turbulent collision kernel
- Hybrid direct numerical simulation
    - Collision efficiency
- Impact on warm rain initiation
- High-resolution simulation and effect of R_λ
- Particle-resolved simulation
- Summary

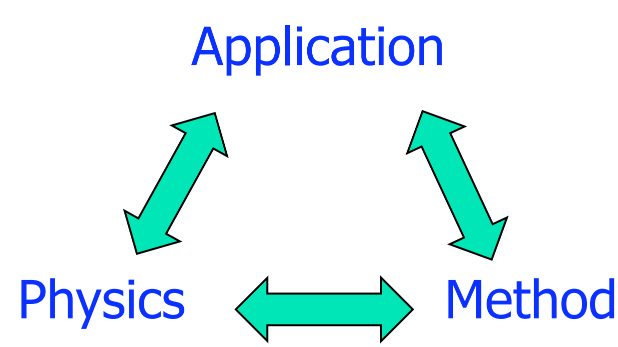

Motivations and applications

Turbulent dispersed two-phase flows are important to a wide variety of natural processes and engineering applications

- dust storm and pollutant transport
- cloud microphysics
- coastal sediment transport
- coal / spray combustion
- plankton dynamics
- combustion
- particle production
- microbubble drag reduction

Key issues

Turbulent particle dispersion
Turbulence modulation
Particle growth by coalescence
Particle sedimentation
Particle-particle collision / agglomeration





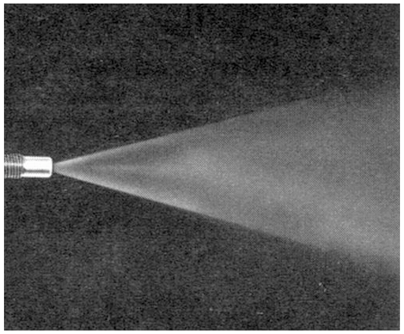


Aerosol-cloud-precipitation-climate interactions

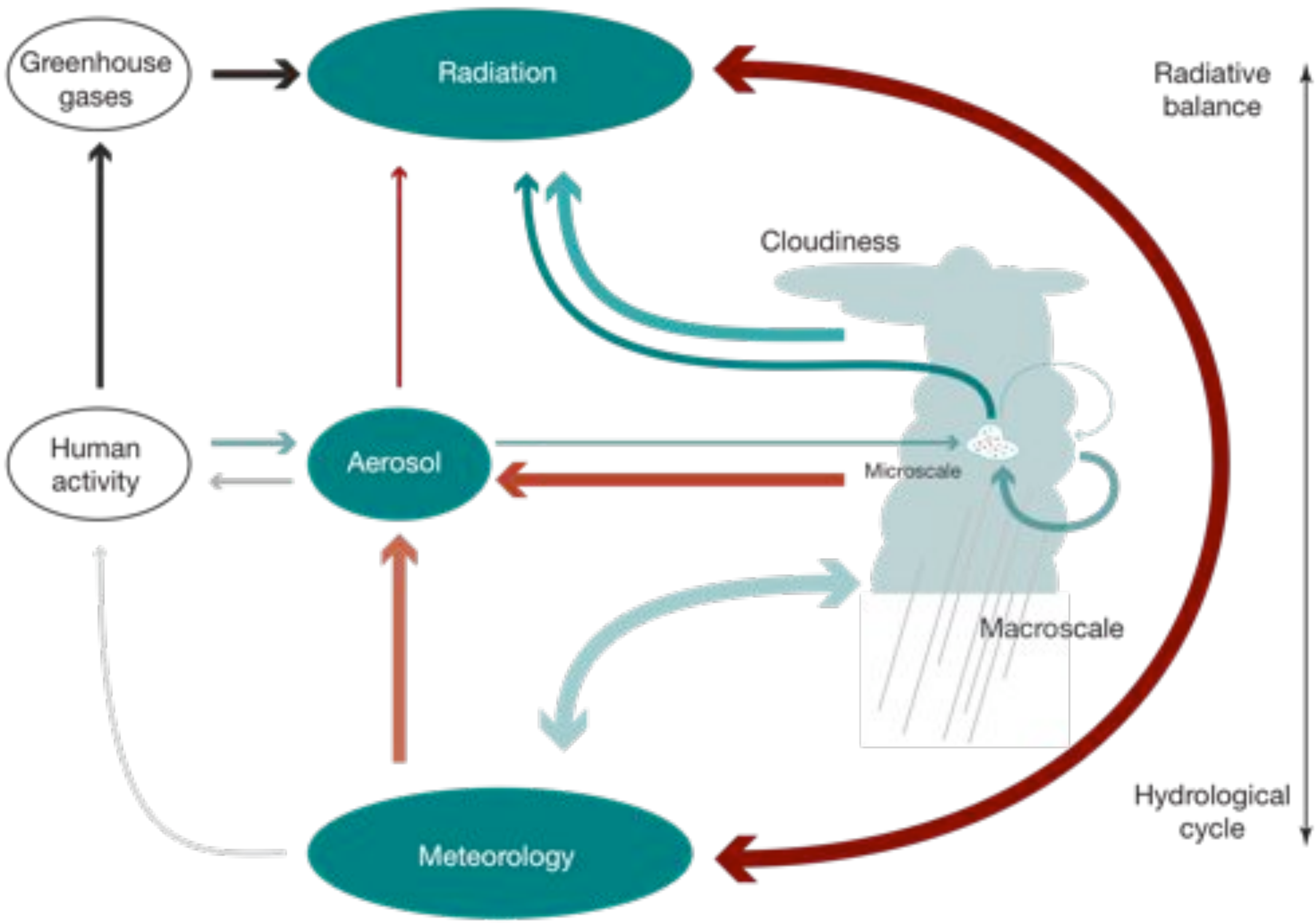

Stevens and Feingold, 2009, Nature, 461, doi:10.1038.

Droplet activation and condensational growth – 1st and 2nd microphysical steps

❖ Aerosols (before activation, interstitial aerosols): 10 nm to 1 μm

sea salt particles [NaCl] over ocean

ammonium sulfate [$(NH_4)_2SO_4$] over continental

❖ Activated aerosols (CCN): ~ 100 nm to 10 μm

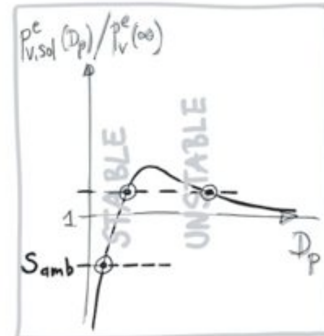

The Köhler theory: kinetic theory, thermodynamics & chemistry

$$p^e_{v,solution} = p^e_v(\infty)\exp\left[\frac{4\sigma \mathrm{v}_l}{kTD_p} - \frac{6\nu n_s \mathrm{v}_l}{\pi D_p^3} - \text{effects due to pollutants}\right]$$

Kelvin effect or curvature effect

Raoult or solute effect

Pollutants reduce the effective interface area, alter intermolecular force & introduce surfactants.

❖ Condensational growth (diffusion theory):

$$\frac{dr}{dt} = \frac{f_{vent} A S}{r}$$

large-scale turbulent fluctuations or stochastic condensation

$$S = \frac{P^e_v(\infty)}{P^e_{v,solution}} - 1, \quad f_{vent} = \text{ventilation coefficient}, \quad A \approx 10^{-10}\ m^2 s^{-1}$$

Kenneth V. Beard & Harry T. Ochs III, An overview …., *J. Applied Meteor.* 32: 608-624 (1993).
F. Raes, Take a glass of water …., *J. Phys. IV France* 139: 63-80 (2006).

Collision-coalescence: effects of small-scale turbulence
The 3rd microphysical step (after CCN activation & condensational growth)

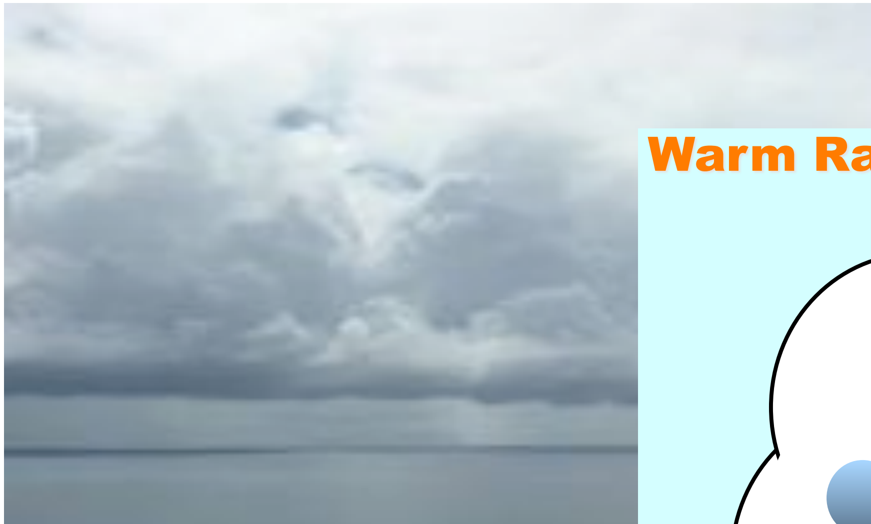

Growth of cloud droplets

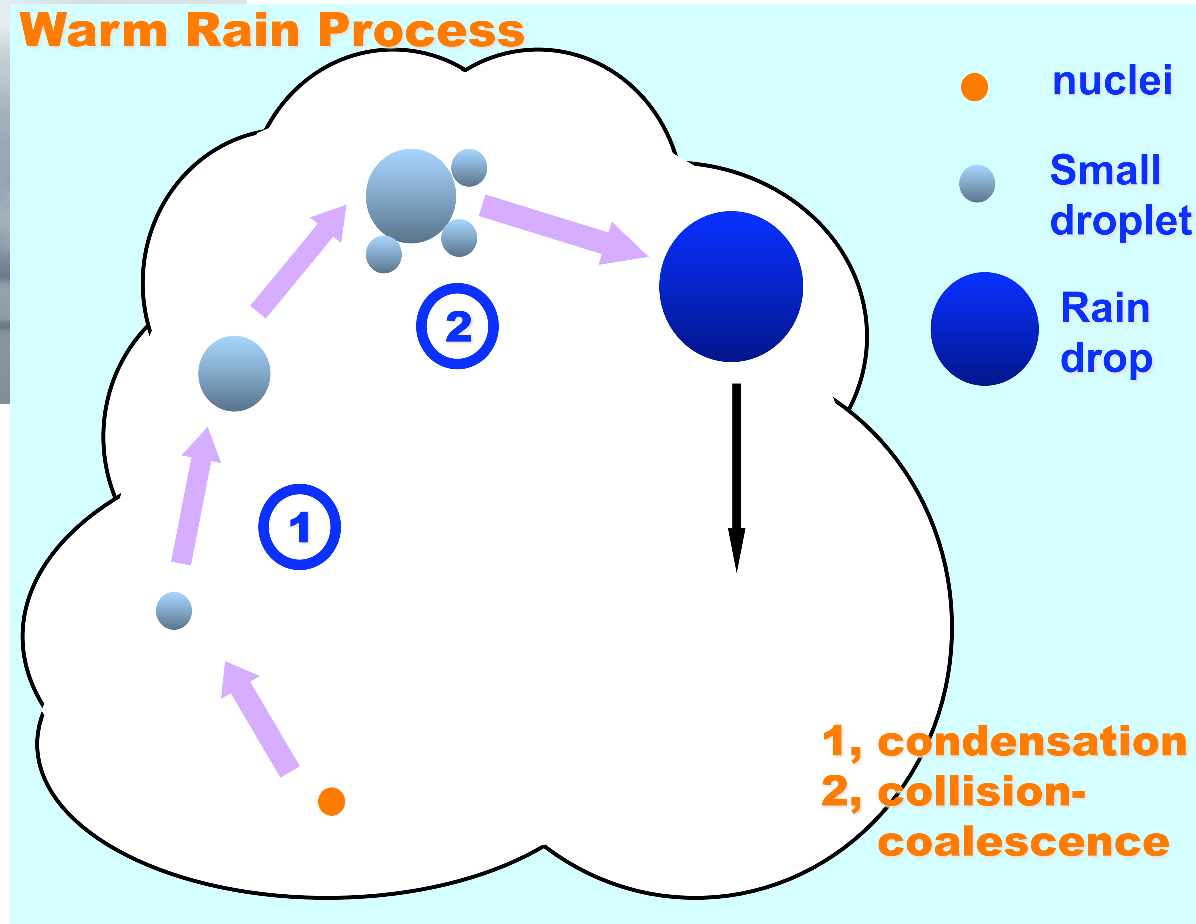

How does air turbulence affect the collision rates and collision efficiency of cloud droplets?

What is the impact on warm rain initiation?

The base case:
Gravitational collision-coalescence

(still the basis of many weather and climate models)

The base kernel: gravitational collision-coalescence

The base case studied by many:

$$K_{12}^{g} = \pi R^2 \left| W_1 - W_2 \right| E_{12}^{g} \quad \text{with } R = a_1 + a_2$$

Swept volume

Collision efficiency

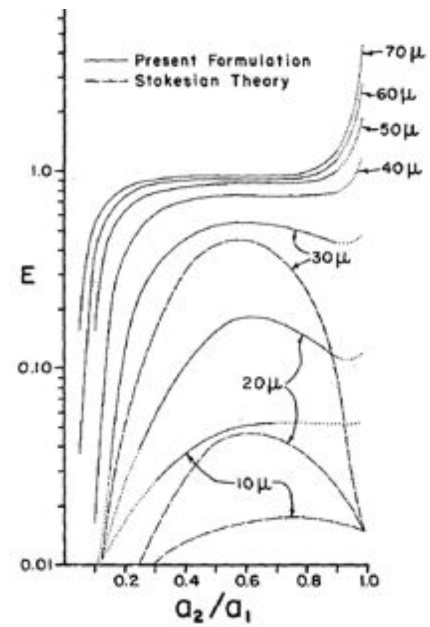

Klett and Davis (1973)

Model for terminal velocity: Beard (1976)

Empirical formula for E_{12}: Long (1974)
Tabulated data of E_{12}: Hall (1980)

How to formulate collision kernel in a turbulent flow?
How to quantify / parameterize the turbulent collision kernel?

Growth of cloud droplets by gravitational collision-coalescence

Linear-Log

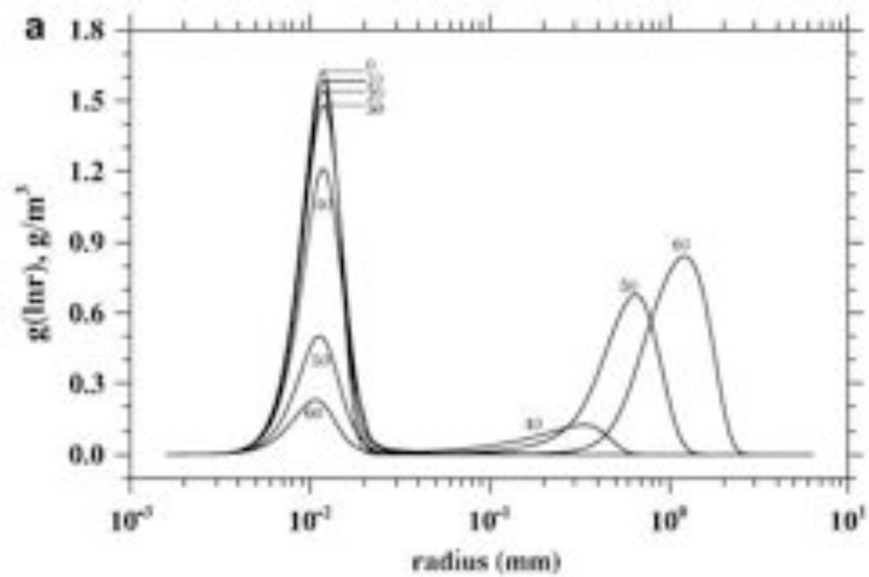

Log-Log

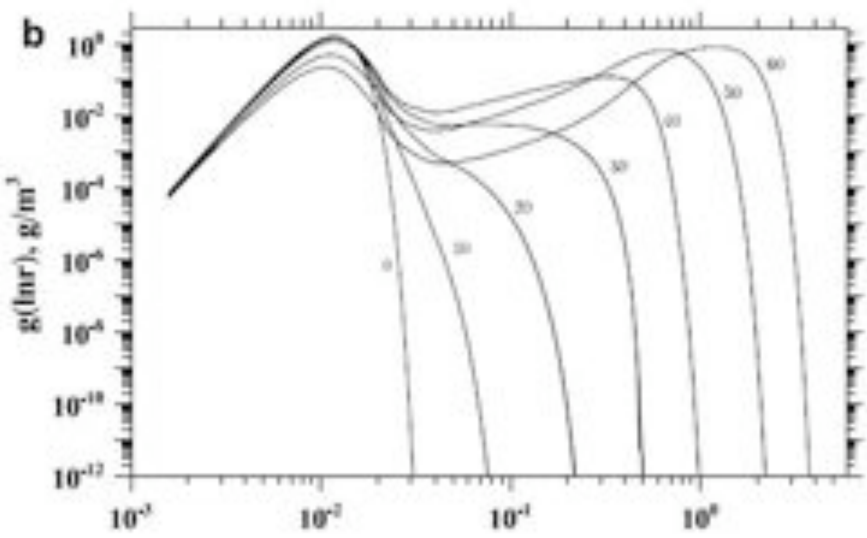

Rapid onset of precipitation in shallow cumulus clouds

?
→

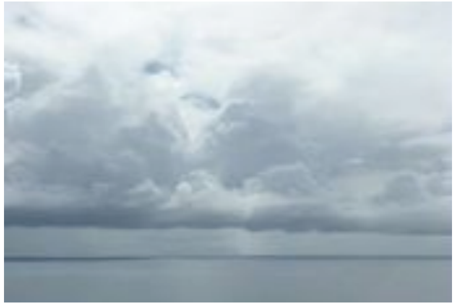

- ❖ Formation of drizzles (>100 μm) from cloud droplets: 15 ~ 30 minutes.

  Hawaiian rainband clouds: Szumowski *et al.* (1997)
  Florida cumulus (SCMS): Knight *et al.* (2002), Blyth *et al.* (2003)

- ❖ Different widths between predicted and measured size distributions

The size gap or bottleneck problem: 10 to 50 μm

Possible explanations

- ❖ Growth by giant and ultragiant particles
- ❖ Effects of air turbulence (on condensations and collision-coalescence)
- ❖ Entrainment-induced spectral broadening
- ❖ Effects of preexisting clouds

Arenberg 1939: Turbulence as a major factor in the growth of cloud droplets. Bull. Amer. Met. Soc. 20, 444-445.

Cloud physics: The multiscale problem down to droplet size!

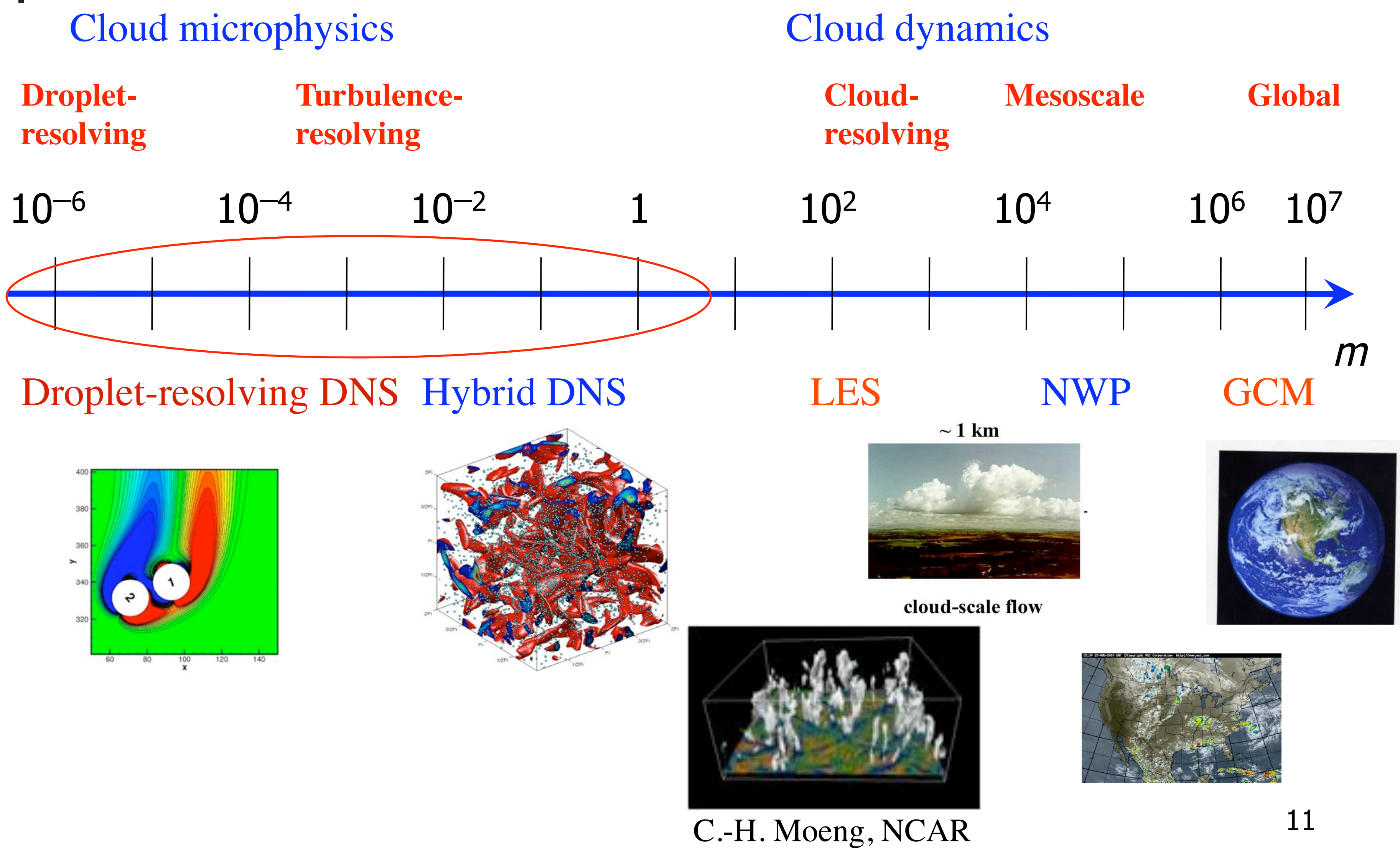

Typical turbulent flow parameters in clouds

	ε (cm^2/s^3)	R_λ	u' (cm/s)
Stratiform clouds	< 100	~5 ,000	~100
Cumulus clouds	100 to 600	~10,000	100 to 200
Cumulonimbus clouds	600 to 2000	~20,000	~ 200

DNS ~ 500

Laboratory experiments ~ 1000

Shaw, Annu. Rev. Fluid Mech. 35 (2003) 183–227.

Khain et al., Atmospheric Research 86 (2007) 1–20.

Turbulence physics: cloud turbulence, scales, scale separations

Large scales

Large eddy size (integral length scale) $l \sim 100\ m$

rms fluctuation velocity $u' \sim 1\ \ m/s$

Large eddy time scale $T \sim \dfrac{l}{u'} \sim 100\ s$

Rate of volumetric energy input

$$\rho\varepsilon \sim \rho\frac{(u')^3}{l} \sim 0.01\ \ \frac{\mathrm{J}}{\mathrm{s \cdot m^3}}$$

$$\frac{l}{\eta} \sim 120{,}000, \quad \frac{T}{\tau_K} \sim 2{,}400, \quad \frac{u'}{v_K} \sim 50$$

Small scales

ϵ ($\mathrm{cm^2\,s^{-3}}$)	τ_k (s)	η (cm)	υ_k ($\mathrm{cm\,s^{-1}}$)
10	0.1304	0.1488	1.142
100	0.0412	0.0837	2.031
400	0.0206	0.0592	2.872

Time evolution of real clouds

2 hours played in 47 seconds
1 s is 2.5 minutes in real time

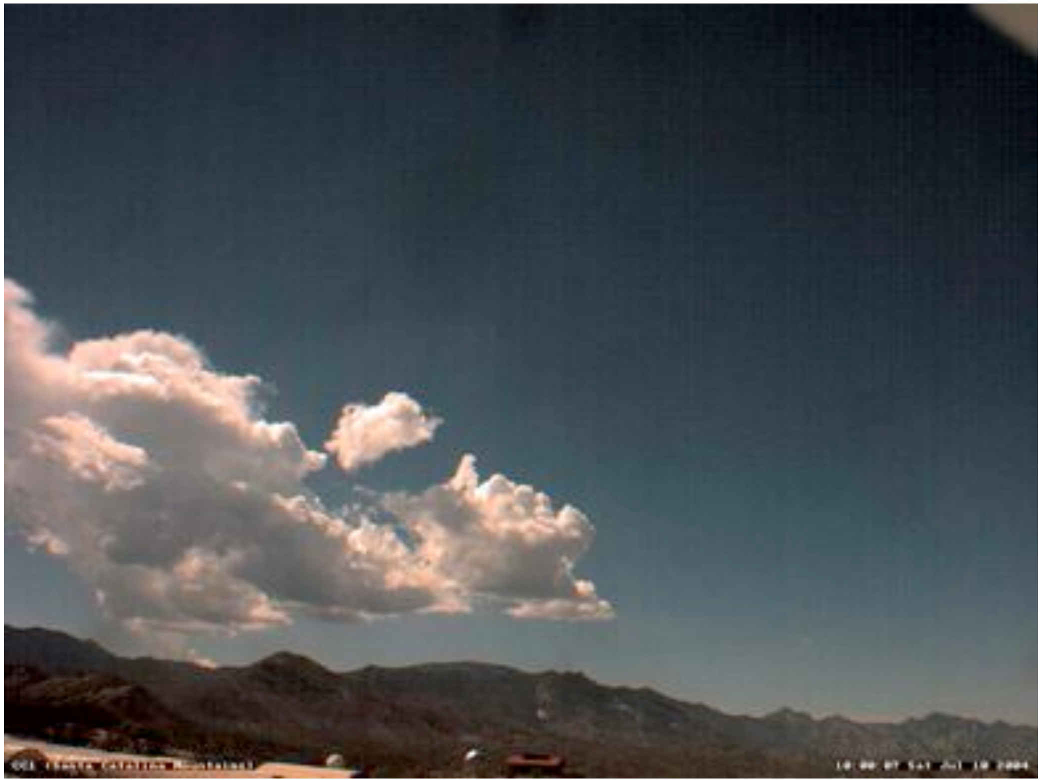

Prof. Joe Zehnder
Department of Atmospheric Sciences
Creighton University

Sketch the problem: cloud droplet as inertial particle

dynamics $$m_p \frac{d\vec{V}(t)}{dt} = -6\pi\, a\, \mu \left[\vec{V}(t) - \vec{U}\left(\vec{Y}(t),t\right)\right] + m_p \vec{g}$$

inertial term Stokes viscous drag gravitational force

kinematics $$\frac{d\vec{Y}(t)}{dt} = \vec{V}(t)$$

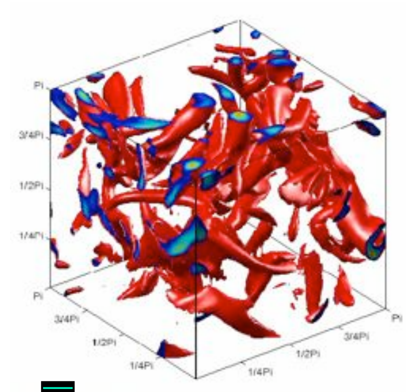

dynamics $$\frac{d\vec{V}(t)}{dt} = \frac{\vec{U}\left(\vec{Y}(t),t\right) - \vec{V}(t) + \vec{W}}{\tau_p}$$

Inertial response time $\tau_p = 2\rho_p a^2/(9\mu)$, still-fluid terminal velocity $\mathrm{W} = \tau_p g$

(Droplets covered with water-insoluble surfactants)

Zero-inertia limit $$\vec{\mathrm{V}}(t) = \vec{\mathrm{U}}\left(\vec{Y}(t),t\right) + \vec{\mathrm{W}}$$

Physics of an heavy particle: importance of inertia and sedimentation

a (μm)	ϵ (cm^2 s^{-3}) 10			100			400		
	St	Sv	a/η	St	Sv	a/η	St	Sv	a/η
10	0.010	1.113	0.007	0.032	0.626	0.011	0.063	0.442	0.017
20	0.040	4.343	0.013	0.127	2.442	0.024	0.253	1.727	0.034
30	0.090	9.385	0.020	0.285	5.278	0.036	0.570	3.732	0.051
40	0.160	15.841	0.027	0.507	8.908	0.047	1.014	6.299	0.067
50	0.250	23.316	0.033	0.792	13.111	0.059	1.585	9.271	0.084
60	0.361	31.478	0.040	1.141	17.701	0.071	2.282	12.516	0.101

$$St = \frac{\tau_p}{\tau_K} \qquad S_V = \frac{W}{v_K}$$

Dependent sensibly on droplet radius and flow dissipation rate

a (μm)	τ_p (s)	v_p (cm s^{-1})	Re_{p0}	$f(Re_{p0})$
10	0.0013	1.272	0.015	1.008
20	0.0052	4.959	0.116	1.034
30	0.0118	10.717	0.378	1.077
40	0.0209	18.089	0.851	1.134
50	0.0327	26.624	1.566	1.204
60	0.0471	35.944	2.537	1.284

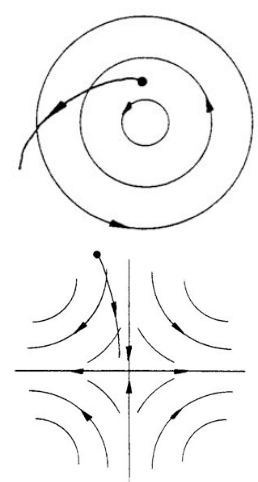

Potential droplet clustering

Maxey (1987)

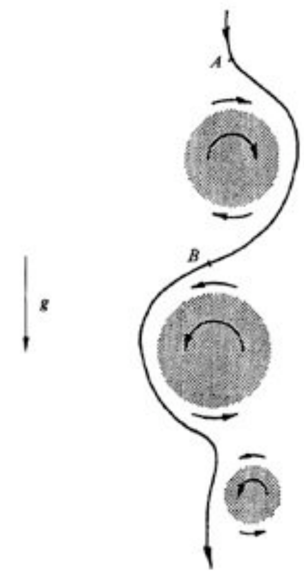

Preferential sweeping

Wang & Maxey (1993)

Droplets as a non-deformable spherical particle

Cloud droplet of a=20 µm, W~0.05 cm/s

Capillary pressure

$$p_C \sim \frac{2\sigma}{a} \sim \frac{2(0.072\ \mathrm{N/m})}{\left(20\times10^{-6} m\right)} \sim 7200\ \ Pa$$

Pressure fluctuations caused by flows

$$p_{flow}^{(1)} \sim \mu\frac{v_K}{\eta} \sim \left(1.5\times10^{-5} kg/(m\cdot s)\right)\frac{(0.02\ m/s)}{\left(8.4\times10^{-4} m\right)}$$

$$\sim 3.8\times10^{-4}\quad Pa$$

$$p_{flow}^{(2)} \sim \mu\frac{u'}{a} \sim \left(1.5\times10^{-5} kg/(m\cdot s)\right)\frac{(1\ m/s)}{\left(20\times10^{-6} m\right)}$$

$$\sim 0.75\ \ Pa$$

$$p_{flow}^{(3)} \sim \mu\frac{W}{a} \sim \left(1.5\times10^{-5} kg/(m\cdot s)\right)\frac{(0.05\ m/s)}{\left(20\times10^{-6} m\right)}$$

$$\sim 0.0375\ \ Pa \quad \text{or} \quad 37.5\ \ Pa$$

$$p_{flow}^{(4)} \sim \rho W^2 \sim \left(1.2\ kg/m^3\right)(0.05\ m/s)^2$$

$$\sim 3.0\times10^{-3}\quad Pa \quad \text{or} \quad 3.0\ \ Pa$$

Cloud droplets do not deform

Rain drop of a=1 mm, W~6 m/s

Capillary pressure

$$p_C \sim \frac{2\sigma}{a} \sim \frac{2(0.072\ \mathrm{N/m})}{\left(1\times10^{-3} m\right)} \sim 144\ \ Pa$$

Pressure fluctuations due to flows

$$p_{flow}^{(1)} \sim \mu\frac{v_K}{\eta} \sim \left(1.5\times10^{-5} kg/(m\cdot s)\right)\frac{(0.02\ m/s)}{\left(8.4\times10^{-4} m\right)}$$

$$\sim 3.8\times10^{-4}\quad Pa$$

$$p_{flow}^{(2)} \sim \mu\frac{u'}{a} \sim \left(1.5\times10^{-5} kg/(m\cdot s)\right)\frac{(1\ m/s)}{\left(1\times10^{-3} m\right)}$$

$$\sim 0.015\ \ Pa$$

$$p_{flow}^{(3)} \sim \mu\frac{W}{a} \sim \left(1.5\times10^{-5} kg/(m\cdot s)\right)\frac{(6\ m/s)}{\left(1\times10^{-3} m\right)}$$

$$\sim 0.09\ \ Pa \quad \text{or} \quad 90\ \ Pa$$

$$p_{flow}^{(4)} \sim \rho W^2 \sim \left(1.2\ kg/m^3\right)(6\ m/s)^2$$

$$\sim 43\ \ Pa \quad \text{or} \quad 43{,}000\ \ Pa$$

Rain drops do deform

Mechanisms for geometric collision

Differential sedimentation

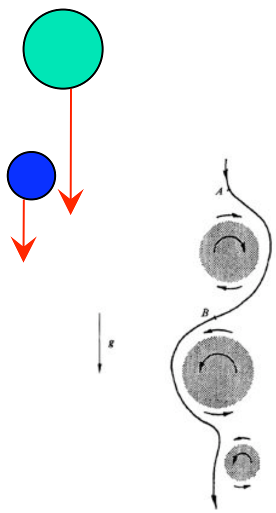

Local flow shear

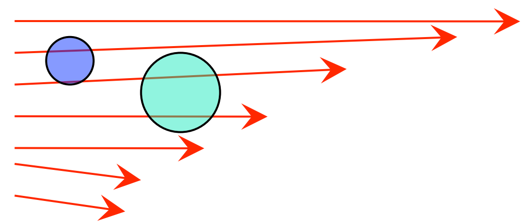

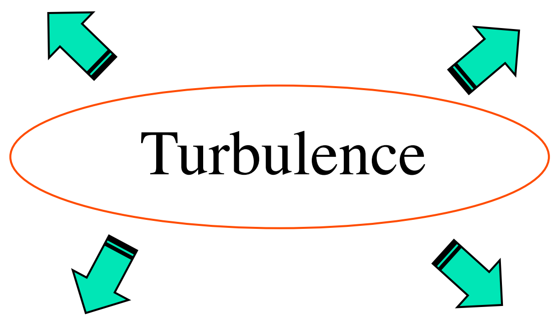

Inertial memory, caustics or sling effect

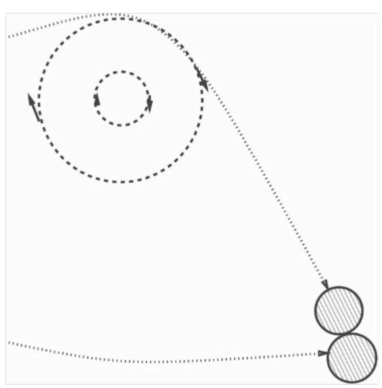

Falkovich & Pumir (2007).

Droplet clustering

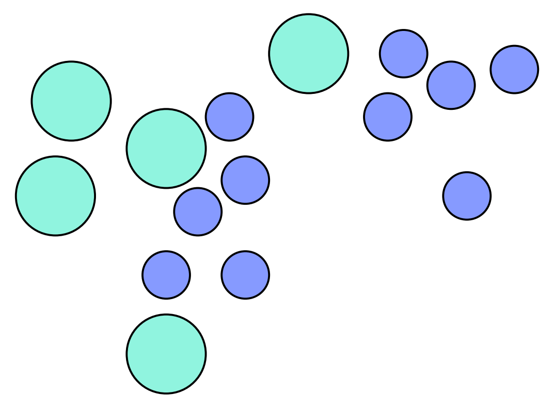

Bottom-up direct numerical simulation of air turbulence (before droplets are introduced)

Turbulence in a one-meter box

Does it produce realistic small-scale turbulent motion?

Does it make sense to study turbulent collision of cloud droplets?

Direct simulation of small-scale air turbulence

Flow field
$$\frac{\partial \vec{U}}{\partial t} = \vec{U}\times\vec{\omega} - \nabla\left(\frac{P}{\rho} + \frac{1}{2}U^2\right) + \nu\,\nabla^2\vec{U} + \vec{f}(\vec{x},t)$$

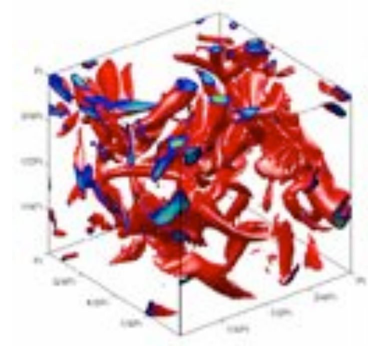

solved with $\nabla\cdot\vec{U} = 0$ in a periodic box

isotropic and homogeneous: $\left\langle \vec{U}(\vec{x},t)\right\rangle = 0$

Kolmogorov scales:

$$\eta = \left(\frac{\nu^3}{\varepsilon}\right)^{1/4};\quad \tau_k = \left(\frac{\nu}{\varepsilon}\right)^{1/2};\quad v_k = (\nu\varepsilon)^{1/4}$$ Primary effect

Effect of large scales:

$$u' = \sqrt{\frac{\left\langle \vec{U}\cdot\vec{U}\right\rangle}{3}} \quad \text{or} \quad R_\lambda = \sqrt{15}\left(\frac{u'}{v_k}\right)^2$$ Secondary effect

Computational / algorithm issues:

Large-scale forcing method
Pseudo-spectral: FFT
Finite-difference: fast Poisson solver, sufficient resolution
Lattice Boltzmann: initialization, acoustic contamination

Air turbulence : compensated energy spectra

$$E(k)k^{5/3}\langle\varepsilon\rangle^{-2/3}$$

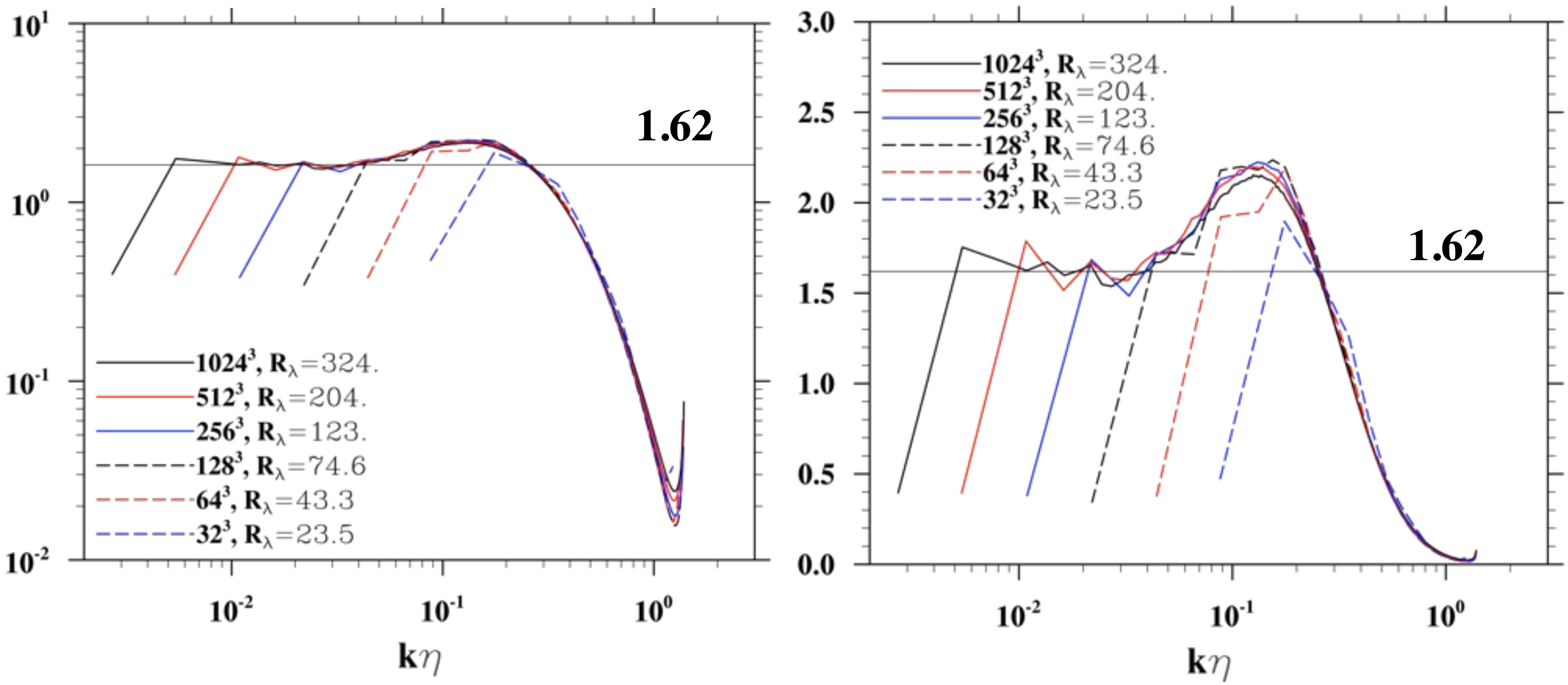

Kolmogorov constant = 1.62: Sreenivasan 1995, Phys. Fluids 7: 2778-2784.
Wang et al., 1996, J. Fluid Mech. 309: 113-156.
Ishihara, Gotoh, and Kaneda, 2009, Annu Rev Fluid Mech 41: 165-180.

Normalized dissipation

Definitions

$$L_f = \frac{\pi}{2(u')^2}\int \frac{E(k)}{k}dk, \quad (u')^2 = \frac{1}{3}\langle \vec{u}\cdot\vec{u}\rangle, \quad \lambda = \lambda_g = \sqrt{\frac{15\nu u'^2}{\varepsilon}}$$

$$\frac{\langle \varepsilon \rangle L_f}{(u')^3}$$

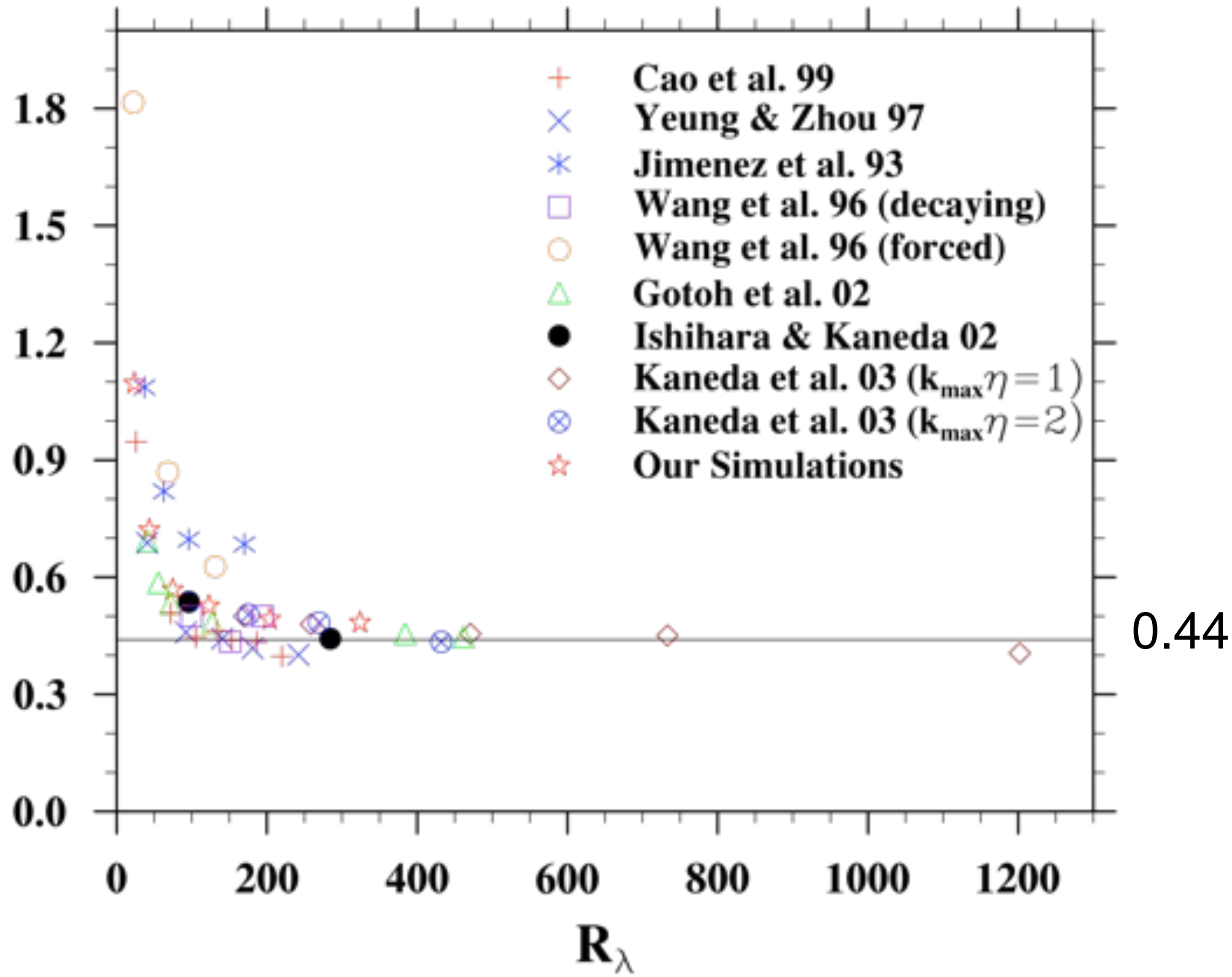

Ishihara, Gotoh, and Kaneda, 2009, *Annu Rev Fluid Mech*. 41: 165-180.

Asymptotic value of 0.44 reached at $R_\lambda = 200$ (when a clearly identifiable inertial subrange exists in the simulated flow).

Implications of increasing DNS grid resolutions

	N	R_λ	Re	<ε> DNS	Domain size (cm) (400 cm²/s³)	Domain size (cm) (100 cm²/s³)	u′
	32	23.5	40.6	3646	4.2	6.0	7.08
Published	64	43.3	90.6	3529	8.4	11.9	9.61
	128	74.6	212	3589	16.9	23.9	12.61
On-going	256	123.	532.	3690	34.0	48.1	16.18
	512	204.	1,373	3900	68.9	97.5	20.84
Target	1024	324.	3,806	3777	137.	193.	26.29

$$\mathrm{Re} = \frac{u' L_f}{\nu}, \qquad R_\lambda = \frac{u'\lambda}{\nu}$$

Cloud conditions

$$\mathrm{Re} = 10^6 \sim 10^8; \qquad R_\lambda = 10^3 \sim 10^4$$

$$\text{Domain size} = 2\pi\left(\frac{\nu_p}{\nu_n}\right)^{0.75}\left(\frac{\varepsilon_n}{\varepsilon_p}\right)^{0.25} = 2\pi\left(\frac{0.17}{\nu_n}\right)^{0.75}\left(\frac{\varepsilon_n}{\varepsilon_p}\right)^{0.25}$$

Implications of increasing DNS grid resolutions (II)

Assume a LWC of $1\ \mathrm{g/m^3}$.

Half $a_1 = 30\ \mu\mathrm{m}$ and half $a_2 = 20\ \mu\mathrm{m}$

	N	R_λ	Box size (cm) (400 cm^2/s^3)	Total number of droplets
Published	32	23.5	4.2	$1.0\mathrm{x}10^3$
	64	43.3	8.4	$8.0\mathrm{x}10^3$
	128	74.6	16.9	$6.6\mathrm{x}10^4$
On-going	256	123.	34.0	$5.4\mathrm{x}10^5$
	512	204.	68.9	$4.5\mathrm{x}10^6$
Target	1024	324.	137.	$3.5\mathrm{x}10^7$

The response of an inertial particle to turbulence: A conceptual model

$$\frac{dV}{dt} = \frac{u - V}{\tau_p}$$

Assume $u = u_0 \sin\left(\frac{2\pi\, t}{T}\right)$, with $T = f\left(l, W, \tau_p, a, ...\right) \approx \frac{l}{u + W}$

The long-time solution is

$$\mathrm{V} = \frac{u_0 \sin\left(\frac{2\pi\, t}{T}\right) - u_0 \frac{2\pi\, \tau_p}{T} \sin\left(\frac{2\pi\, t}{T}\right)}{1 + \left(\frac{2\pi\, \tau_p}{T}\right)^2}$$

Therefore,

$$\frac{|\mathrm{V}|}{|\mathrm{u}|} = \frac{1}{\sqrt{1 + \left(\frac{2\pi\, \tau_p}{T}\right)^2}} = \frac{1}{\sqrt{1 + \left(\frac{2\pi\, \tau_p (u + W)}{l}\right)^2}}$$

For the inertial subrange, we set

$$l \sim \frac{2\pi}{k}, \quad u \sim (\varepsilon l)^{1/3} \sim \left(\varepsilon \frac{2\pi}{k}\right)^{1/3}, \quad \text{then} \quad \frac{|\mathrm{V}|}{|\mathrm{u}|} = \frac{1}{\sqrt{1 + \left\{(k\eta) \cdot St \cdot \left[Sv + \left(\frac{2\pi}{k\eta}\right)^{1/3}\right]\right\}^2}}$$

The response function

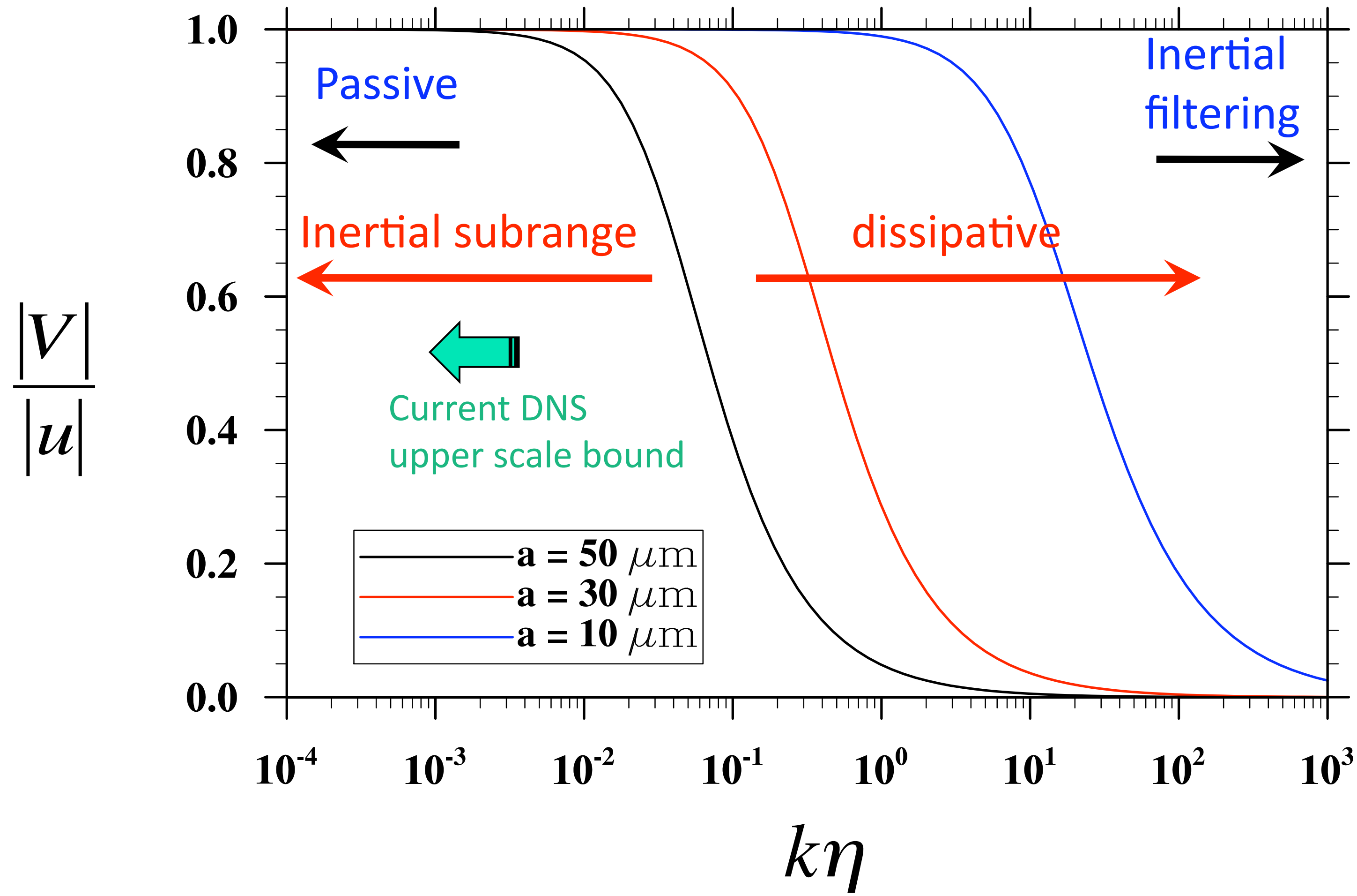

Direct numerical simulations of particle-laden turbulent flows

In parallel to the development of DNS of single-phase turbulent flows

Point-particle simulation (late1980 -)

Point-particle simulation with particle-particle and particle-wall interactions (late 1990 -)

Hybrid direct numerical simulation (2000 -)

Particle-resolved simulation (2005 -)

Point-Particle Based

Direct Numerical Simulation:

Geometric collision

Droplets as ghost particles

Equation of motion (modeled, Maxey and Riley 1983)

$$m_p \frac{d\vec{V}(t)}{dt} = \left(m_p - m_f\right)\vec{g} + m_f \frac{D\vec{U}}{Dt} + \frac{1}{2}\left(\frac{D\vec{U}}{Dt} - \frac{d\vec{V}(t)}{dt}\right) + 6\pi a\mu\left(U - V\right)$$

$$+ \text{ Basset history } + \text{ lift } + \text{ others}$$

Droplets as heavy particles: $\rho_p >> \rho_f$

$$\frac{d\vec{V}(t)}{dt} = -\frac{\vec{V}(t) - U(\vec{Y}(t),t)}{\tau_p} - \vec{g}$$

$$\frac{d\vec{Y}(t)}{dt} = \vec{V}(t)$$

$$\tau_p = 2\rho_p a^2/(9\mu), \quad W = \tau_p g$$

Algorithm issues: interpolation of $\vec{U}(\vec{Y}(t),t)$
MPI

Wang et al, 2009, *Int. J. Multiphase Flow* 35: 854-867.

Dynamic collision detection

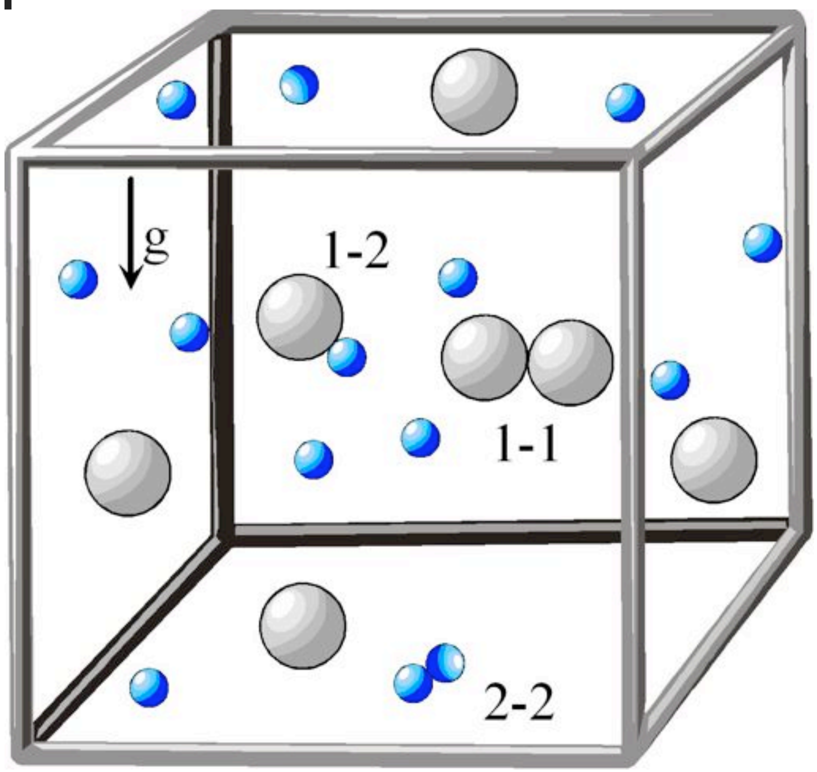

Dynamic collision kernels:

$$K_{12}^{D} = \langle \dot{N}_{12} \rangle / (n_1 n_2)$$

$$K_{11}^{D} = \langle \dot{N}_{11} \rangle / (n_1^2 / 2)$$

$$K_{12}^{D} = \langle \dot{N}_{22} \rangle / (n_2^2 / 2)$$

where

$$n_1 = N_1 / V_B, \qquad n_2 = N_2 / V_B$$

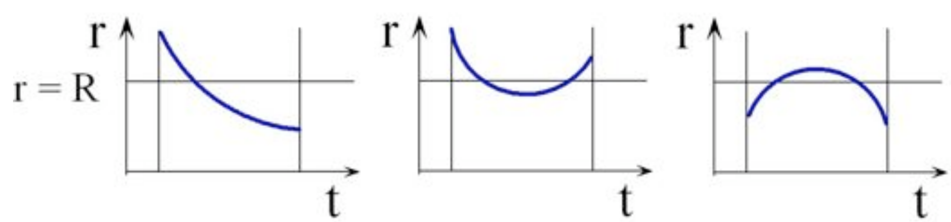

Numerical detection: The efficient cell-index method and the concept of linked lists
Allen & Tildesley (1987), ***Computer Simulation of Liquids*****. Oxford University Press.**

General kinematic collision kernel: inertial droplets in a turbulent flow

$$K_{12} = 2\pi R^2 \langle | w_r(r = R) | \rangle g_{12}(r = R)$$

Radial relative velocity   Radial distribution function

$$\langle | w_r | \rangle = \frac{1}{N_{pair}} \sum_{all\ pairs} \left| \vec{r} \cdot \frac{(\vec{V}_1 - \vec{V}_2)}{r} \right|$$

$$g_{12}(R) = \lim_{\delta << r} \frac{N_{pair}(r - \delta \le d \le r + \delta) / 4\pi \left[(r+\delta)^3 - (r-\delta)^3 \right]}{N_1 N_2 / V_B}$$

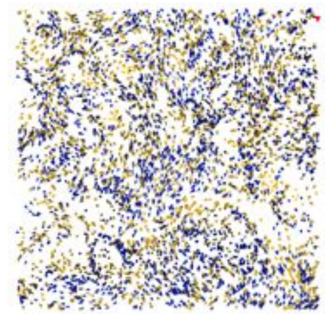

- Based on the spherical formulation
- Confirmed by DNS for all different situations
- Easy to calculate in DNS, but could be very difficult to measure!

Important for parameterization of collection kernel.

Saffman & Turner, J. Fluid Mech. (1956).
Sundaram & Collins, J. Fluid Mech. 335: 75-109 (1997).
Wang, *et al.* J. Atmos. Sci. 62: 2433-2450 (2005).

The mean settling velocity of droplets in turbulent flow

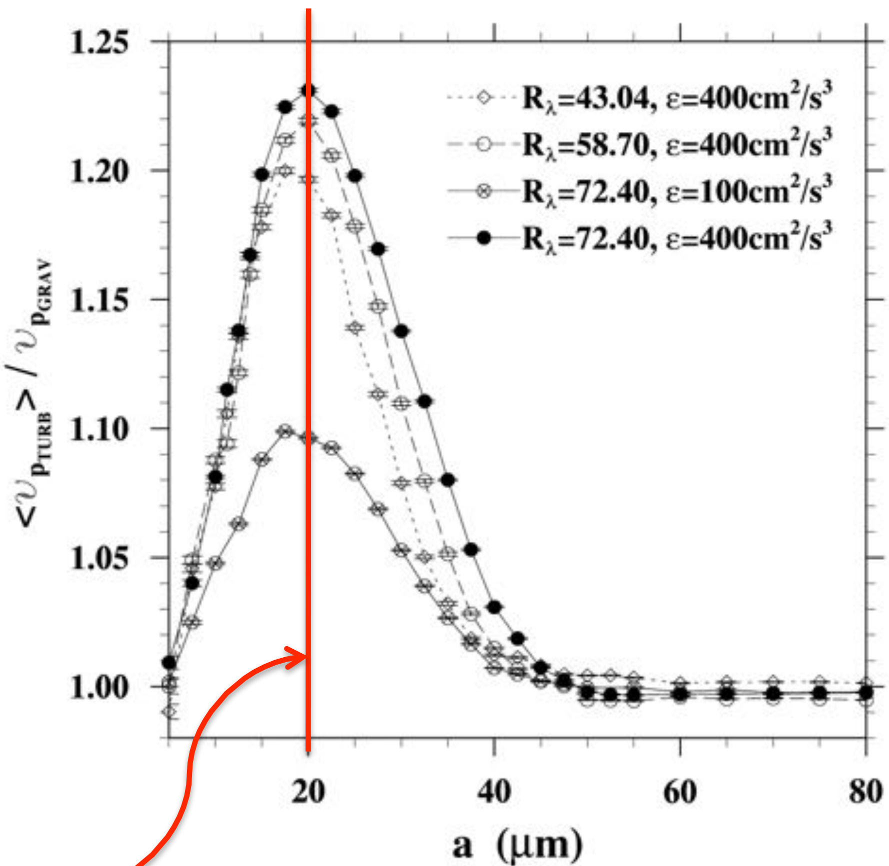

A nondimensional parameter

$$\frac{\tau_p W_p^2}{\Gamma_{vort}} = \frac{\tau_p^3 g^2}{\nu}$$

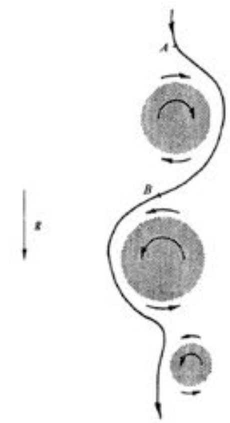

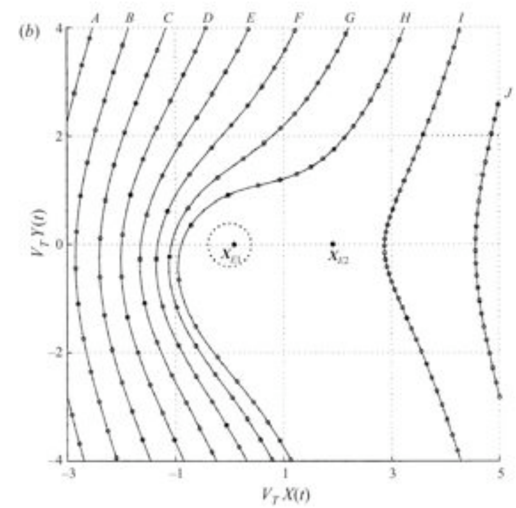

$$\tau_p \sim \frac{\Gamma_{vort}}{W_p^2} \sim \frac{v_k \eta}{(\tau_p g)^2} \sim \frac{\nu}{(\tau_p g)^2}$$

$$a \sim 20 \quad \mu m$$

Wang & Maxey, J. Fluid Mech. 256 (1993).
Davila & Hunt, J. Fluid Mech. 440 (2001). Falkovich et al., Nature, 419 (2002).
Ayala et al., New J. Physics, 10: 075015 (2008).

Geometric collision: radial relative velocity and radial distribution function

$$a_1 = 30\mu m, \quad R_\lambda = 72.4, \quad \varepsilon = 400\ cm^2/s^3$$

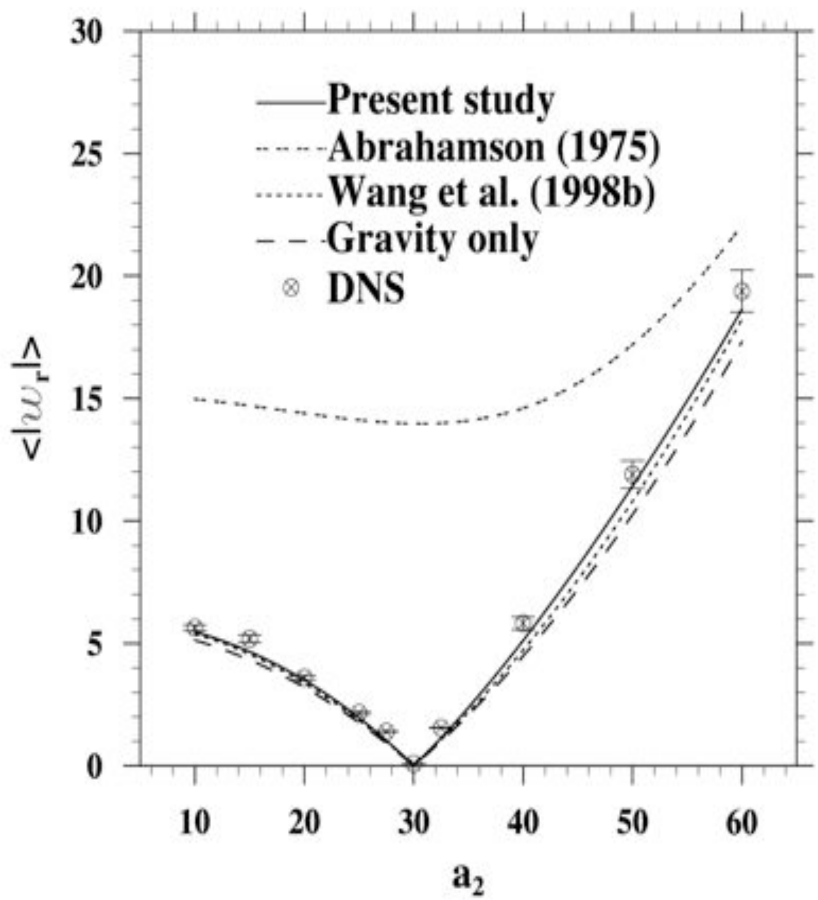

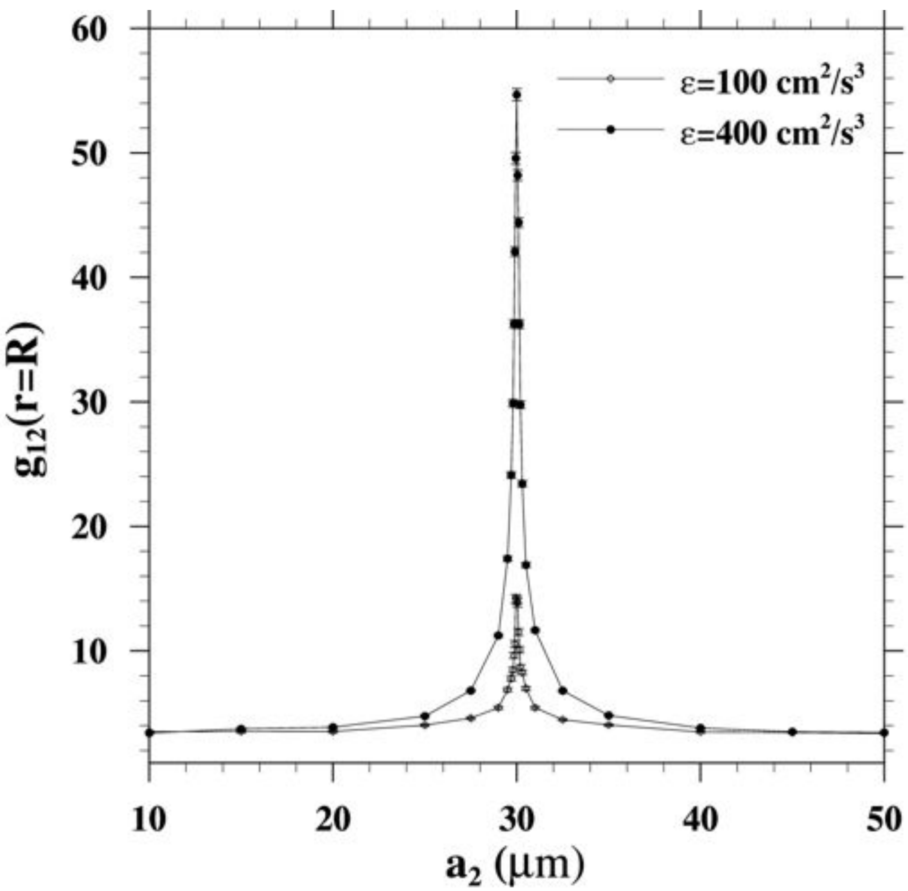

Droplet positions (a thin 2D slice):
blue cones for 30 μm (St=0.570)
yellow cones for 20 μm (St=0.253)

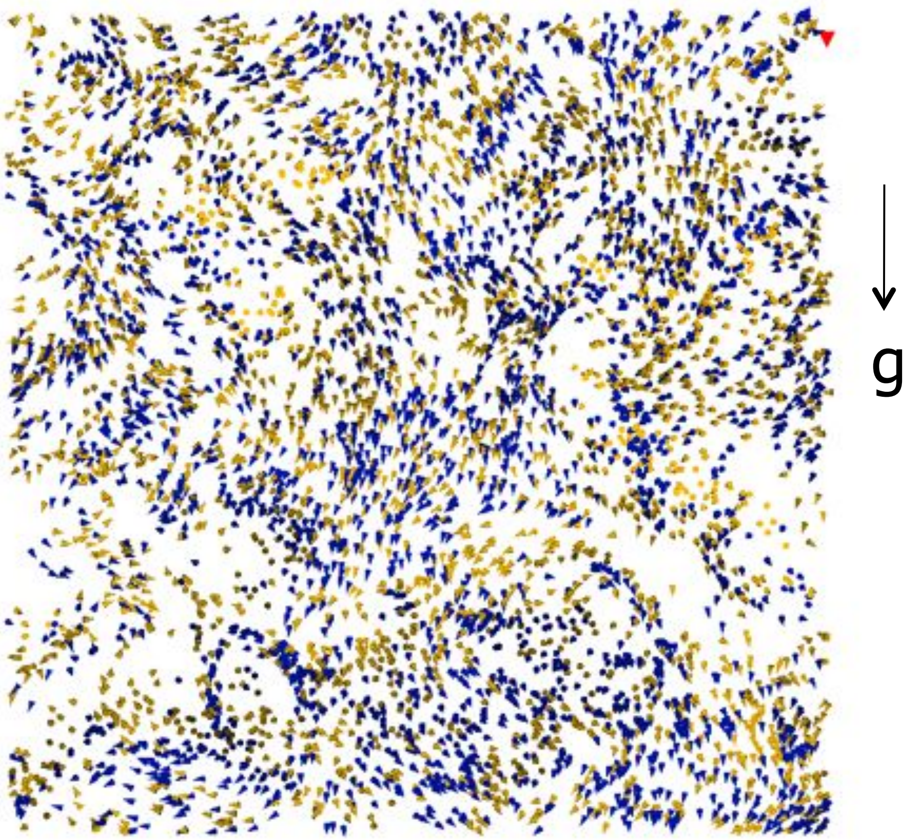

$g_{12} = 1.125,$

$g_{11} = 16.824,$

$g_{22} = 5.087$

Flow enstrophy field

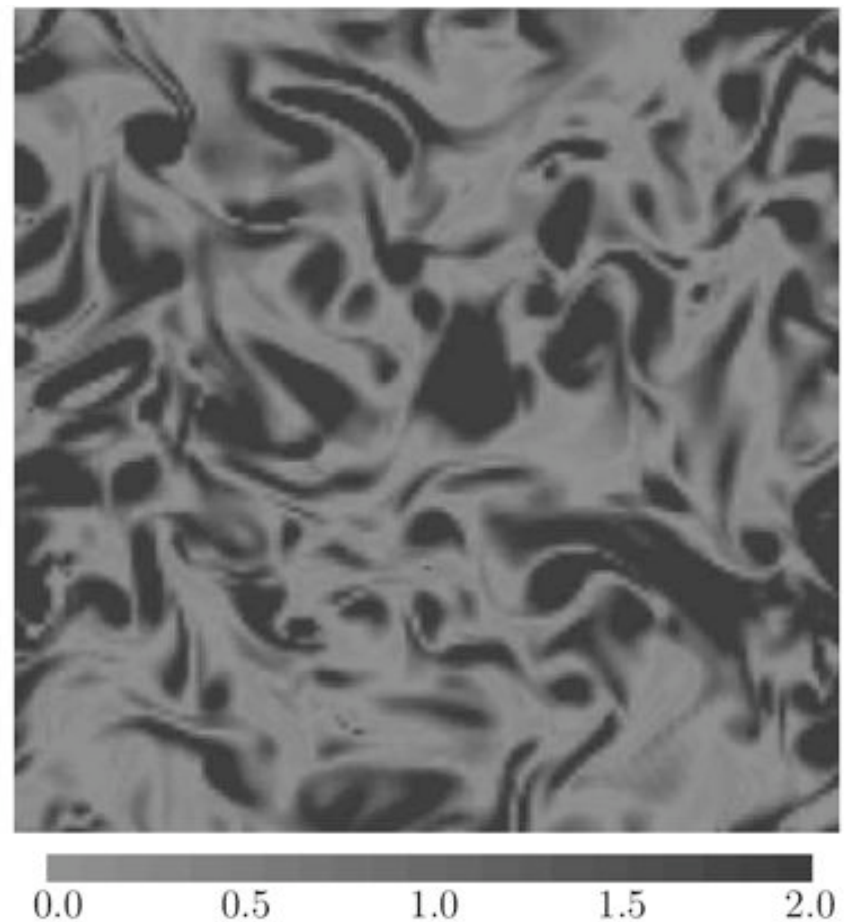

$R_\lambda = 72, \quad \varepsilon = 400\ cm^2/s^3$

Theoretical parameterization: $\langle | w_r(r = R) | \rangle$

Random part
due to turbulence

Deterministic part
due to gravity

$$w_r(\theta) = \xi(\theta) + h(\theta)$$

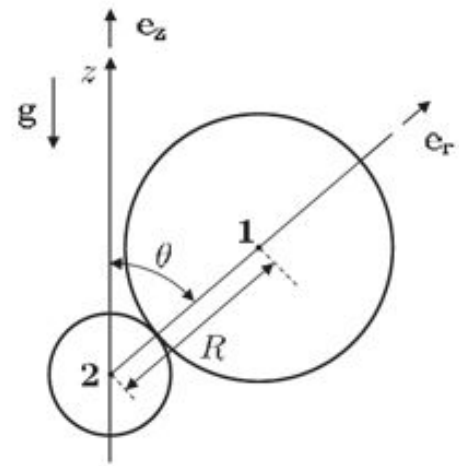

$$\langle |w_r| \rangle = \tfrac{1}{2} \int_0^{\pi} \overline{|w_r(\theta)|} \sin\theta d\theta$$

Dodin & Elperin (2002)

$$\langle |w_r| \rangle = \int_0^{\pi/2} \int_{-\infty}^{\infty} |w_r(\theta)| \frac{1}{\sqrt{2\pi}\sigma(\theta)} \times \exp\left(-\frac{[w_r(\theta) - |\mathbf{g}||\tau_{\mathbf{p1}} - \tau_{\mathbf{p2}}| \cos\theta]^2}{2\sigma(\theta)^2} \right) dw_r \sin\theta d\theta$$

Assume Gaussian PDF for the random part

Ayala et al., New Journal of Physics 10 (2008) 075016.

Table 3. Characteristic scales of cloud droplets.

a (μm)	ϵ (cm^2 s^{-3}) 10			100			400		
	St	Sv	a/η	St	Sv	a/η	St	Sv	a/η
10	0.010	1.113	0.007	0.032	0.626	0.011	0.063	0.442	0.017
20	0.040	4.343	0.013	0.127	2.442	0.024	0.253	1.727	0.034
30	0.090	9.385	0.020	0.285	5.278	0.036	0.570	3.732	0.051
40	0.160	15.841	0.027	0.507	8.908	0.047	1.014	6.299	0.067
50	0.250	23.316	0.033	0.792	13.111	0.059	1.585	9.271	0.084
60	0.361	31.478	0.040	1.141	17.701	0.071	2.282	12.516	0.101

Ayala et al. 2008 New J. Phys. 10 (2008) 075015.

VARIANCE σ^2 (θ =90^o)

$$\sigma^2 \equiv < (v_z'^{(1)} - v_z'^{(2)})^2 > = < (v_z'^{(1)})^2 > + < (v_z'^{(2)})^2 > -2 < (v_z'^{(1)} v_z'^{(2)}) >$$

$$v_z'^{(k)} = \int_{-\infty}^{t} \frac{U_1(\mathbf{Y}^{(k)}(\tau),\tau)}{\tau_{pk}} \exp\left(\frac{\tau - t}{\tau_{pk}}\right) d\tau \quad \text{(Reeks, 1977)}$$

Integration on particle trajectory

$$< (v_z'^{(1)} v_z'^{(2)}) > = \frac{1}{\tau_{P1}\tau_{P2}} \int_{-\infty}^{0} d\tau_1 \int_{-\infty}^{0} d\tau_2 < U_1(\mathbf{Y}^{(1)}(\tau_1),\tau_1) U_1(\mathbf{Y}^{(2)}(\tau_2),\tau_2) > \times \exp\left(\frac{\tau_1}{\tau_{P1}}\right) \exp\left(\frac{\tau_2}{\tau_{P2}}\right)$$

$$< (v_z'^{(k)})^2 > = \frac{1}{\tau_p} \int_{-\infty}^{0} d\tau < U_1(\mathbf{Y}^{(k)}(0),0) U_1(\mathbf{Y}^{(k)}(\tau),\tau) > \exp\left(\frac{\tau}{\tau_{P1}}\right)$$

The fluid velocity correlations

$$\frac{< U_1(\mathbf{Y}^{(1)}(0),0) U_1(\mathbf{Y}^{(1)}(\tau),\tau) >}{u'^2} \approx R_{11}(v_{p_k}\mathbf{e}_z\tau) D_L(\tau) \approx g(v_{p_k}\tau) D_L(\tau)$$

Introduce approximations

$$\frac{< U_1(\mathbf{Y}^{(1)}(\tau_1),\tau_1) U_1(\mathbf{Y}^{(2)}(\tau_2),\tau_2) >}{u'^2} \approx R_{11}(\mathbf{R} + v_{p_1}\mathbf{e}_z\tau_1 - v_{p_2}\mathbf{e}_z\tau_2) D_L(\tau_1 - \tau_2) \approx f(R) g(v_{p_1}\tau_1 - v_{p_2}\tau_2) D_L(\tau_1 - \tau_2)$$

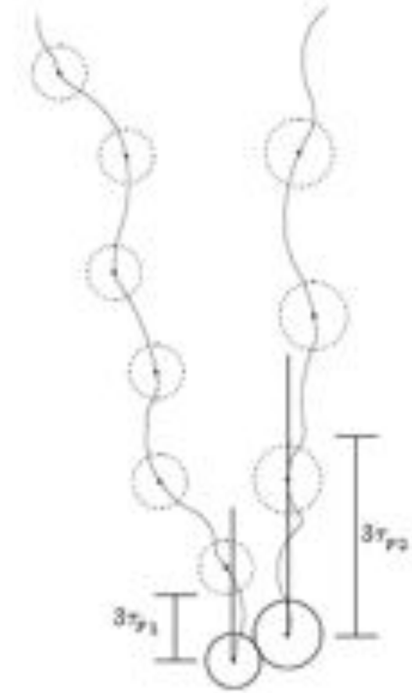

Ayala et al. 2008 New J. Phys. 10 (2008) 075015.

Using the bi-exponential forms for $D_L(\tau)$ and $f(r)$ (Sawford, 1991; Zaichick *et al.* 2003a), along with the expression for $g(r)$

$$g(r) = f(r) + \frac{r}{2}\frac{df}{dr}$$

We obtain

$$< (v_x'^{(1)} v_x'^{(2)}) >= \frac{u'^2 f(R)}{\tau_{p1}\tau_{p2}}[b_1 d_1 \Phi(c_1, e_1) - b_1 d_2 \Phi(c_1, e_2) - b_2 d_1 \Phi(c_2, e_1) + b_2 d_2 \Phi(c_2, e_2)]$$

$$< (v_x'^{(k)})^2 >= \frac{u'^2}{\tau_{pk}}[b_1 d_1 \Psi(c_1, e_1) - b_1 d_2 \Psi(c_1, e_2) - b_2 d_1 \Psi(c_2, e_1) + b_2 d_2 \Psi(c_2, e_2)]$$

THE FINAL RESULT FOR $\langle |w_r| \rangle$

$$\langle |w_r| \rangle = \sqrt{\frac{2}{\pi}}\sigma f(b)$$

$$f(b) = \frac{1}{2}\sqrt{\pi}\left(b + \frac{0.5}{b}\right)\mathrm{erf}(b) + \frac{1}{2}\exp\left(-b^2\right)$$

$$b = \frac{|\mathbf{g}||\tau_{p1} - \tau_{p2}|}{\sigma\sqrt{2}}$$

Dodin and Elperin (2002)

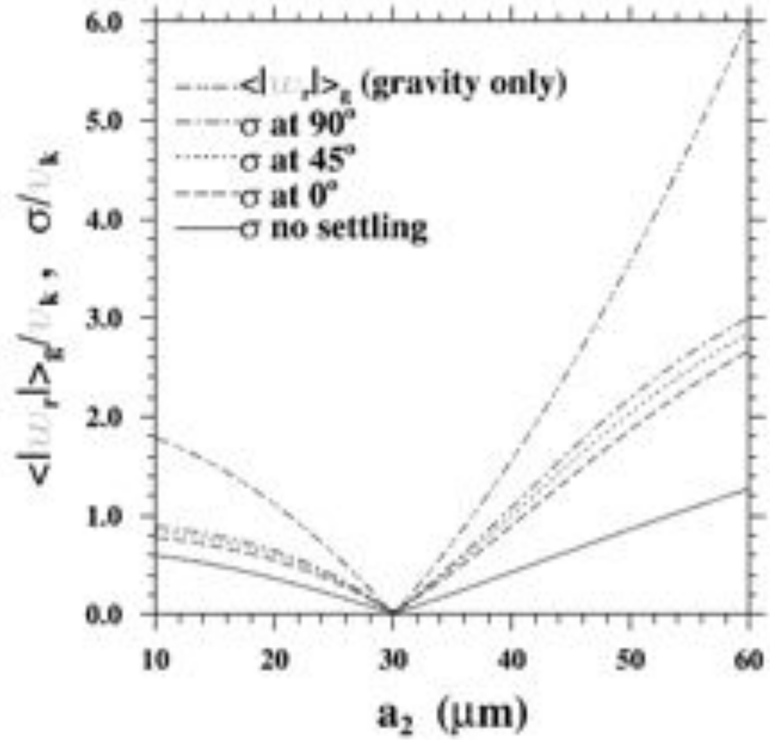

$$\langle |w_r| \rangle = \sqrt{\frac{2}{\pi}}\left(\sigma + \frac{\pi}{8}(\tau_{p1} - \tau_{p2})^2|\mathbf{g}|^2\right)^{1/2}$$

Wang *et al.* (1998b)

Comparing with DNS results

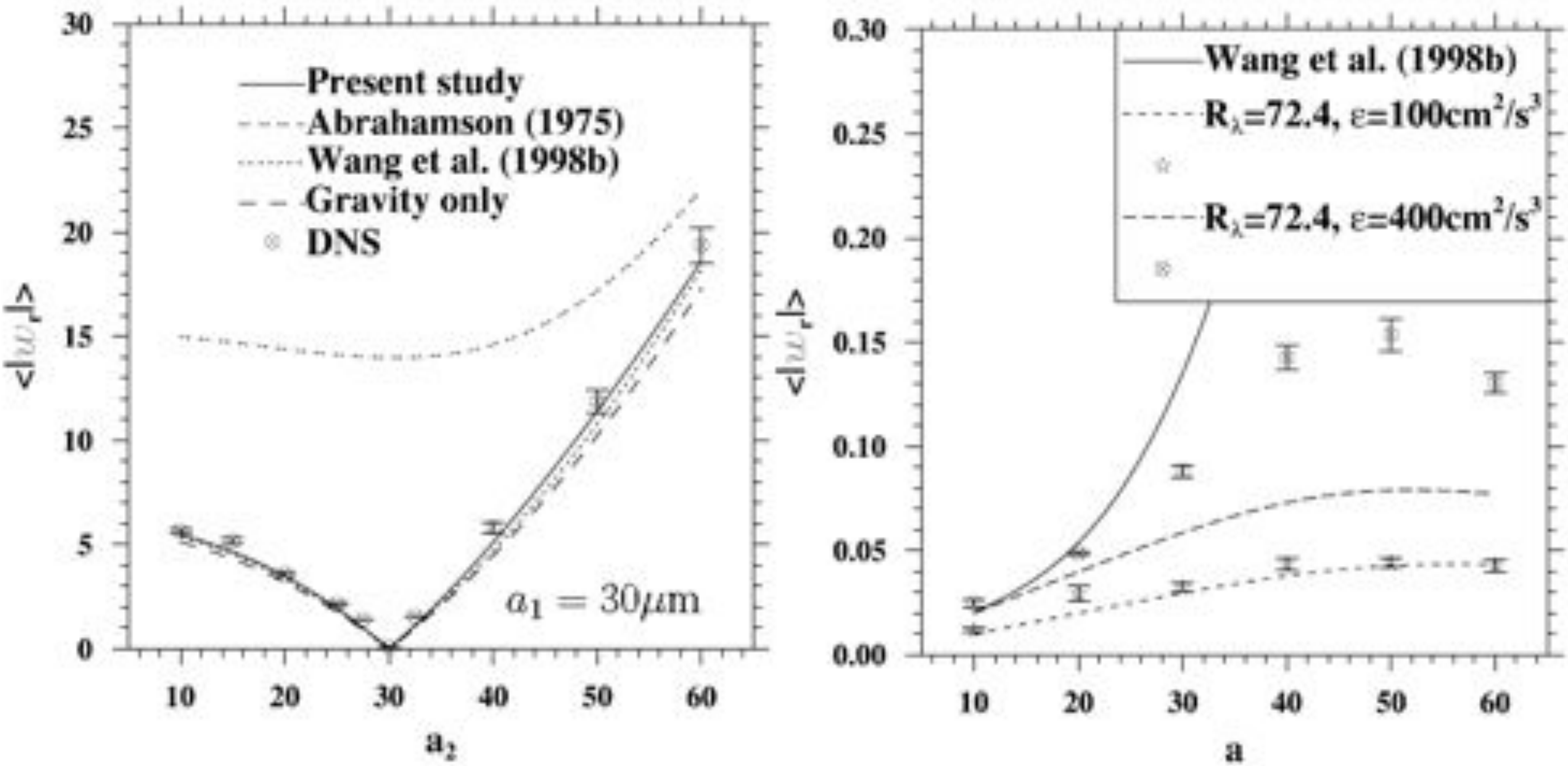

R_λ =72.4 and ϵ =400 cm^2/s^3

Radial distribution function g_{12}: empirical fitting

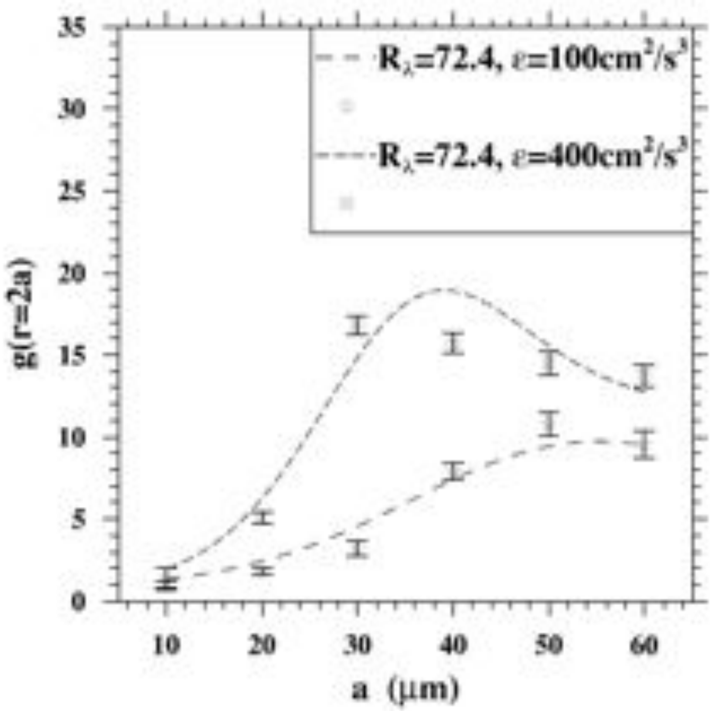

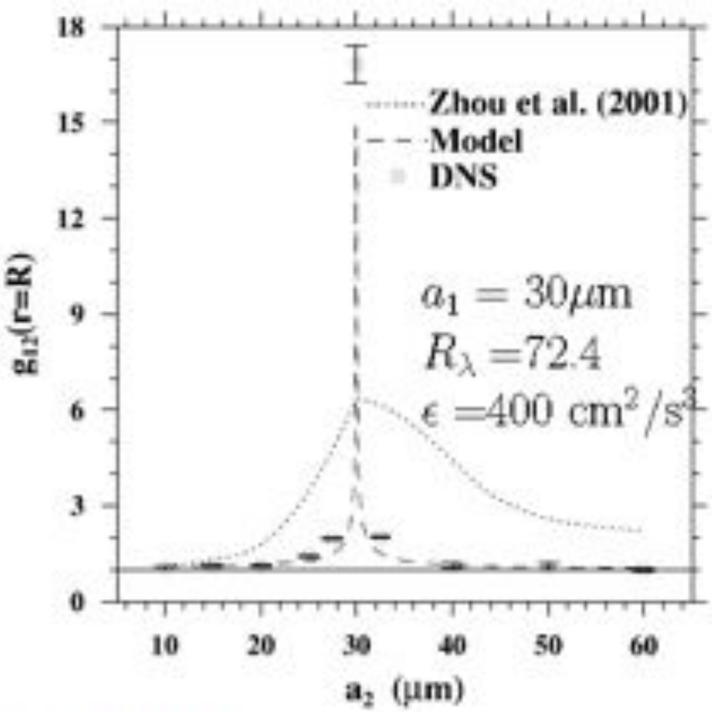

$$g_{12}(r) = \left(\frac{\eta^2 + r_c^2}{r^2 + r_c^2}\right)^{C_1/2}$$ Chun *et al.* (2005)

$$C_1 = \frac{f_2(St)}{(|\mathbf{g}|/(v_k/\tau_k))^{f_1(R_\lambda)}}, \qquad St \equiv \max(St_2, St_1) \qquad \left(\frac{r_c}{\eta}\right)^2 = |St_2 - St_1| F(a_{o_g}, R_\lambda)$$

$$f_1(R_\lambda) = 0.1886 \exp\left(\frac{20.306}{R_\lambda}\right) \qquad a_{o_g} = a_o + \frac{\pi}{8}\left(\frac{|\mathbf{g}|}{v_k/\tau_k}\right)^2$$

$$f_2(St) = -0.1988 St^4 + 1.5275 St^3 - 4.2942 St^2 + 5.3406 St \qquad F(a_{o_g}, R_\lambda) = 20.115\left(\frac{a_{o_g}}{R_\lambda}\right)^{1/2}$$

Alternative approach: fit the empirical theory of Falkovich et al. (2002)

GEOMETRIC COLLISION KERNEL

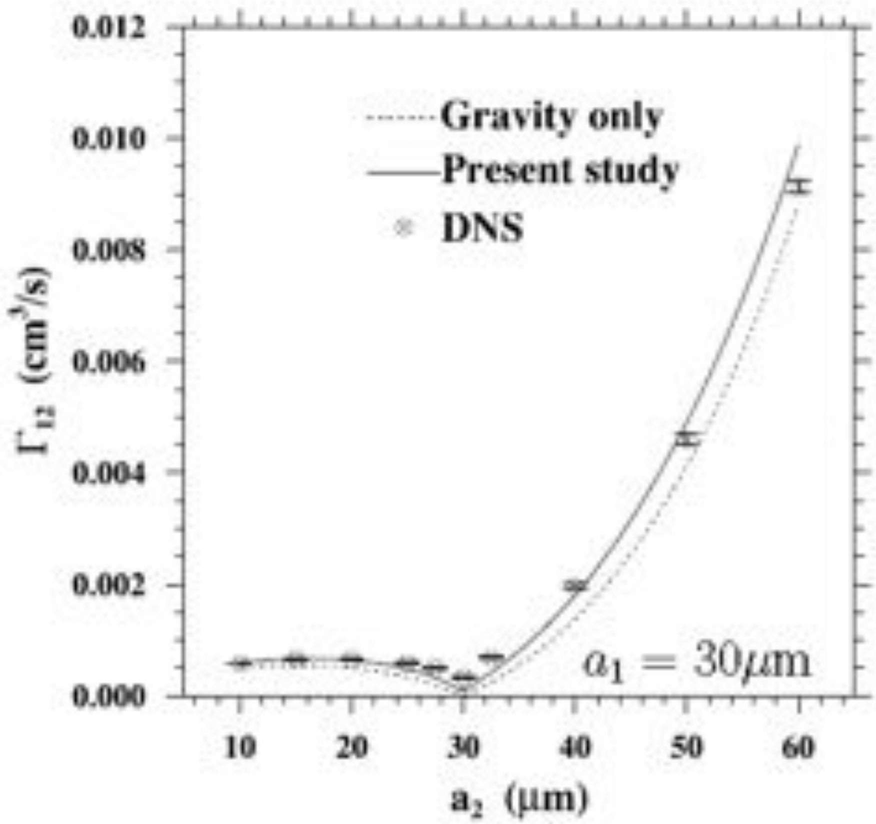

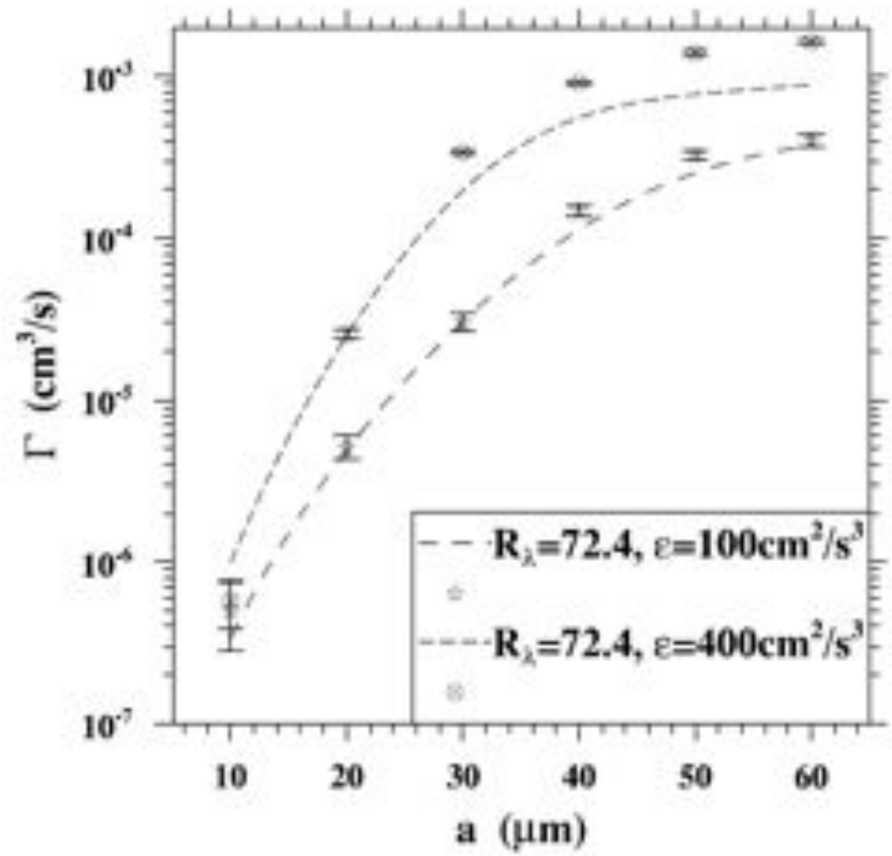

R_λ =72.4 and ϵ =400 cm^2/s^3

Overall enhancement factor on geometric collision kernel

Ayala kernel $\varepsilon = 300\ cm^2/s^3; \quad u' = 202\ \ cm/s$

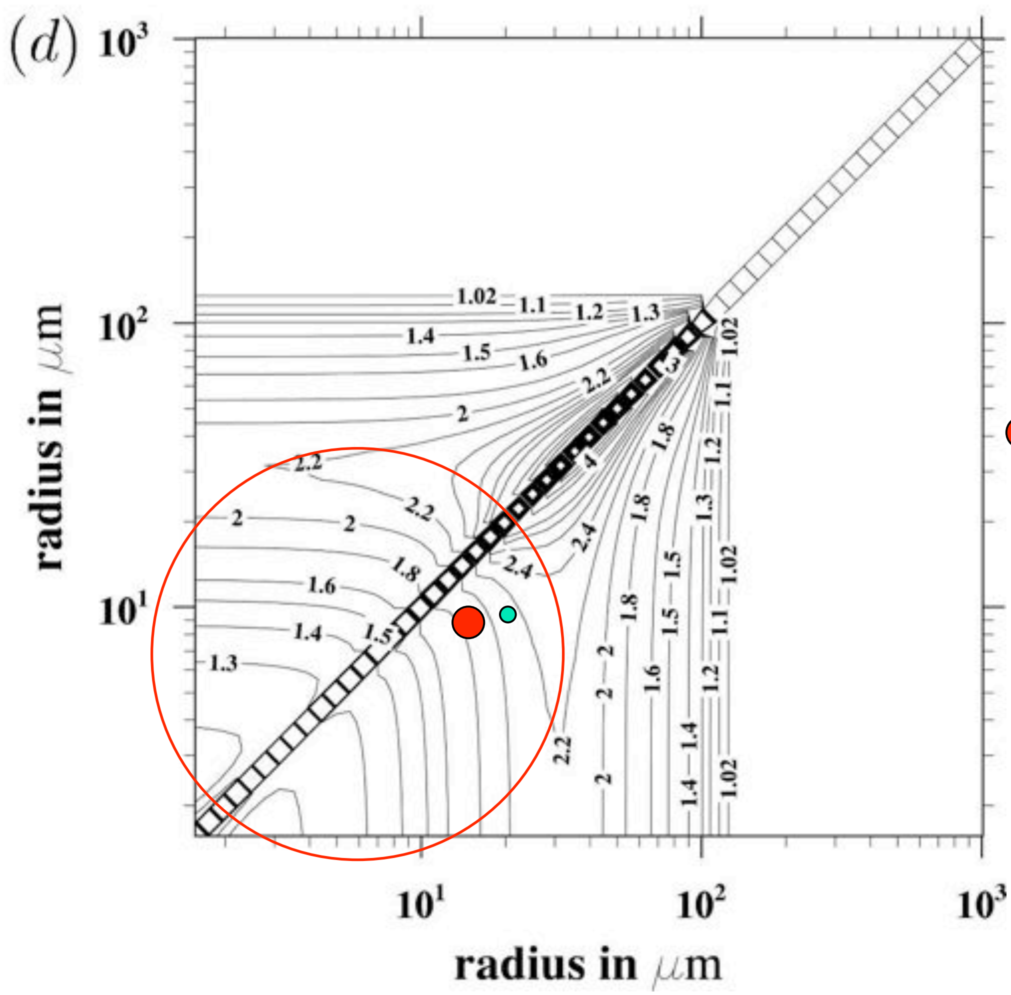

- Franklin et al. (2005): 10µm-20µm
  a factor of 1.2 to 2.1 for
  $280\ cm^2/s^3 \le \varepsilon \le 1535\ cm^2/s^3;$
  $9\ \ cm/s \le u' \le 21\ \ cm/s$

- Pinsky et al. (2006): 10µm-15µm, a factor of 1.6 for
  $\varepsilon = 1000\ cm^2/s^3$

Pinsky et al. (1997):
a factor of 10 for
$\varepsilon = 600\ cm^2/s^3$

Hybrid Direct Numerical Simulation

Beyond point step

A half step forward

Requirement 1: treat a very large number of particles moving in 3D fluid turbulence

Requirement 2: include the effect of droplet-droplet local aerodynamic interaction

Wang et al, 2009, *Int. J. Multiphase Flow* 35: 854-867.

Physics: droplet-droplet local aerodynamic interaction

a_1=10 μm and a_2=30 μm
W_1=0.107 m/s and W_2=0.0127 m/s

Aerodynamic interaction time

$$\tau_{\mathrm{AI}} \sim \frac{10(a_1 + a_2)}{|W_1 - W_2|} \sim \frac{40 \times 10^{-5}\ m}{(0.107 - 0.0127)\ \mathrm{m/s}}$$

$$\sim 4.24\ ms$$

Inertial response time

$$\tau_{p,1} = 1.3\ \ ms, \qquad \tau_{p,2} = 11.8\ \ ms$$

Droplets can respond to the disturbance flows

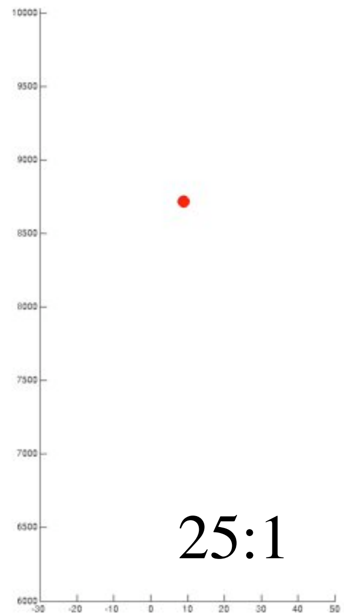

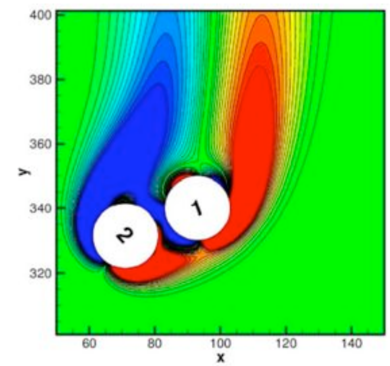

Klett and Davis (1973)

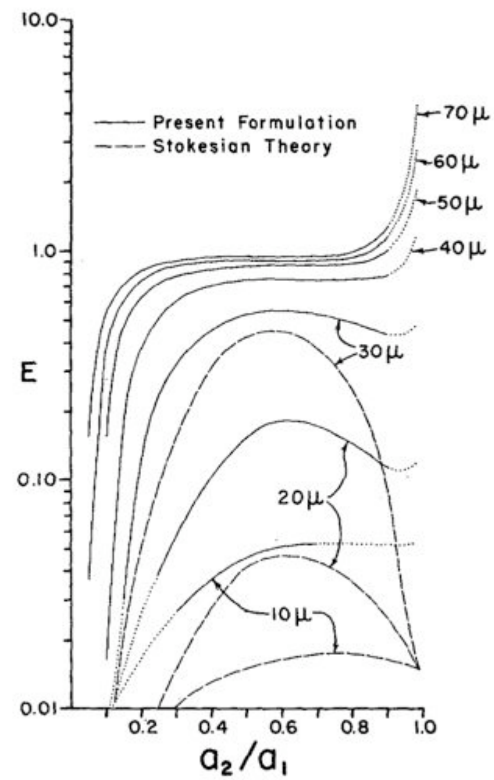

a_1=100 μm and a_2=30 μm
W_1=1 m/s and W_2=0.107 m/s

Aerodynamic interaction time

$$\tau_{\mathrm{AI}} \sim \frac{10(a_1 + a_2)}{|W_1 - W|_2} \sim \frac{130 \times 10^{-5}\ m}{(1.0 - 0.107)\ \mathrm{m/s}}$$

$$\sim 1.45\ ms$$

Inertial response time

$$\tau_{p,1} = 102\ \ ms, \qquad \tau_{p,2} = 11.8\ \ ms$$

Droplets do not have time to respond to the disturbance flows

Equation of motion for droplets

$$\frac{d\vec{V}^{(\alpha)}(t)}{dt} = \frac{\left[\vec{U}\left(\vec{Y}^{(\alpha)}(t),t\right) + \vec{u}(\vec{Y}^{(\alpha)},t)\right] - \vec{V}^{(\alpha)}(t)}{\tau_p^{(\alpha)}} + \vec{g}$$

$$\frac{d\vec{Y}^{(\alpha)}(t)}{dt} = \vec{V}^{(\alpha)}(t)$$

Where $\tau_p^{(\alpha)} = 2\rho_p\left(a^{(\alpha)}\right)^2/(9\mu),\qquad \mathrm{W}^{(\alpha)} = \tau_p^{(\alpha)}g$

If hydrodynamic interaction is considered: $\vec{u}(\vec{Y}^{(\alpha)},t) \neq 0$

Self-consistent: no ambiguity in defining undisturbed fluid velocity

Typically tracking $10^5 \sim 10^7$ droplets with hydrodynamic interactions.

A lot of quantitative information can be extracted!

The hybrid DNS approach

A grid volume in DNS of background turbulence

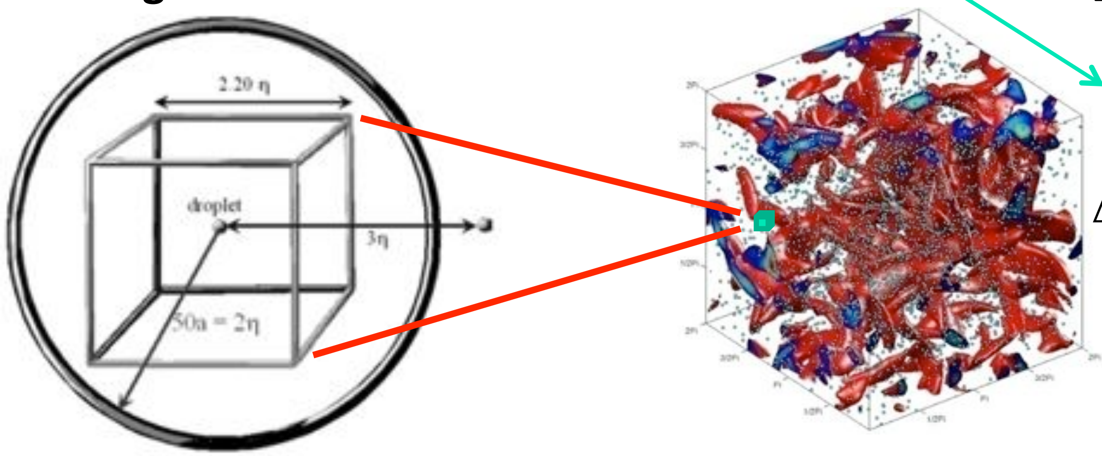

Resolve ~5 orders of magnitude in length scales!

200 to 1000 mm

Resolved numerically

Δx ~ 1 to 2 mm

Treated analytically

a ~ 0.02 to 0.05 mm

Assumptions:

(1) There is scale separation between Δx and disturbance flows are localized

(2) The disturbance flow is Stokes flow

$$\vec{U}(\vec{x},t) + \sum_{m=1}^{N_p} \vec{u}_s\left(\vec{r}_m; a_m, \vec{V}_m - \vec{U}(\vec{Y}_m,t) - \vec{u}_m\right)$$

Background turbulent flow

Disturbance flows due to droplets

$$\text{where} \quad \vec{r}_m = \vec{x} - \vec{Y}_m, \quad \vec{u}_s\left(\vec{r}; a, \vec{V}\right) \equiv \left[\frac{3a}{4r} - \frac{3}{4}\left(\frac{a}{r}\right)^3\right]\frac{\vec{r}}{r^2}\left(\vec{V}\cdot\vec{r}\right) + \left[\frac{3a}{4r} + \frac{1}{4}\left(\frac{a}{r}\right)^3\right]\vec{V}$$

The hybrid DNS approach: no slip boundary condition

$$\vec{U}(\vec{x},t)+\sum_{k=1}^{N_p}\vec{u}_s\left(\vec{r}_k;a_k,\vec{V}_k-\vec{U}(\vec{Y}_k,t)-\vec{u}_k\right)$$

Background turbulent flow

Disturbance flows due to droplets

$$\vec{V}_k=\left\{\vec{U}(\vec{x},t)+\sum_{\substack{m=1\\ m\neq k}}^{N_p}\vec{u}_s\left(\vec{x}-\vec{Y}_m;a_m,\vec{V}_m-\vec{U}(\vec{Y}_m,t)-\vec{u}_m\right)\right\}_{\vec{x}=\vec{Y}_k}$$

Leading to

$$\vec{u}_k=\sum_{\substack{m=1\\ m\neq k}}^{N_p}\vec{u}_s\left(\vec{Y}_k-\vec{Y}_m;a_m,\vec{V}_m-\vec{U}(\vec{Y}_m,t)-\vec{u}_m\right),\qquad \text{for}\qquad k=1,2,3,\ldots,N_p$$

A large linear system of $3N_p$ DOF solved by Gauss-Seidel

or block Gauss Seidel

The drag force acting on the droplet k is $\vec{\mathrm{D}}_{\mathrm{k}}=-6\pi\mu a_k\left[\vec{V}_k-\vec{U}(\vec{Y}_k,t)-\vec{u}_k\right]$.

The hybrid DNS approach: disturbance flows due to droplets

$$\vec{U}(\vec{x},t) + \sum_{k=1}^{N_p} \vec{u}_s\left(\vec{r}_k; a_k, \vec{V}_k - \vec{U}(\vec{Y}_k,t) - \vec{u}_k\right)$$

Background turbulent flow

Disturbance flows due to droplets

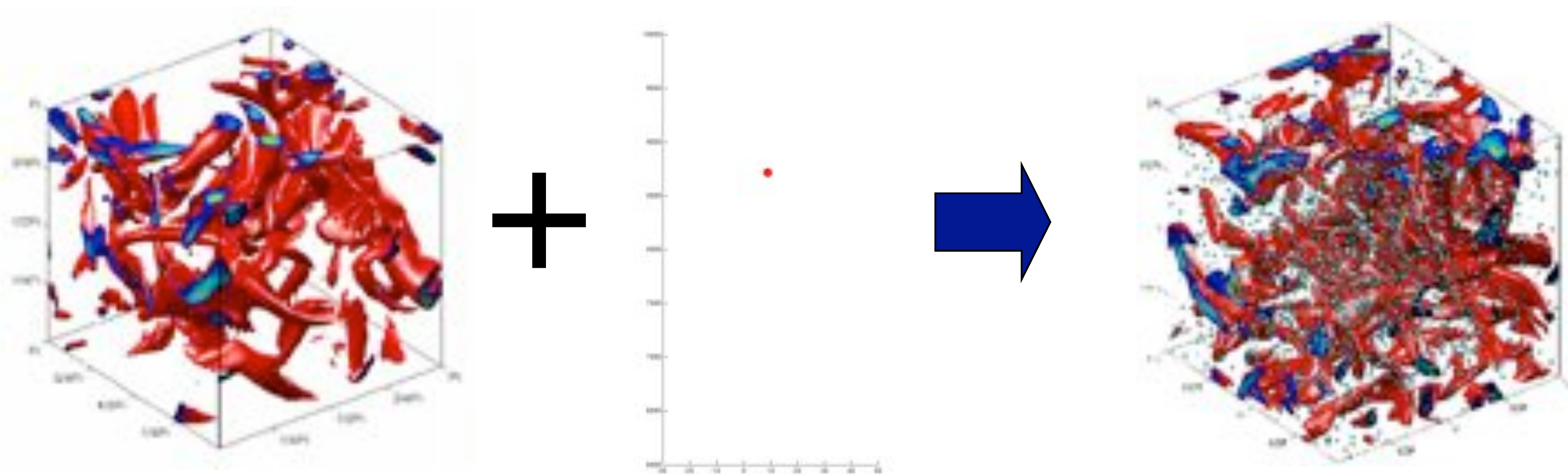

Features: Background turbulent flow can affect the disturbance flows;
No-slip condition on the surface of each droplet is satisfied on average;
Both near-field and far-field interactions are considered.

Wang, Ayala, and Grabowski, J. Atmos. Sci. 62(4): 1255-1266 (2005).
Ayala, Wang, and Grabowski, J. Comp. Phys, 225, 51-73 (2007).

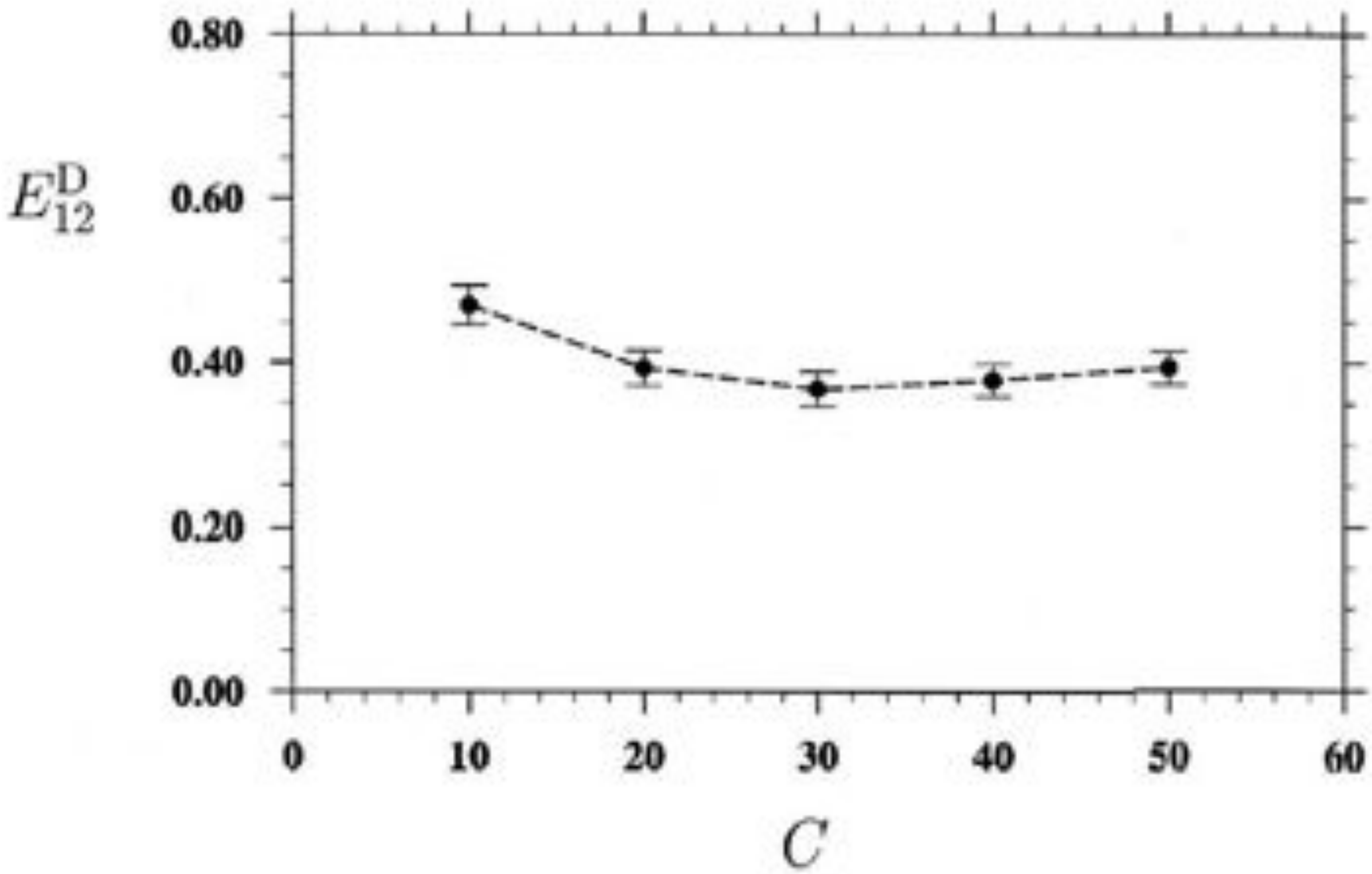

FIG. 4. Sensitivity of the computed dynamic collision efficiency with C.

***C* is the normalized truncation radius**

How to define collision efficiency in a turbulent flow?

$$E_{12}^{g} = \frac{y_c^2}{R^2}$$

$$E_{12}^{D} = \frac{\Gamma_{12}^{D}(\mathrm{AI})}{\Gamma_{12}^{D}(\mathrm{NO\ \ AI})}$$

Geometric collision

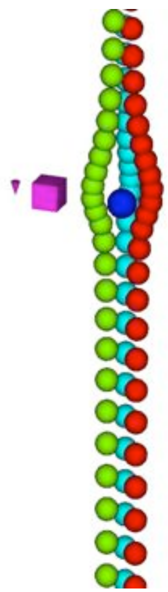

No air turbulence

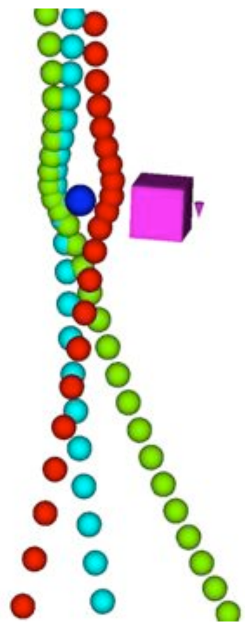

With air turbulence

$$E_{12}^{K} = \frac{\Gamma_{12}^{K}(\mathrm{AI})}{\Gamma_{12}^{K}(\mathrm{NO\ \ AI})} = \frac{\langle |w_r| \rangle_{12}(\mathrm{AI})}{\langle |w_r| \rangle_{12}(\mathrm{NO\ \ AI})} \times \frac{g_{12}(\mathrm{AI})}{g_{12}(\mathrm{NO\ \ AI})}$$

Geometric collision

Enhancement factors by air turbulence

$$\eta \equiv \frac{\Gamma_{12}(\mathrm{AI})}{\Gamma_{12}^{g}(\mathrm{AI})} = \frac{\Gamma_{12}(\mathrm{No\ \ AI}) \times E}{\Gamma_{12}^{g}(\mathrm{No\ \ AI}) \times E^{g}} = \frac{\Gamma_{12}(\mathrm{No\ \ AI})}{\Gamma_{12}^{g}(\mathrm{No\ \ AI})} \times \frac{E}{E^{g}} = \eta_G \times \eta_E$$

Total enhancement factor

Enhancement factor on geometric collision

Enhancement factor on collision efficiency

Data on enhancement factors are compiled in

Wang et al., New J. Phys. 10 (2008) 075013.

Typical enhancement factors by air turbulence

TABLE II. A case study: $a_1 = 25\ \mu m$, $a_2 = 20\ \mu m$, $R_\lambda = 40$

$\epsilon\ (cm^2/s^3)$		No HI	HI	E	$\eta/\eta_G/\eta_E$
0	$\Gamma_{12}^{D}/\Gamma_{12}^{g}$	1.000 ± 0.026	0.257 ± 0.012	0.257	
	$\Gamma_{12}^{K}/\Gamma_{12}^{g}$	1.026 ± 0.046	0.286 ± 0.023	0.279	
	$<\lvert w_r\rvert>^{K}/\Delta W$	0.516 ± 0.013	0.132 ± 0.005		
	g_{12}^{K}	0.99 ± 0.04	1.08 ± 0.04		
100	$\Gamma_{12}^{D}/\Gamma_{12}^{g}$	1.117 ± 0.032	0.315 ± 0.016	0.282	1.23/1.12/1.10
	$\Gamma_{12}^{K}/\Gamma_{12}^{g}$	1.180 ± 0.130	0.302 ± 0.048	0.256	
	$<\lvert w_r\rvert>^{K}/\Delta W$	0.533 ± 0.020	0.129 ± 0.011		
	g_{12}^{K}	1.11 ± 0.08	1.17 ± 0.09		
400	$\Gamma_{12}^{D}/\Gamma_{12}^{g}$	1.420 ± 0.032	0.584 ± 0.021	0.411	2.27/1.42/1.60
	$\Gamma_{12}^{K}/\Gamma_{12}^{g}$	1.544 ± 0.109	0.656 ± 0.052	0.425	
	$<\lvert w_r\rvert>^{K}/\Delta W$	0.561 ± 0.015	0.218 ± 0.007		
	g_{12}^{K}	1.38 ± 0.06	1.50 ± 0.07		

Wang, *et al.* J. Atmos. Sci. 62: 2433-2450 (2005).

Enhancement factors (Turbulent kernel / gravitational kernel)

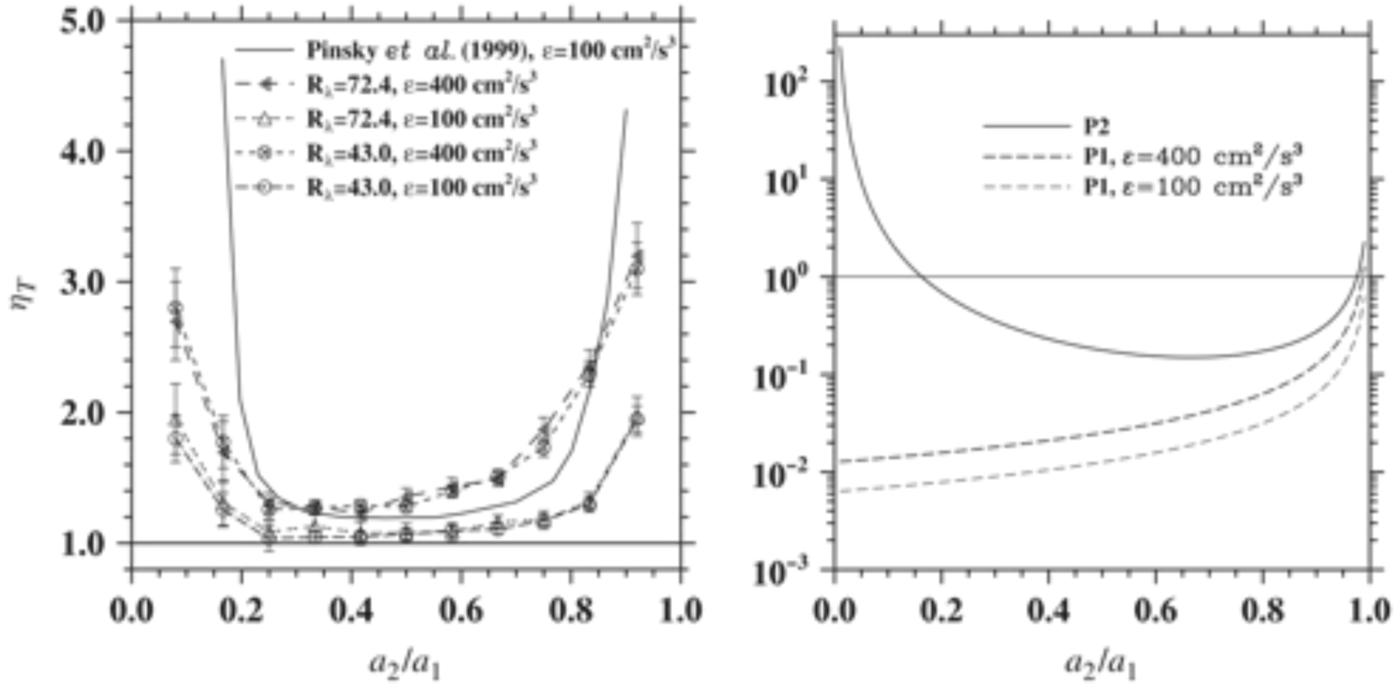

$a_1 = 30\ \mu\text{m}$

Turbulent fluctuation $R(v_k/\eta) \sim (v_{p1} - v_{p2})$

Aerodynamic interaction time $\dfrac{R}{(v_{p1} - v_{p2})} \sim \tau_{p2}$

$$P_1 = \frac{R(v_k/\eta)}{\mathrm{v}_{p1} - \mathrm{v}_{p2}}$$

$$P_2 = \frac{R}{\left(\mathrm{v}_{p1} - \mathrm{v}_{p2}\right)\tau_{p2}}$$

Clustering: $\tau_p \sim \tau_K$ and $\tau_{p1} \sim \tau_{p2}$

Eddy – particle interaction: $\tau_p \sim \dfrac{\Gamma_{vort}}{W_p^2} \sim \dfrac{\nu}{\left(\tau_p g\right)^2}$

Wang & Grabowski, *Atmos. Sci. Let.*, 10: 1-8 (2009).

Turbulent kernel / Hall kernel (with turbulent collision efficiency)

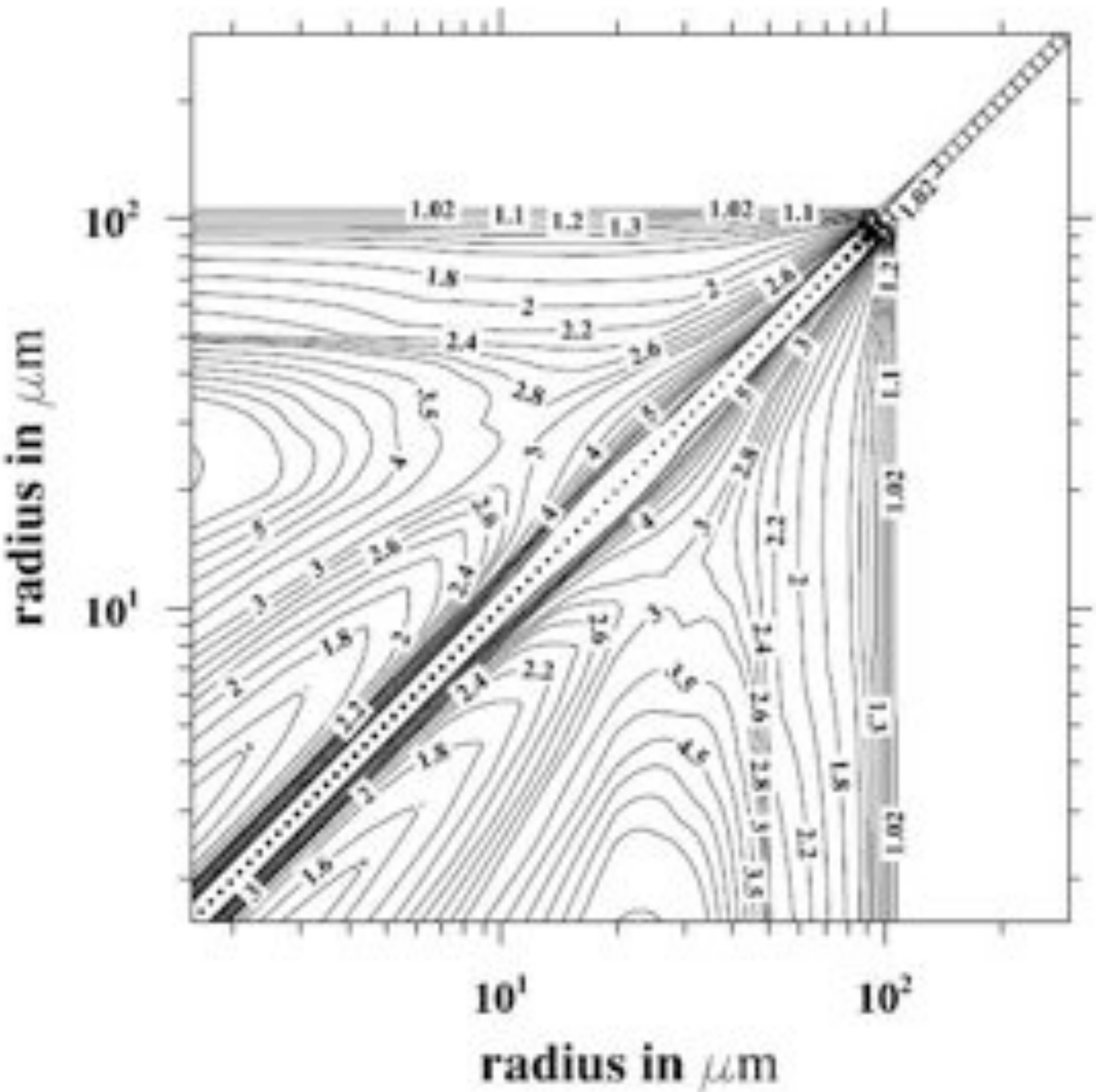

The overall enhancement factor of collection kernel by air turbulence.

Flow dissipation rate is 300 cm^2/s^3; r.m.s. velocity 202 cm/s.

Wang, *et al.,* Turbulent collision efficiency of heavy particles relevant to cloud droplets. *New J. Physics*, 10, 075013 (2008).

Summary: Observations from direct numerical simulations

Droplet settling velocity

- ✧ Significant enhancement around a=20 μm as predicted by $\frac{\tau_p W_p^2}{\Gamma_{vort}} = \frac{\tau_p^3 g^2}{\nu} \sim 1$
- ✧ Depend on scale separation or flow Reynolds number
- ✧ Need to parameterize and include in turbulent collision kernel

Geometric collision kernel

- ✧ Both turbulent fluctuations and clustering moderately enhance the kernel
- ✧ Rapid concentration decorrelation and sedimentation reduce the effect of clustering on collision between unequal size droplets
- ✧ Turbulence causes collision between nearly equal size droplets
- ✧ A first parameterization has been developed, much remains to be done.

Turbulent collision efficiency

- ✧ A hybrid simulation method has been developed
- ✧ Enhancement for droplets of nearly equal size or very different sizes

All increase with flow dissipation rate and Reynolds number

UNIVERSITY OF DELAWARE

Numerical studies of turbulent collision of cloud particles. Part 2.

Lian-Ping Wang

Department of Mechanical Engineering
University of Delaware
lwang@udel.edu

International School on
Fluctuations and turbulence in the microphysics and dynamics of clouds
Porquerolles, France, September 2-10, 2010

Acknowledgments:
Dr. Wojtek Grabowski (NCAR)
Dr. Y. Zhou, Dr. O. Ayala, Dr. Y. Xue, Dr. B. Rosa, Mr. H. Gao, Mr. H. Parashani, ……
U.S. National Science Foundation**,** U.S. National Center for Atmospheric Research

Outline

❖ The application: collision-coalescence of cloud droplets

❖ Simulation of small-scale air turbulence

❖ Point-particle based simulation

Geometric collision

Parameterization of turbulent collision kernel

❖ Hybrid direct numerical simulation

Collision efficiency

❖ Impact on warm rain initiation time

❖ High-resolution simulations

The effect of flow Reynolds number

❖ Particle-resolved simulation: some next-level dreams

❖ Summary

Impact of turbulent collection kernel on warm rain initiation

Does turbulent collision kernel make a difference, when compared to the gravitational base kernel?

How to solve the Smoluchowski kinetic collection equation accurately?

Kinetic collection equation

$$\frac{\partial n(x,t)}{\partial t} = \frac{1}{2}\int_{x_0}^{x-x_0} n(x-y,t)n(y,t)K(x-y,y)dy - n(x,t)\int_{x_0}^{\infty} n(y,t)K(x,y)dy$$

x_0 is the mass of the smallest droplet in the system.
n(x,t) is continuous number density distribution
K(x,y) is the collection kernel, a non-negative, symmetric function of x and y

Initial distribution

$$n(x,t=0) = A\frac{L_0}{\bar{x}_0^2}\exp\left[-\left(\frac{Bx}{\bar{x}_0}\right)^{\alpha}\right]$$

Numerical method: Bin Integral Method with Gauss Quadrature
Converged solution without numerical diffusion/dispersion errors

Numerical Solutions to KCE

- Difficulties:
  - Highly nonlinear integral differential equation
  - Collection kernel varies by many orders of magnitude
  - The magnitude of size distribution also varies by several orders of magnitude, along with a large range of sizes
- Challenge: to obtain an accurate numerical solution with a small number of discrete size bins

Bin moments definition

$$m_0(t;i) \equiv N(t;i) = \int_{x_i}^{x_{i+1}} n(x,t;i)dx$$

$$m_1(t;i) \equiv L(t;i) = \int_{x_i}^{x_{i+1}} xn(x,t;i)dx$$

Realizability condition

$$n(x,t;i) \geq 0 \qquad x_i \leq \frac{m_1(t;i)}{m_0(t;i)} \leq x_{i+1}$$

Kinetic Spectral moments equation (KSME)

$$\frac{\partial m_k(t;i)}{\partial t} = \int_{x_i}^{x_{i+1}} x^k dx \int_{x_0}^{x/2} n(x-y,t)K(x-y,y)n(y,t)dy - \int_{x_i}^{x_{i+1}} x^k n(x,t)dx \int_{x_0}^{\infty} K(x,y)n(y,t)dy$$

The concept of the closure problem

Bin integral method with Gauss Quadrature (BIMGQ)

bin-based pair-interactions for the source bins

$$\Delta\tilde{n}(i) = \Delta\tilde{n}(j) = -dt\int_{x_{1,i}}^{x_{2,i}} dx \int_{x_{1,j}}^{x_{2,j}} n(x,t;i)K(x,y)n(y,t;i)dy$$

$$\Delta\tilde{m}(i) = -dt\int_{x_{1,i}}^{x_{2,i}} dx \int_{x_{1,j}}^{x_{2,j}} xn(x,t;i)K(x,y)n(y,t;i)dy$$

$$\Delta\tilde{m}(j) = -dt\int_{x_{1,i}}^{x_{2,i}} dx \int_{x_{1,j}}^{x_{2,j}} yn(x,t;i)K(x,y)n(y,t;i)dy$$

Wang, Xue & Grabowski 2007, *J. Comp. Physics*, 226, 59-88.

BIMGQ:
3 possible Scenarios of the local distribution

$$n(x,t;i) = n_{1,i}\frac{x - x_{2,i}}{x_{1,i} - x_{2,i}} + n_{2,i}\frac{x - x_{1,i}}{x_{2,i} - x_{1,i}}$$

$$x_i \le x_{1,i} < x_{2,i} \le x_{i+1}$$

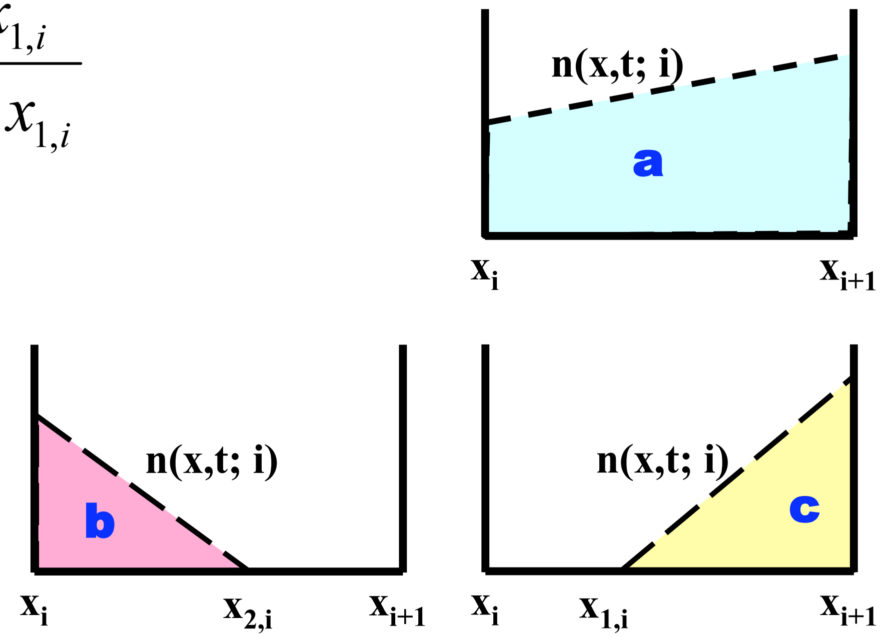

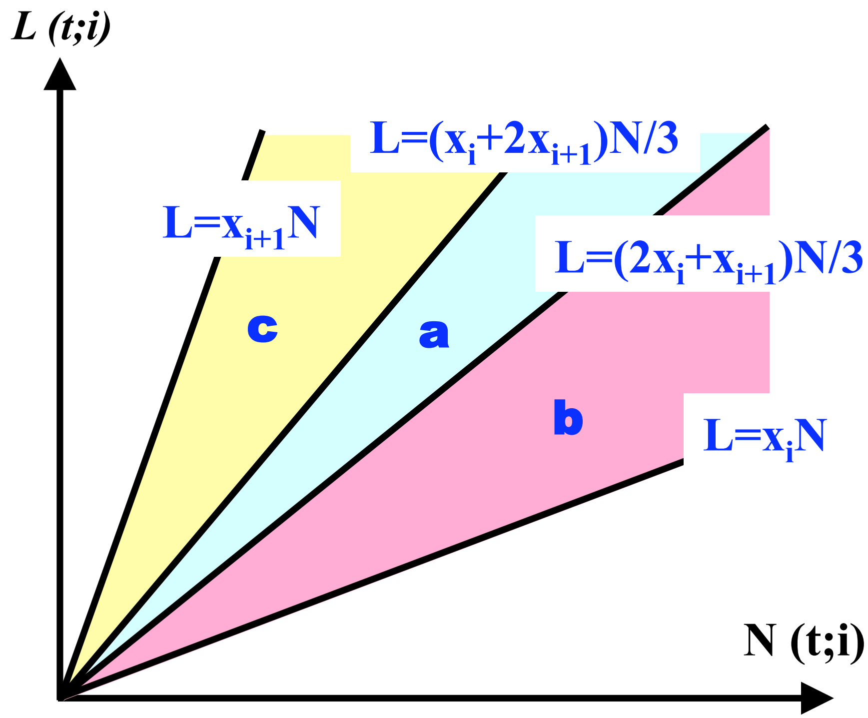

$$N(t;i) = \int_{x_{1,i}}^{x_{2,i}} n(x,t;i)dx$$

$$L(t;i) = \int_{x_{1,i}}^{x_{2,i}} xn(x,t;i)dx$$

Pair interactions for the target bins (BIMGQ)

$$\Delta\tilde{n}(k) = dt \iint_{\Omega_k} n(x,t;i)K(x,y)n(y,t;j)dxdy$$

$$\Delta\tilde{n}(k+1) = dt \iint_{\Omega_{k+1}} n(x,t;i)K(x,y)n(y,t;j)dxdy$$

$$\Delta\tilde{m}(k) = dt \iint_{\Omega_k} (x+y)n(x,t;i)K(x,y)n(y,t;j)dxdy$$

$$\Delta\tilde{m}(k+1) = dt \iint_{\Omega_{k+1}} (x+y)n(x,t;i)K(x,y)n(y,t;j)dxdy$$

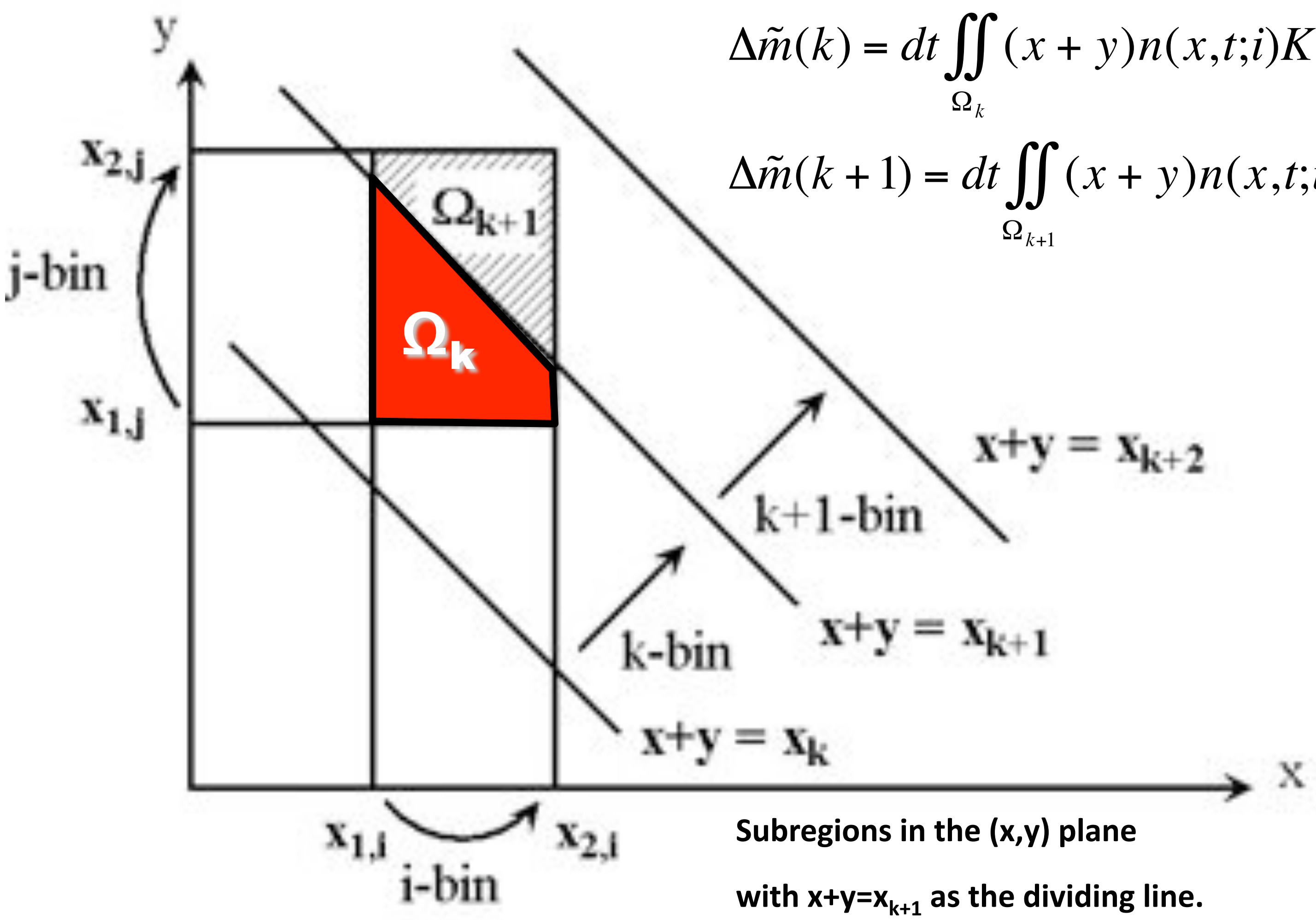

Subregions in the (x,y) plane

with $x+y=x_{k+1}$ as the dividing line.

Number and mass conservations

$$\Delta\tilde{n}(i)+\Delta\tilde{n}(j)+\Delta\tilde{n}(k)+\Delta\tilde{n}(k+1)=-dt\int dx\int dy n(x,t;i)K(x,y)n(y,t;j)$$

$$\Delta\tilde{m}(i)+\Delta\tilde{m}(j)+\Delta\tilde{m}(k)+\Delta\tilde{m}(k+1)=0$$

Orders of polynomial and number of Gauss quadrature points required

term	Order of polynomial		m	
	x	y	x	y
$\Delta\tilde{n}(i)=\Delta\tilde{n}(j)$	2	2	2	2
$\Delta\tilde{m}(i)$	3	2	2	2
$\Delta\tilde{m}(j)$	2	3	2	2
$\Delta\tilde{n}(k+1)$	5	2	3	2
$\Delta\tilde{m}(k+1)$	6	3	4	2
$\Delta\tilde{n}(k)$	5	2	3	2
$\Delta\tilde{m}(k)$	6	3	4	2

$$\Delta\tilde{n}(i)=\Delta\tilde{n}(j)=-dt\int_{x_{1,i}}^{x_{2,i}}dx\int_{x_{1,j}}^{x_{2,j}}n(x,t;i)K(x,y)n(y,t;i)dy$$

Basic steps of BIMGQ

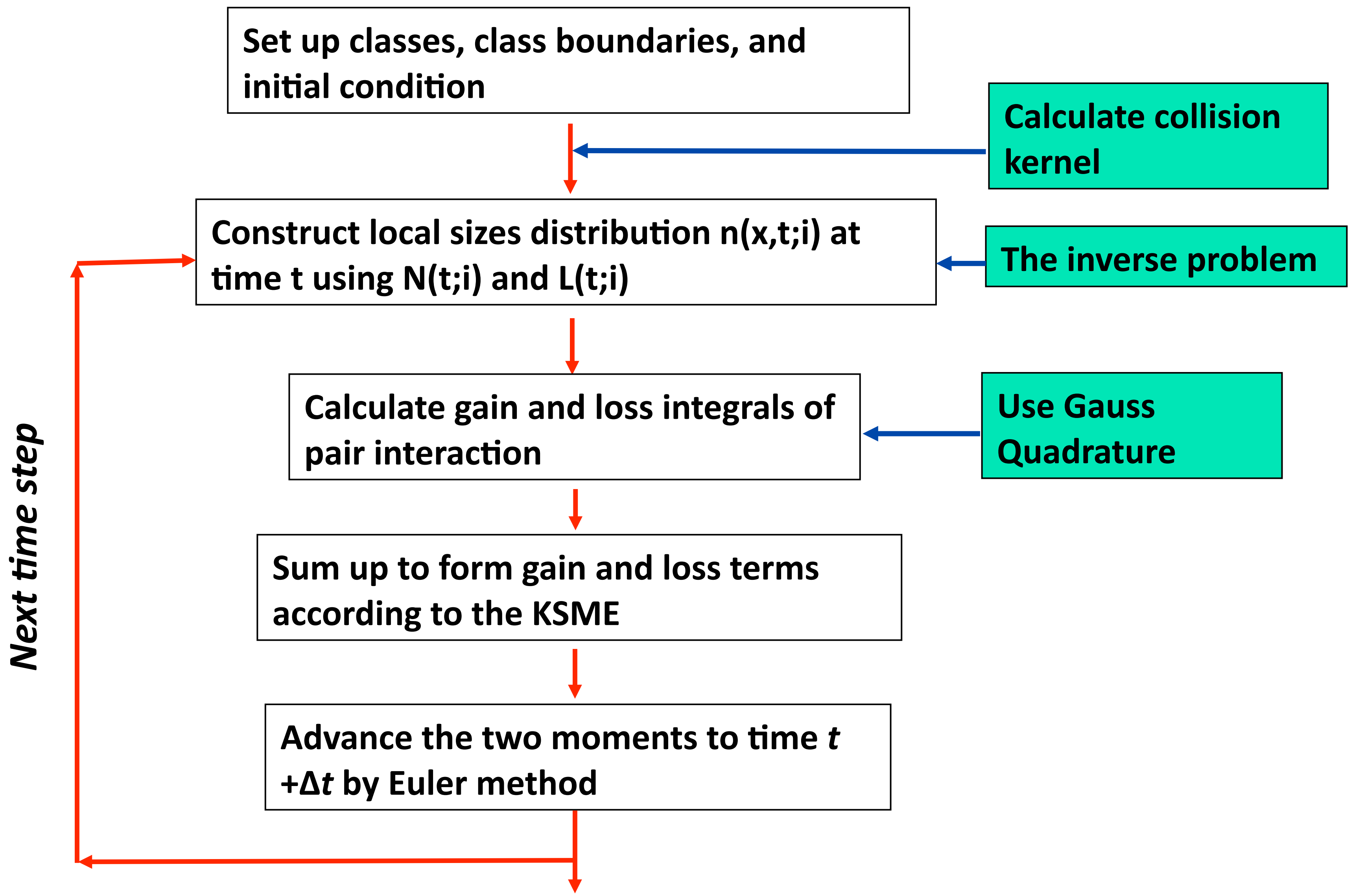

The base kernel: gravitational collision-coalescence

The base case studied by many:

$$K_{12}^{g} = \underbrace{\pi R^2 \left| W_1 - W_2 \right|}_{\text{Swept volume}} \, E_{12}^{g}$$

with $R = a_1 + a_2$

Collision efficiency

Model for terminal velocity: Beard (1976)

Empirical formula for E_{12}: Long (1974)
Tabulated data of E_{12}: Hall (1980)

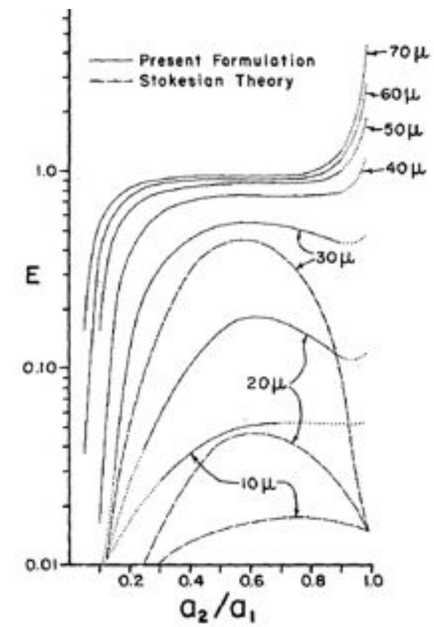

Klett and Davis (1973)

How to formulate collision kernel in a turbulent flow?
How to quantify / parameterize the turbulent collision kernel?

Growth of cloud droplets by gravitational collision-coalescence

Linear-Log

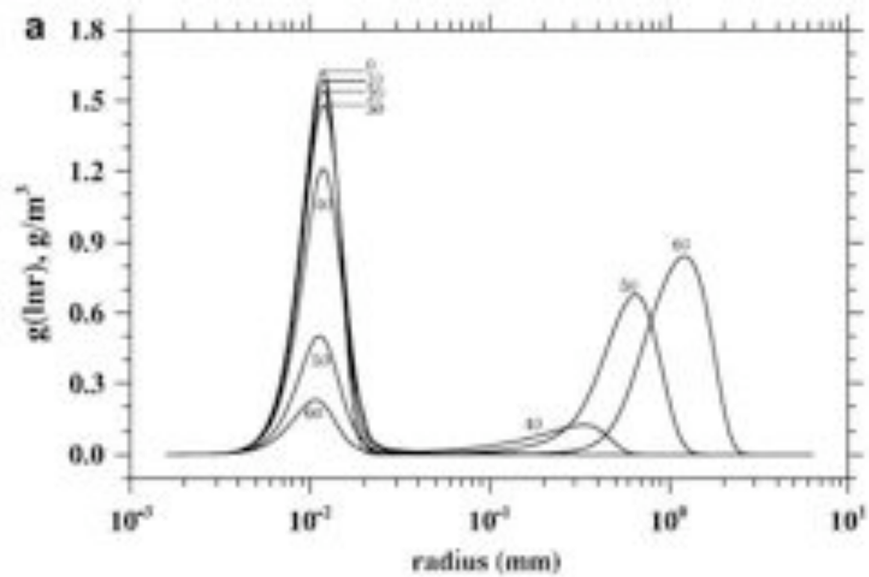

Log-Log

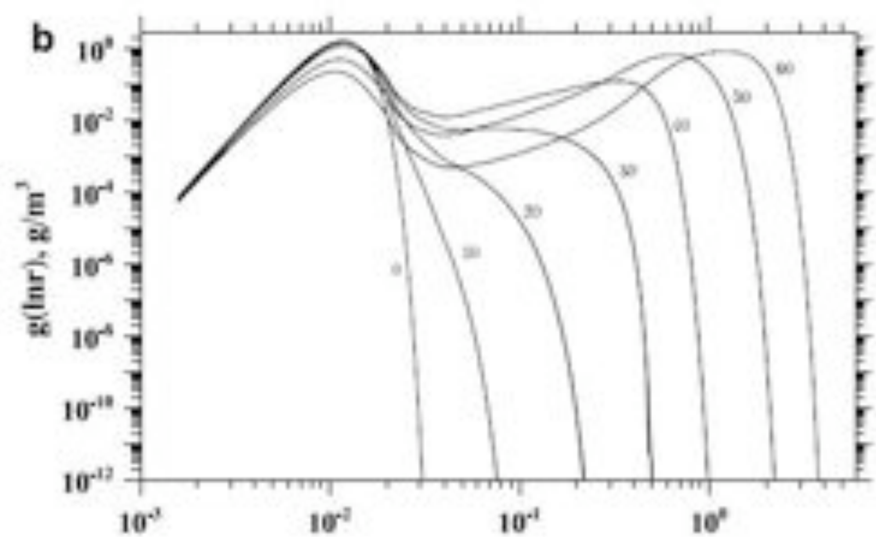

1. Autoconversion; 2. Accrection; 3. Hydrometeor self-collection (Berry and Reinhardt, 1974)

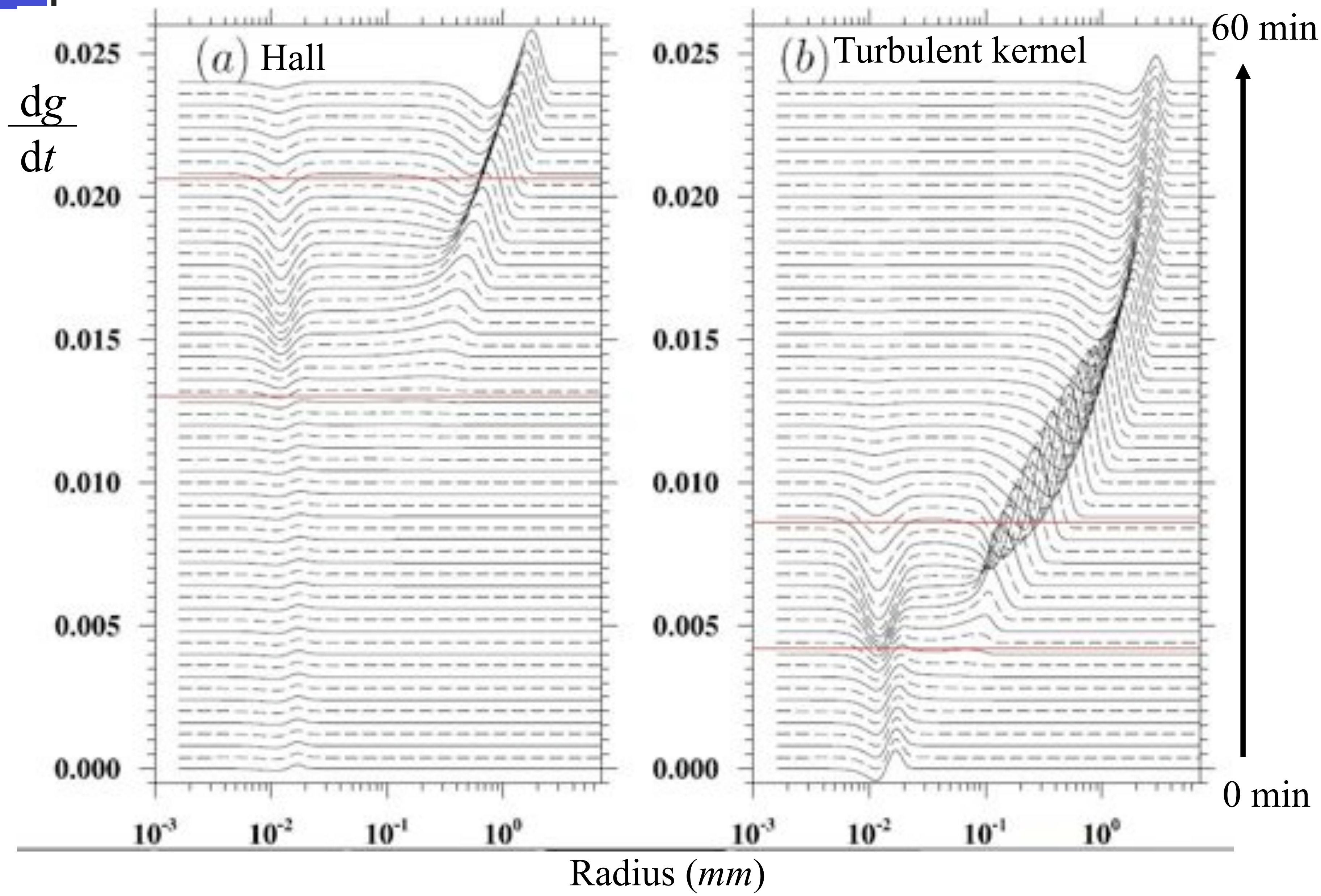

Method to identify the three phases

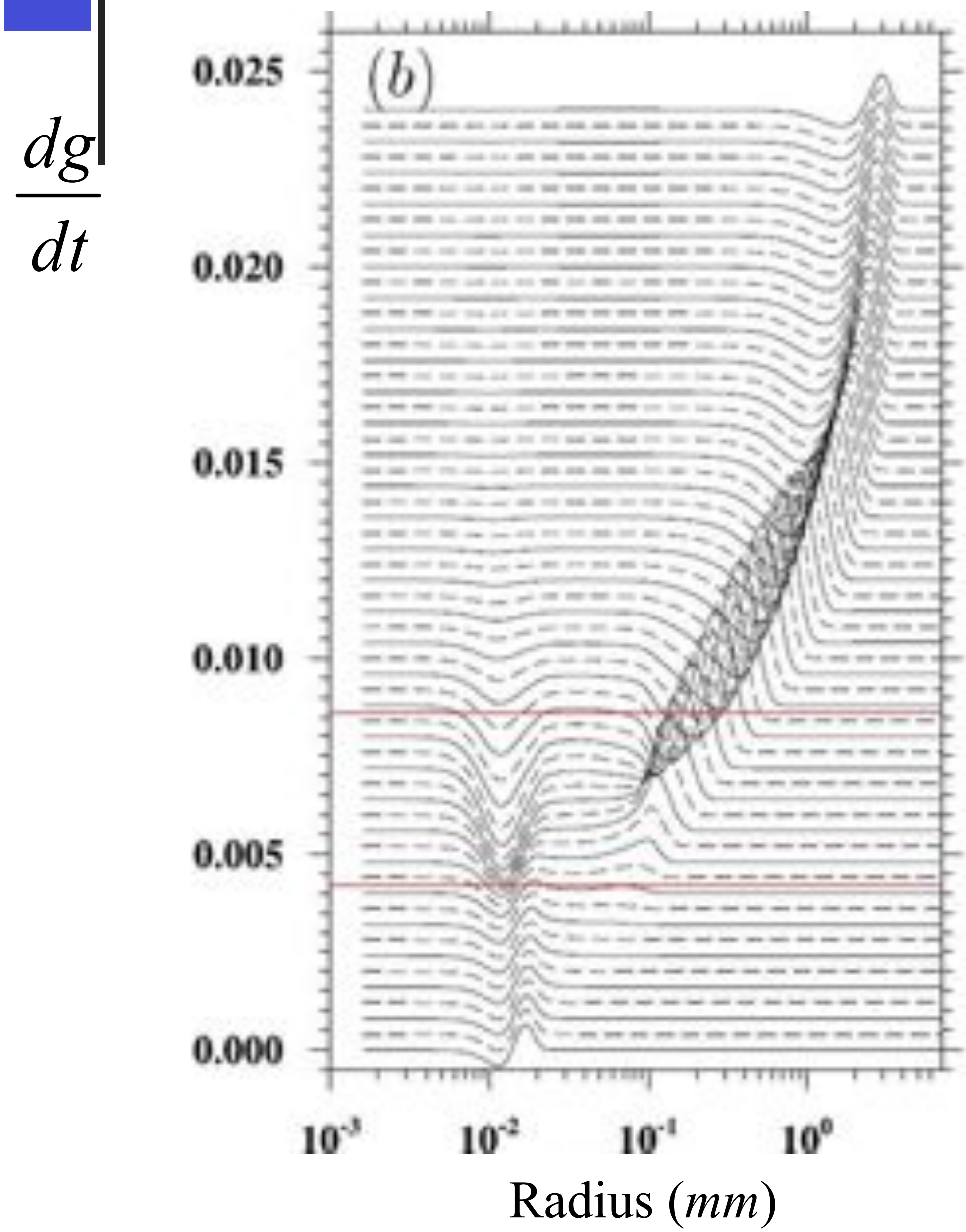

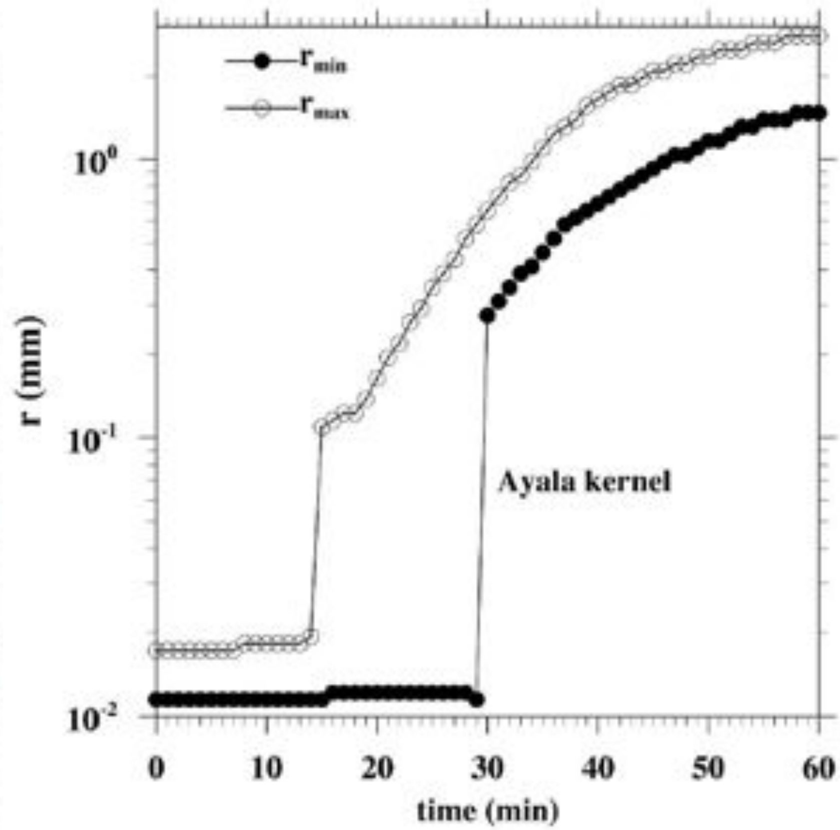

Time before rapid growth of droplets

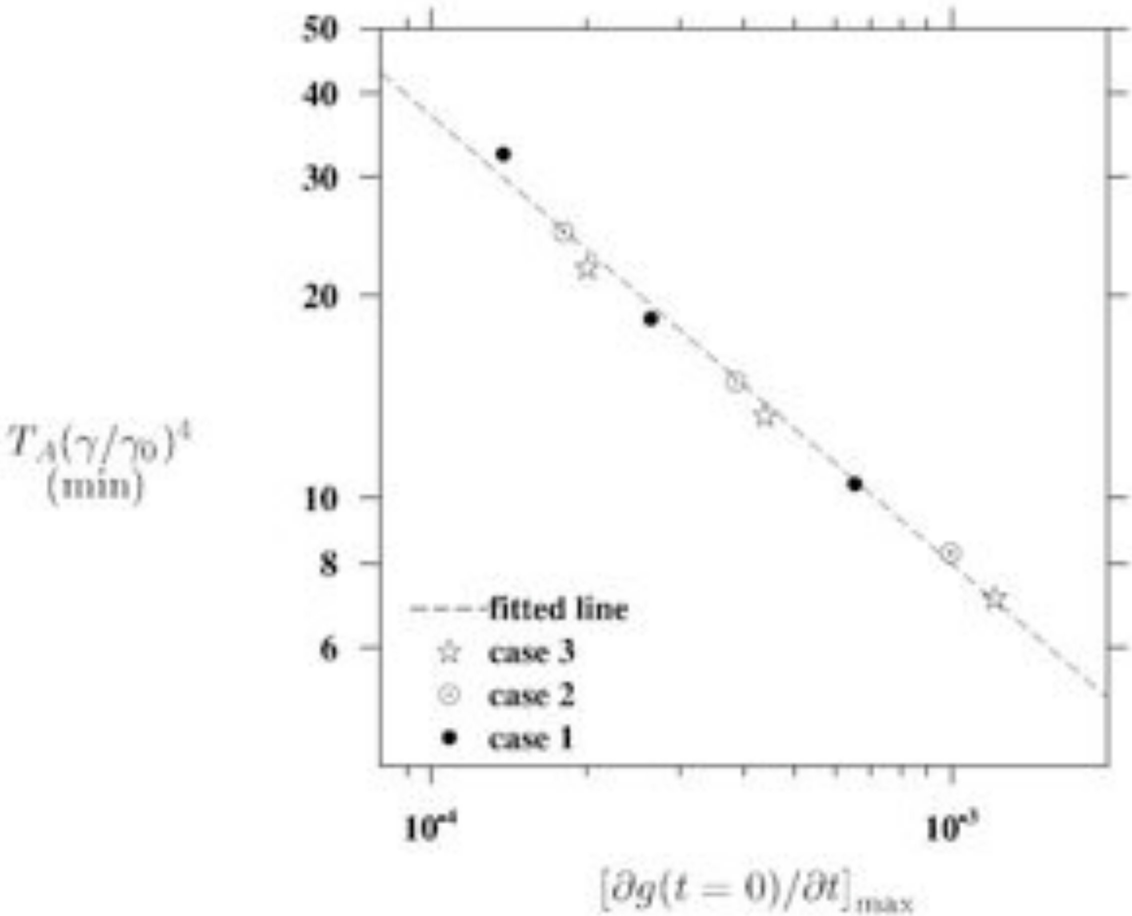

$$T_A \approx 0.08 \times \left(\frac{\partial g(\ln r, t=0)}{\partial t}\right)_{max}^{-2/3} \times \left(\frac{\gamma}{\gamma_0}\right)^{-4}$$

Wang and Grabowski 2009, Atmos. Sci. Letters, 10: 1-8.

Dependence of growth time on ε, u'

For Ayala kernel

ε cm^2/s^3	u' cm/s	t_1 s	t_2 s	Δt_1 %	Δt_2 %
100	100	1949	1972	20.4	20.3
	150	1832	1855	25.2	25.0
	202	1738	1761	29.0	28.8
200	100	1816	1837	25.8	25.7
	150	1685	1707	31.2	31.0
	202	1584	1605	35.3	35.1
300	100	1736	1757	29.1	28.9
	150	1602	1623	34.6	34.4
	202	1498	1519	38.8	38.6
400	100	1681	1702	31.3	31.2
	150	1547	1568	36.8	36.6
	202	1443	1464	41.1	40.8
With turbulent collision efficiency: 400	202	1230	1250	49.8	49.4

Reduction relative to the Hall kernel

Xue, Wang & Grabowski 2007, *J. Atmos. Sci,* 65: 331-356.
Wang & Grabowski 2009, *Atmos. Sci. Let.*, 10: 1-8.

Impact study using a parcel model

Conservation of the moist static energy and total water in a rising adiabatic parcel

$\phi^{(i)}dr$ droplet concentration in a bin

T parcel temperature

P parcel pressure

q_v water vapor mixing ratio

w rising velocity (prescribed)

$$C_p \frac{dT}{dt} = -gw + LC$$

$$\frac{dq_v}{dt} = -C$$

$$\frac{dp}{dt} = -\rho_0 wg$$

$$\frac{\partial \phi^{(i)}}{\partial t} = \left(\frac{\partial \phi^{(i)}}{\partial t}\right)_{activation} + \left(\frac{\partial \phi^{(i)}}{\partial t}\right)_{condensation} + \left(\frac{\partial \phi^{(i)}}{\partial t}\right)_{coalescence}$$

supplemented with an activation model

$$N_{CCN} = C_0 (100S)^k$$

The speed up factor by air turbulence

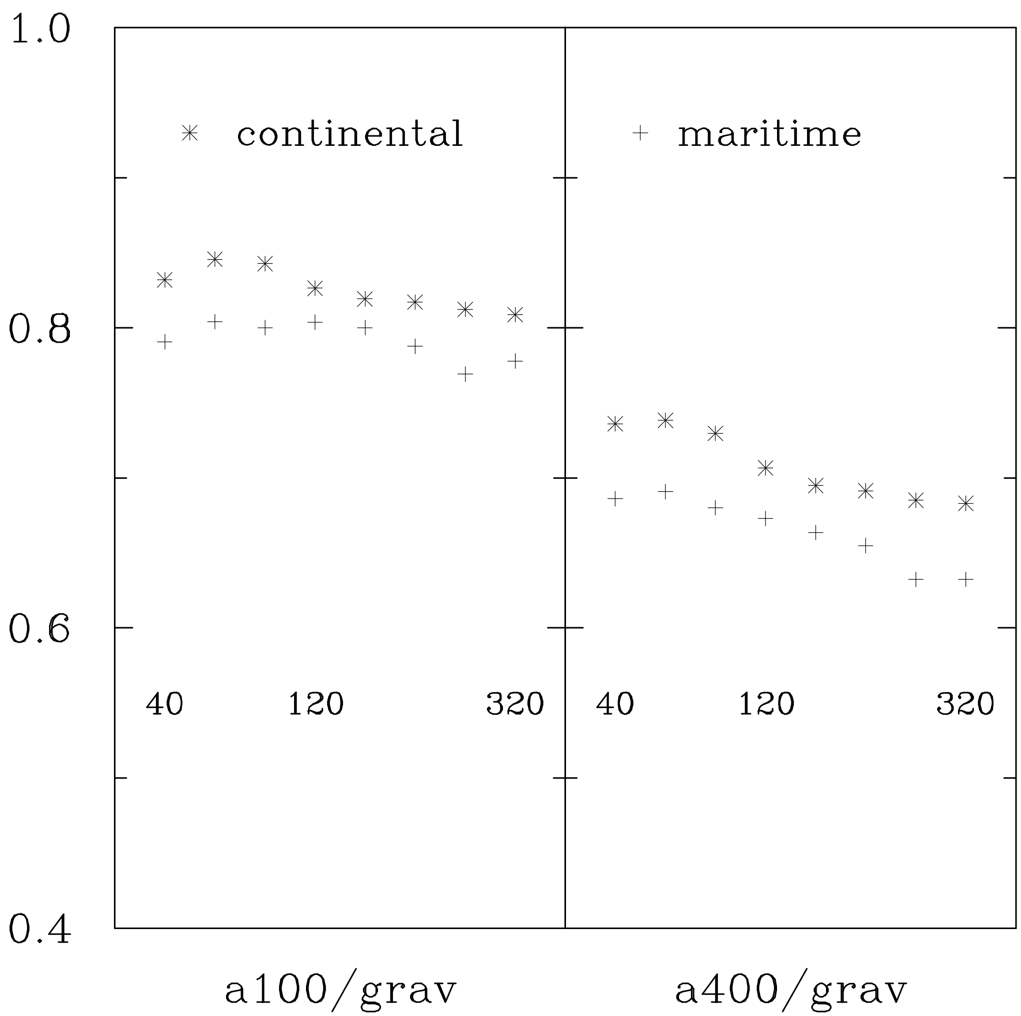

Parcel rising velocity
w=1 m/s

Grabowski & Wang 2008, Diffusional and accretional growth of water drops in a rising adiabatic parcel: effects of turbulent collision kernel, *Atmos. Chem. Phys.*, 9, 2335–2353.

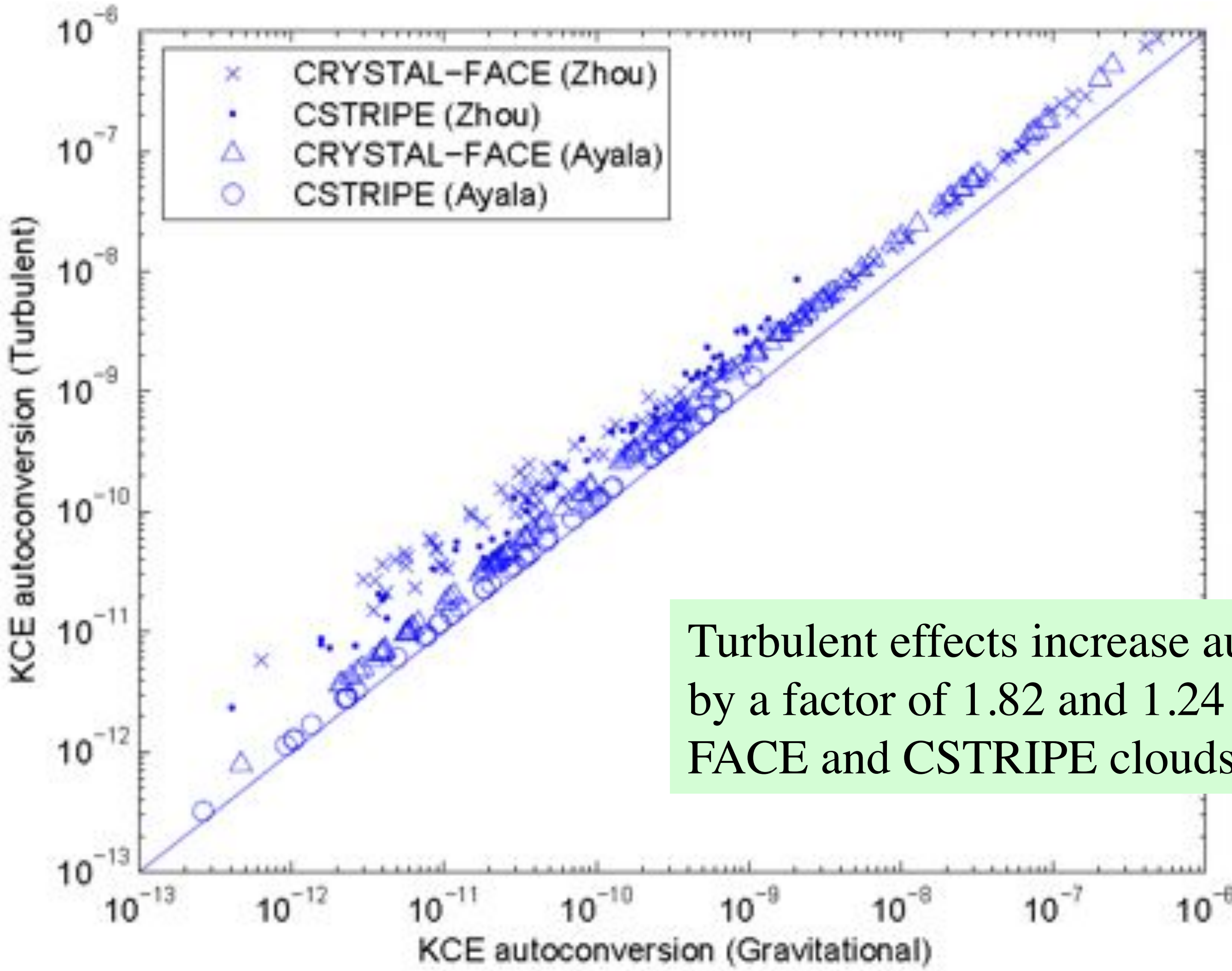

Turbulent effects increase autoconversion by a factor of 1.82 and 1.24 for CRYSTAL-FACE and CSTRIPE clouds.

W. C. Hsieh et al., 2009, On the representation of droplet coalescence and autoconversion: Evaluation using ambient cloud droplet size distributions. J. Geophysical Res., 114, D07201.

Summary

An accurate numerical integration method for KCE has been developed

- Combining the advantages of several previous methods
- Converged solutions for realistic kernels have been demonstrated

Numerical solutions of KCE alone show that

- Air turbulence can reduce the rain initiation time by as much as 50%.
- Turbulence has the strongest impact on the growth phase by autoconversion

A parcel model is also used to test our turbulent collision kernel

- Air turbulent reduces the rain initiation time by 15% –25% and 25% –40% for the energy dissipation rates of 100 and 400 cm^2/s^3, respectively.

Using measured droplet size distribution, it is shown that turbulent effects increase autoconversion by a factor of 1.82 and 1.24 for CRYSTAL-FACE and CSTRIPE clouds.

High-resolution simulation

The effect of flow Reynolds number?

Implications of increasing DNS grid resolutions

	N	R_λ	Re	<ε> DNS	Domain size (cm) (400 cm^2/s^3)	Domain size (cm) (100 cm^2/s^3)	u′
Published	32	23.5	40.6	3646	4.2	6.0	7.08
	64	43.3	90.6	3529	8.4	11.9	9.61
	128	74.6	212	3589	16.9	23.9	12.61
On-going	256	123.	532.	3690	34.0	48.1	16.18
	512	204.	1,373	3900	68.9	97.5	20.84
Target	1024	324.	3,806	3777	137.	193.	26.29

$$\mathrm{Re} = \frac{u' L_f}{\nu}, \qquad R_\lambda = \frac{u'\lambda}{\nu}$$

Cloud conditions

$$\mathrm{Re} = 10^6 \sim 10^8; \qquad R_\lambda = 10^3 \sim 10^4$$

$$\text{Domain size} = 2\pi\left(\frac{\nu_p}{\nu_n}\right)^{0.75}\left(\frac{\varepsilon_n}{\varepsilon_p}\right)^{0.25} = 2\pi\left(\frac{0.17}{\nu_n}\right)^{0.75}\left(\frac{\varepsilon_n}{\varepsilon_p}\right)^{0.25}$$

Droplet parameters

$$St = \frac{\tau_p}{\tau_k}, \qquad Sv = \frac{\tau_p g}{v_k}, \qquad Fr_p = \frac{\tau_p}{\Gamma_{vort}/V_p^2} = \frac{\tau_p^3 g^2}{\upsilon} = St \cdot Sv^2$$

a (µm)	St	Sv	Fr_p
10	0.0634	0.446	0.0126
20	0.254	1.78	0.808
30	0.571	4.01	9.20
40	1.015	7.14	51.7
50	1.585	11.15	197.
60	2.283	16.06	589.

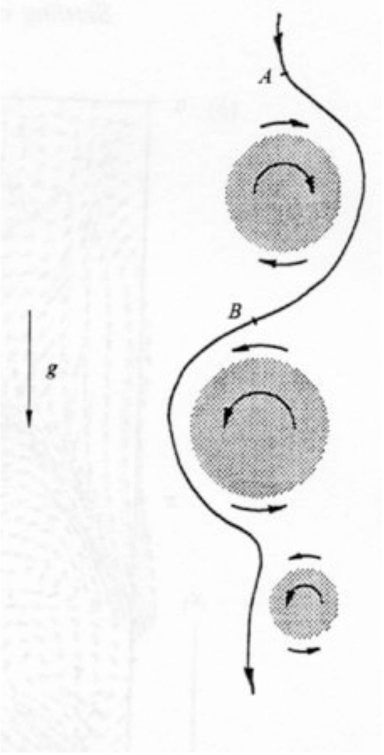

$\varepsilon = 400 \quad cm^2/s^3$ Stokes drag

Rapid increase of Stokes numbers and Sv with size.
Settling through Kolmogorov eddy very quickly: limited eddy-droplet interaction
Inertial effect is partially weakened by the crossing-trajectory effect

Droplet settling velocity: a single-particle statistics

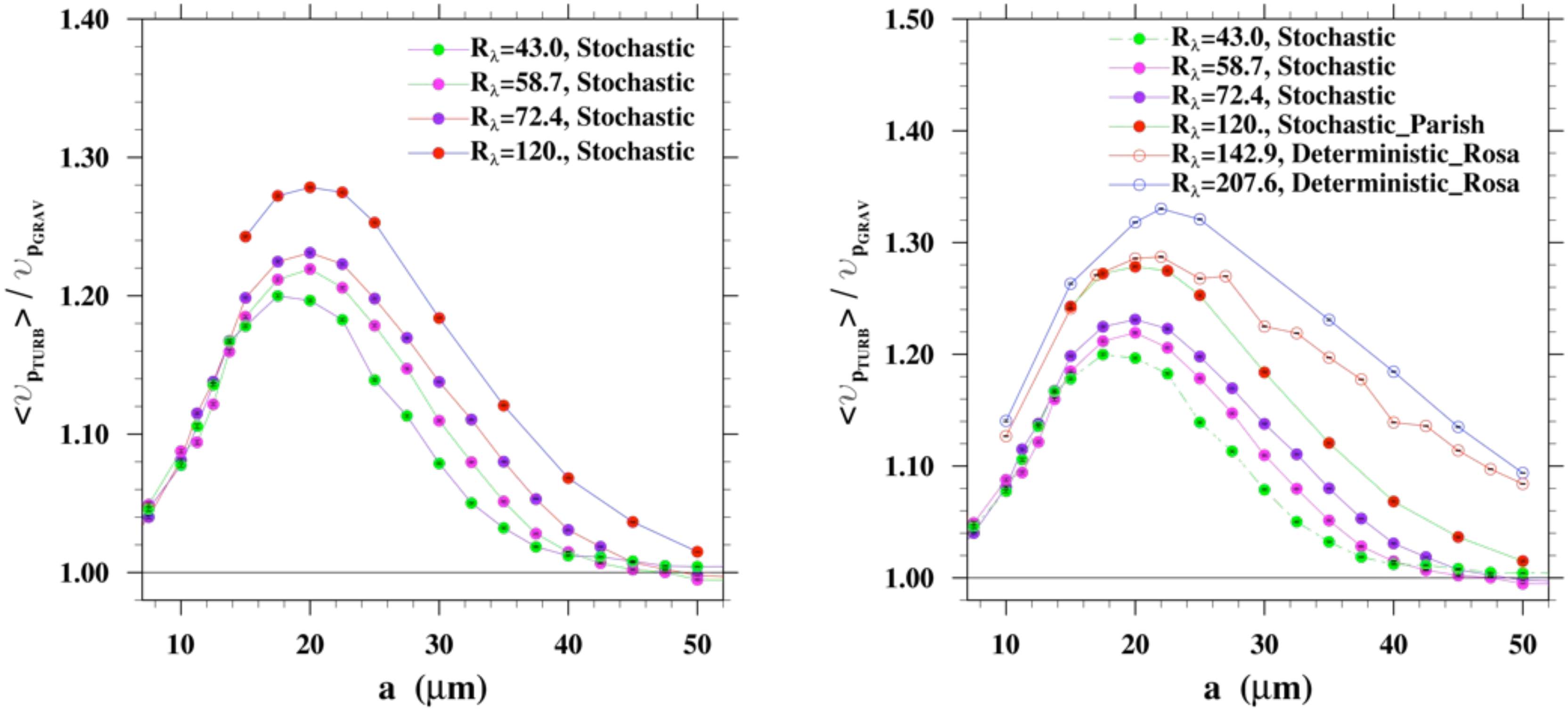

Depend on R_λ and large-scale forcing scheme

Single-particle statistics depend on the large-scale flow field

Wang & Maxey, J. Fluid Mech. 256 (1993).

Davila & Hunt, J. Fluid Mech. 440 (2001). Falkovich et al., Nature, 419 (2002).

Ayala et al., New J. Physics, 10: 075015 (2008).

Droplet r.m.s. fluctuation velocity: a single-particle statistics

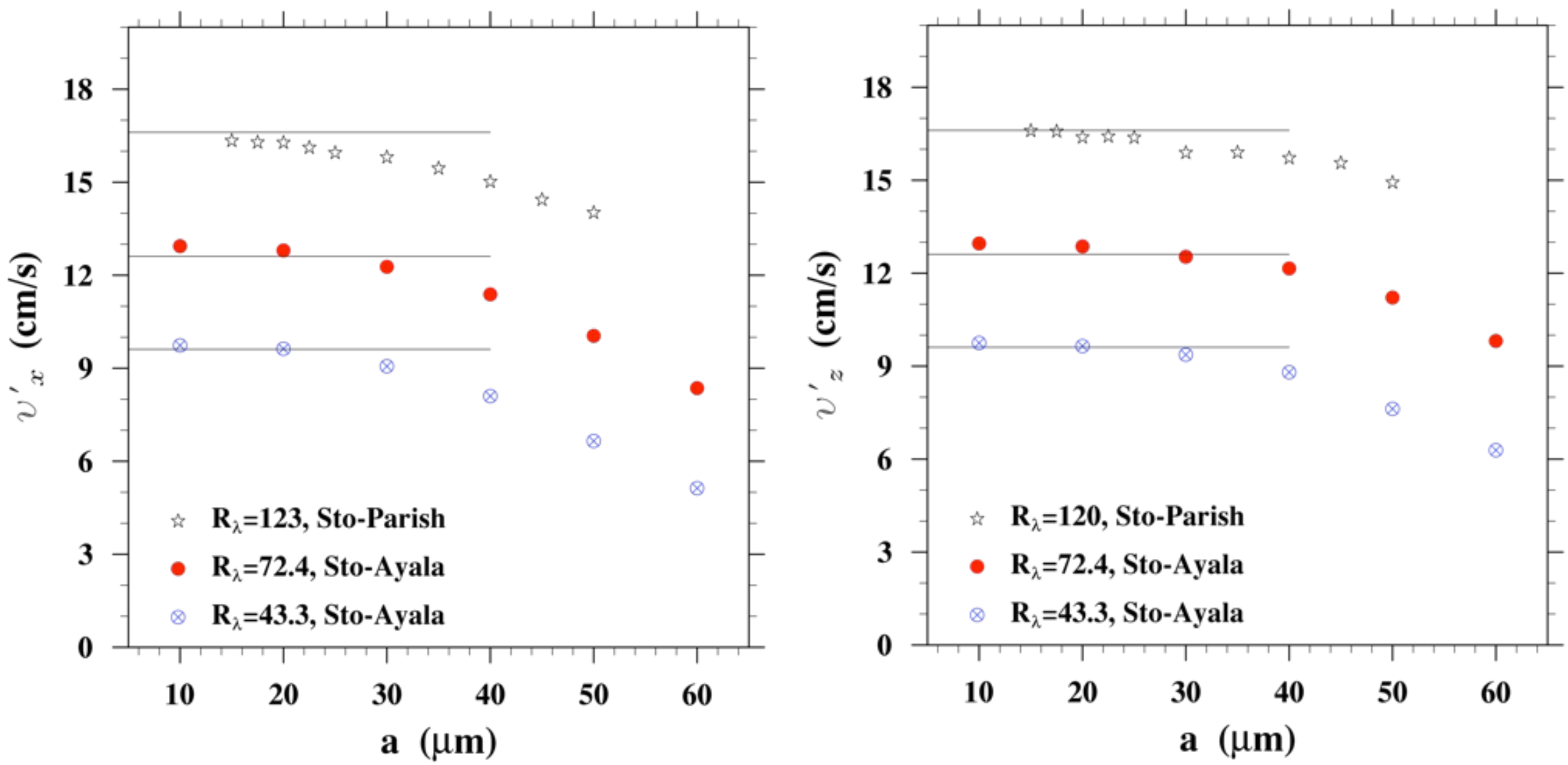

Lines mark the fluid r.m.s. fluctuation velocity *u'*

The effect of R_λ on relative velocity

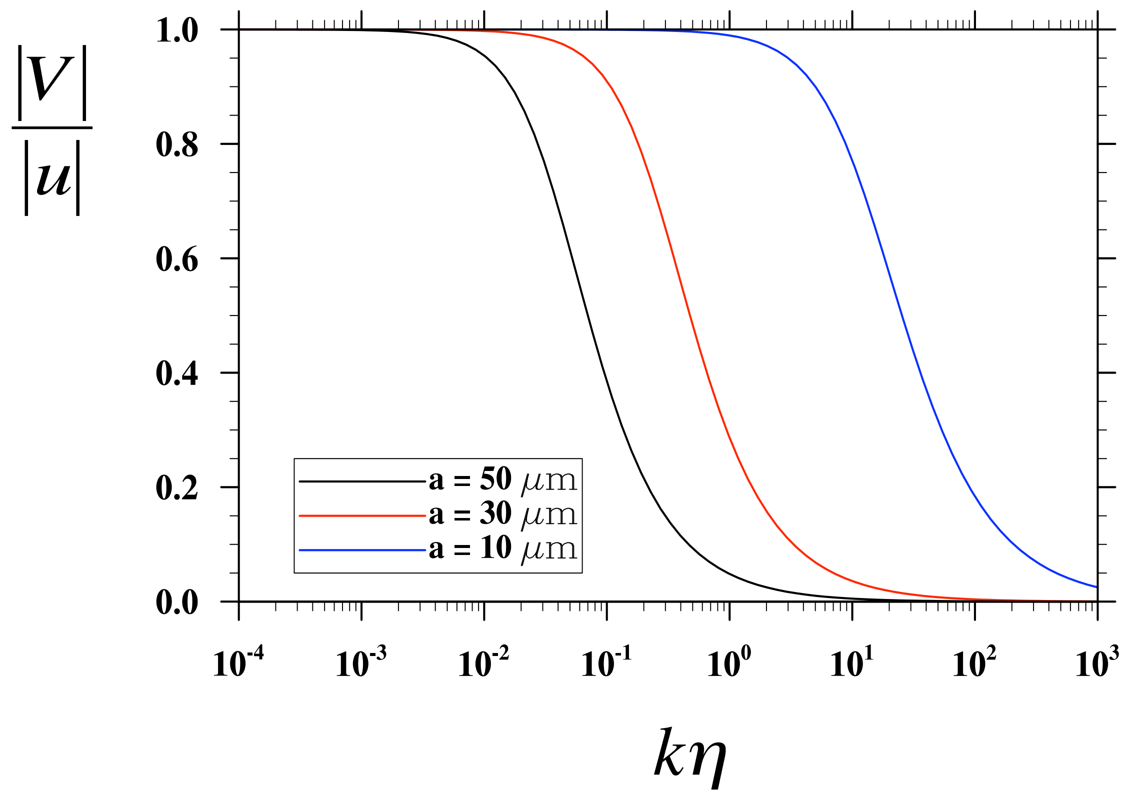

- Saturation is expected if all scales of motion of relevance are included
- Saturation should be achieved first for smaller droplet size

Radial relative velocity vs size and R_λ

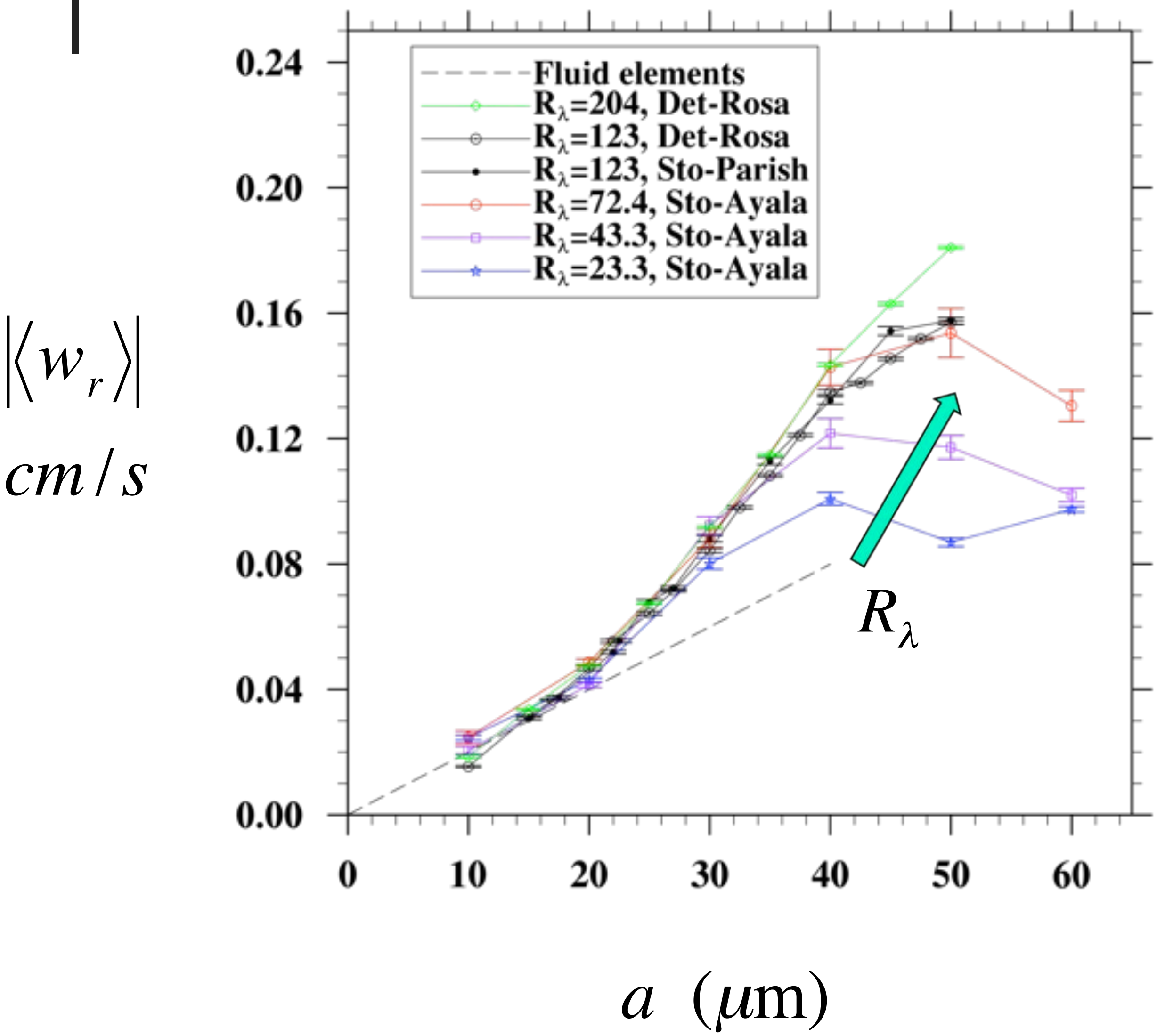

$\varepsilon = 400 \quad cm^2/s^3$

For fluid elements (e.g., ST56)

$$|\langle w_r \rangle|_0 = \sqrt{\frac{2}{15\pi}} \frac{(2a)}{\tau_k}$$

Monodisperse RDF vs droplet radius and R_λ

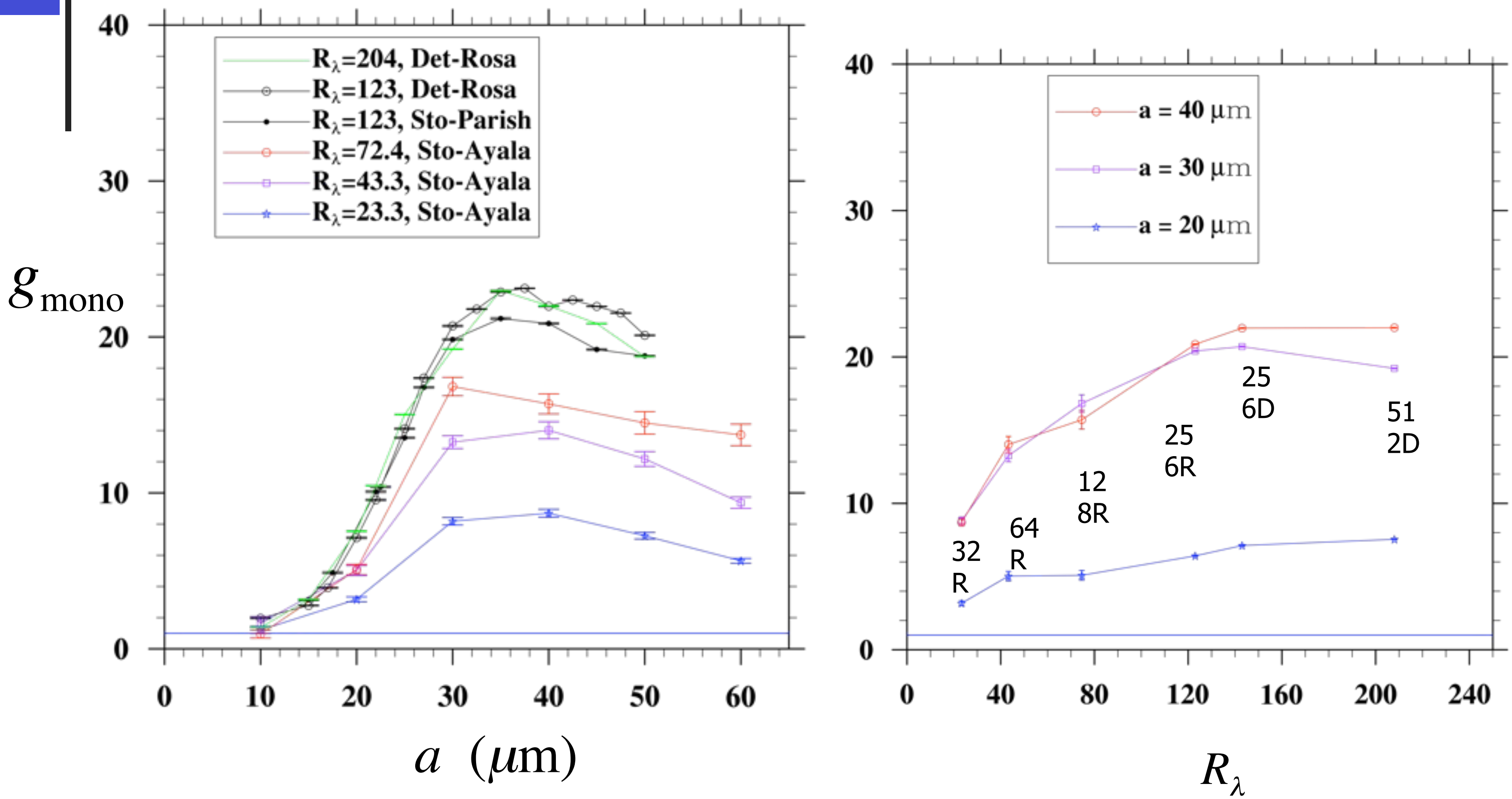

Stokes drag $\varepsilon = 400 \quad \mathrm{cm^2/s^3}$

Saturation with R_λ for sedimenting droplets when $R_\lambda > 100$.

a (μm)	St	Sv
20	0.254	1.78
30	0.571	4.01
40	1.015	7.14

The effect of R_λ on RDF: Collins and Keswani (2004)

Arguments :

- K41 : fixing ε and ν, increasing R_λ will only introduce a correction to the fluid vorticity that scales as $\left(1 - R_\lambda^2\right)$
- K62 : Dissipation intermittency increases with R_λ

$$\frac{\left\langle \varepsilon^2 \right\rangle}{\left(\left\langle \varepsilon \right\rangle\right)^2} \sim R_\lambda^{3/8} \quad \text{and} \quad St \sim \sqrt{\varepsilon}$$

$\Rightarrow$ it is possible that RDF increase indefinitely with R_λ

Simulations appear to support saturation of RDF at high Reynolds number

$57 \le R_\lambda \le 152$, forced turbulence

non - sedimenting, monodisperse, ghost particles

$$\frac{a}{\eta} \sim 0.01$$

Collins and Keswani (2004), New J. Phys. 6, 199. Their largest grid is 192^3 and R_λ is 152.

The effect of R_λ on RDF: Sedimenting particles

The more relevant particle - flow interaction time is the residence time

$$\tau_{\text{res}} \sim \frac{\Gamma}{W^2} \sim \frac{\eta\, \mathrm{v}_k}{W^2} \sim \frac{\nu}{W^2}$$

or the nondimensional ratio

$$\frac{\tau_p}{\tau_{\text{res}}} \sim \frac{\tau_p W^2}{\nu} \sim St \cdot S\mathrm{v}^2 \quad \text{independent of local dissipation rate}$$

$\Rightarrow$ There is more reason to believe satuation of RDF with R_λ.

Dynamic geometric collision kernel: 30 μm – 30 μm

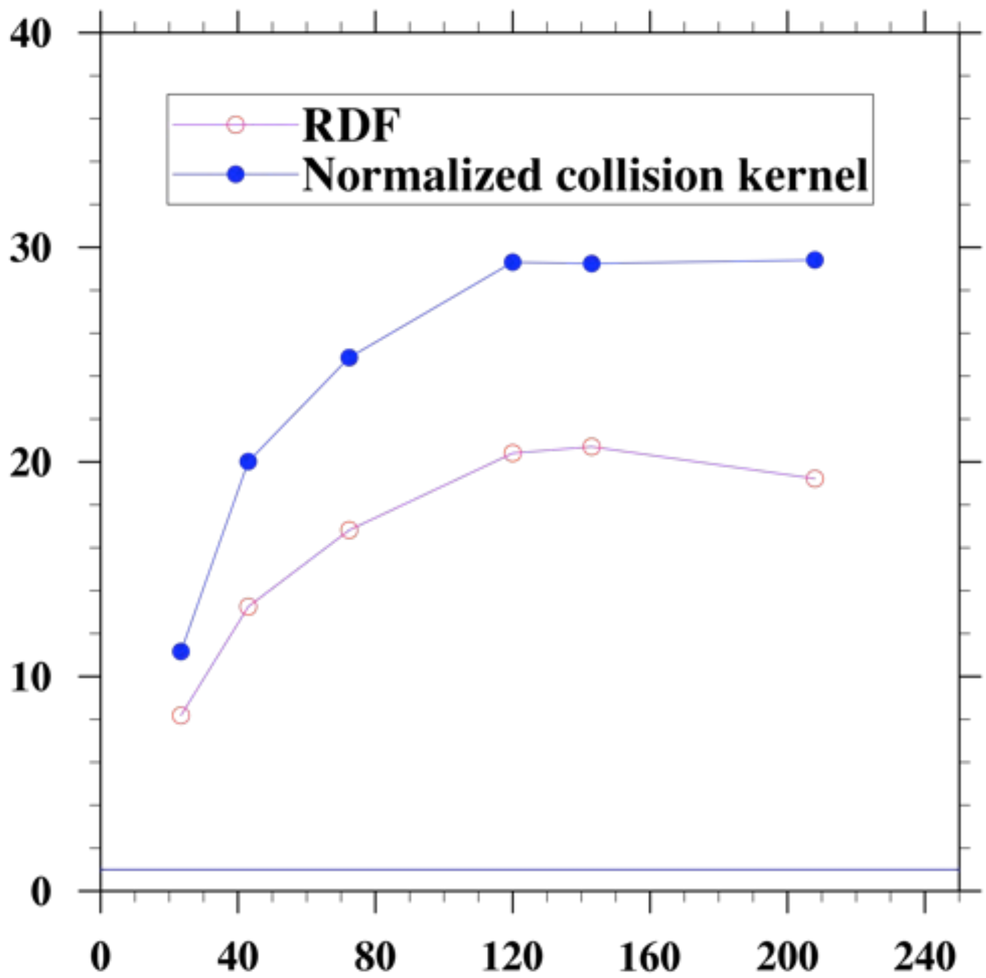

R_λ

$$\frac{\Gamma_{11}}{2\pi R^2 \left|\langle w_r \rangle\right|_0}$$

g_{11}

$\varepsilon = 400 \quad cm^2/s^3$

Stochastic forcing

Enhancement factors of geometric collision: 20 µm – 30 µm

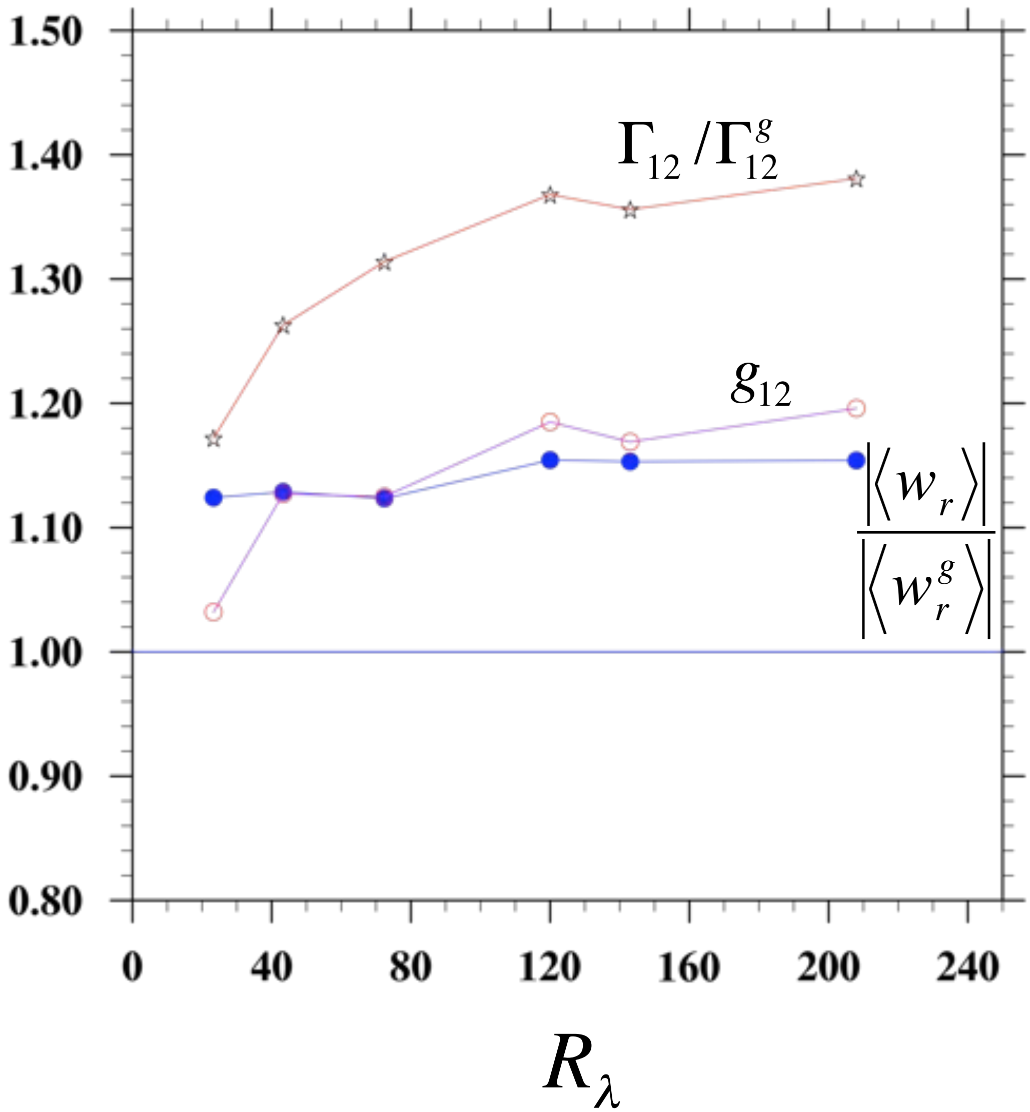

$\varepsilon = 400 \quad cm^2/s^3$

Stochastic forcing

Enhancement factor on collision efficiency

$\varepsilon = 400 \quad cm^2/s^3$

Stochastic forcing

a_1 (μm)	a_2 (μm)	a_2/a_1	R_λ		
			43.0	72.4	120. Dynamic / kinematic
30.0	15.0	0.500	1.1230	1.1272	1.1216/1.2042
	17.5	0.583	1.1819	1.1635	1.1366/1.1587
	20.0	0.667	1.2019	1.1371	1.3191/1.2383
	22.5	0.750	1.2460	1.2671	1.2202/1.2589
	25.0	0.833	1.3767	1.3459	1.3815/1.3961
50	30.	0.60	1.1190	1.0857	1.2223/1.1535
	35.	0.70	1.1209	1.0629	1.0881/1.1855
	40.	0.80	1.0982	1.1027	1.1040/1.1483
	45.	0.90	1.2629	1.1158	1.1632/1.1722

Data at 512^3 are needed here.

Summary

❖ MPI implementations allow HDNS at 256^3 and above so that some inertial subrange of fluid turbulence can be included, with converged small-scale flow features.

❖ Droplet pair statistics relevant to collision-coalescence show saturation with flow Reynolds number, at least for $a < 40\ \mu m$.

❖ The R_λ dependence in previous low-resolution simulations is a result of narrow scale-separation.

On-going

❖ More data at 512^3, with a goal of obtaining data at 1024^3 in the near future.

❖ Improved parameterization of turbulent collision kernel

Particle-Resolved

Direct Numerical Simulation

What is it?

What can you do with it?

Fluid turbulence and particle motion are fully-coupled

Flow in a domain containing a large number of moving boundary surfaces

Explicit no-slip condition on moving particle surface

Tractable theoretically only when $Re_p = \rho\, d_p |V-u| / \mu << 1$ **and** $a_p / \eta << 1$

Particle-resolved methods

– necessary when particle size overlaps with flow scale

– a variety of approaches are available

- body-fitted finite element scheme (Hu *et al*., 2001; Johnson and Tezduyar, 1999)
- fixed structured grid, with proper coupling at the boundary
  - Immersed boundary method (Peskin 2002; Uhlmann 2005 & 2008)
  - Fictitious domain method (Glowinski *et al*.,2001; Patankar *et al*.,2000 & 2009)
  - Force coupling method (Maxey and Patel, 2001; Yeo *et al*. 2010)
  - **Physalis method** (Takagi *et al*. 2003; Zhang and Prosperetti, 2003 & 2005)
  - **LBM method** (Aidun *et al*., 1998; Ladd 1994 a,b; Ten Cate *et al*., 2004)
  - IB-LBM method (Feng and Michaelides, 2004, 2005 & 2009)
  - Pseudo-penalization method (Homann & Bec 2010)

Relevant work: Particle-resolved simulations

Chronological	Method	Physical issues studied
Ten Cate *et al.* (04)	LBM	Turbulence modulation, particle-particle hydrodynamic interactions & collision. Forced.
Burton & Eaton (05)	Finite volume / Overset grid	Dissipation rate and kinetic energy as a function of distance from the particle surface; force acting on the particle. Decaying.
Zhang & Prosperetti (05), Naso & Prosperetti (10)	Finite-difference / Stokes flow expansion	Turbulence modulation and force on particle. Decaying. Also single fixed particle in a turbulence
Uhlmann (08)	LBM with IBM	Turbulent suspension in a vertical channel
Lucci et al. (10)	Finite-difference with IBM	Turbulence modulation, local variation around particle, energy spectra. Decaying.
Yeo et al. (10)	Force coupling method	Turbulence modulation by particles and bubbles. Lagrangian statistics. Forced.
Homann & Bec (10)	*a pseudo-penalization method within pesudospectral*	A single neutrally buoyant particles in a forced turbulent flow

key findings

– reduced energy at large scales and enhanced dissipation at small scales
– Clear finite-size effect related to the Faxen term
– less diffusion and stronger tendency of clustering compared with point-particle model

Suspension flows: Ladd (1994, …), Qi (1999), Aidun et al (1998), Ding and Aidun (2000), ….

Methodology

➢ Mesoscopic approach by solving the multiple-relaxation-time (MRT) lattice-Boltzmann equation (d'Humières et al. 2002, Lallemand and Luo, 2000)

$$\left|f(\mathbf{r}_i+\mathbf{e}_\alpha\delta_t,t+\delta_t)\right\rangle-\left|f(\mathbf{r}_i,t)\right\rangle=-\mathbf{M}^{-1}\hat{\mathbf{S}}\left[\left|m(\mathbf{r}_i,t)\right\rangle-\left|m^{(eq)}(\mathbf{r}_i,t)\right\rangle\right]$$

$$\hat{\mathbf{S}}=\mathbf{M}\cdot\mathbf{S}\cdot\mathbf{M}^{-1}\equiv diag(0,s_1,s_2,0,s_4,0,s_4,0,s_4,s_9,s_{10},s_9,s_{10},s_{13},s_{13},s_{13},s_{16},s_{16},s_{16})$$

$$\left|m(\mathbf{r}_i,t)\right\rangle=\left(\rho,e,\varepsilon,j_x,q_x,j_y,q_y,j_z,q_z,3p_{xx},3\pi_{xx},p_{ww},\pi_{ww},p_{xy},p_{yz},p_{xz},m_x,m_y,m_z\right)^T$$

➢ D3Q19 model for incompressible N-S eqn. (He and Luo, 1997)

$$f_i^{(eq)}(\mathbf{x},t)=W_i\left[\rho+\frac{\rho_0\mathbf{e_i}\cdot\mathbf{u}}{c_s^2}+\frac{\rho_0\mathbf{uu}:\left(\mathbf{e_i}\mathbf{e_i}-c_s^2\mathbf{I}\right)}{2c_s^4}\right]$$

$$\rho=\sum_i f_i\ ,\quad \rho_0\mathbf{u}=\sum_i f_i\,\mathbf{e}_i$$

➢ No-slip boundary condition on the moving particle surface: 2nd-order interpolated bounce-back scheme (Bouzidi *et al*. 2001, Lallemand and Luo, 2003)

Interpolated bounce back (q < 0.5)

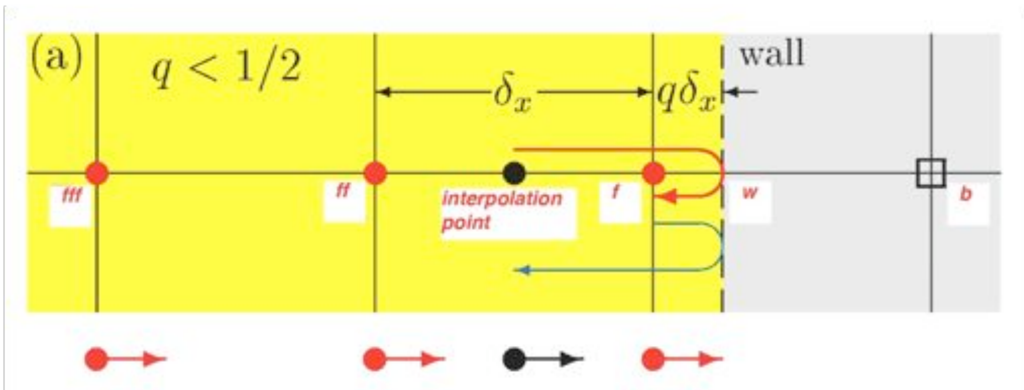

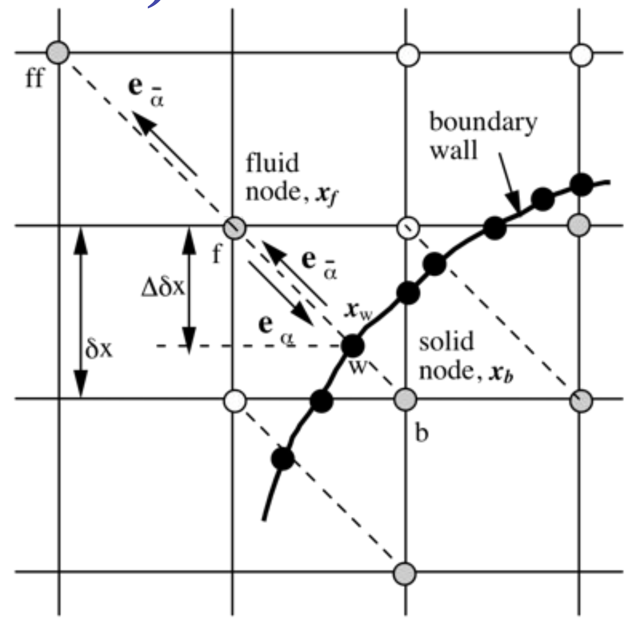

First consider $0 < q \le 0.5$, the strategy is to interpolate before streaming

$$f_{\bar{\alpha}}\left(\vec{x}_f, t+1\right) \equiv \tilde{f}_{\bar{\alpha}}\left(\vec{x}_b, t\right) = \begin{cases} 2q\tilde{f}_{\alpha}\left(\vec{x}_f, t\right) + (1-2q)\tilde{f}_{\alpha}\left(\vec{x}_{ff}, t\right), & \text{2 - point} \\ q(2q+1)\tilde{f}_{\alpha}\left(\vec{x}_f, t\right) + (1+2q)(1-2q)\tilde{f}_{\alpha}\left(\vec{x}_{ff}, t\right) - q(1-2q)\tilde{f}_{\alpha}\left(\vec{x}_{fff}, t\right) \\ & \text{3 - point} \end{cases}$$

Note that the coefficient add up to one.

And reduces to simple bounce back when $q = 0.5$.

Interpolated bounce back (q > 0.5)

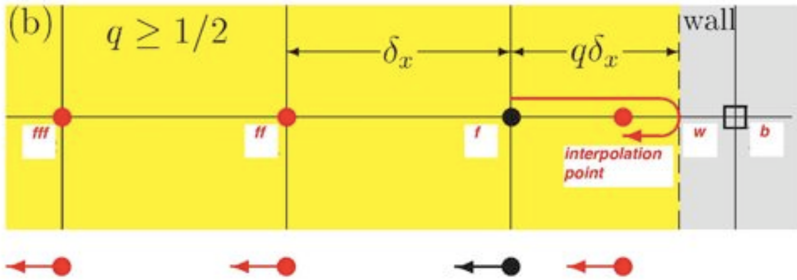

Now consider $0.5 < q \leq 1$, the strategy now is to interpolate after streaming

$$f_{\bar{\alpha}}\left(\vec{x}_f, t+1\right) \equiv \tilde{f}_{\bar{\alpha}}\left(\vec{x}_b, t\right) = \begin{cases} \dfrac{1}{2q}\tilde{f}_{\alpha}\left(\vec{x}_f, t\right) + \dfrac{2q-1}{2q} f_{\bar{\alpha}}\left(\vec{x}_{ff}, t+1\right) & \text{2 - point} \\ \dfrac{1}{q(2q+1)}\tilde{f}_{\alpha}\left(\vec{x}_f, t\right) + \dfrac{2q-1}{q} f_{\bar{\alpha}}\left(\vec{x}_{ff}, t+1\right) + \dfrac{1-2q}{1+2q} f_{\bar{\alpha}}\left(\vec{x}_{fff}, t+1\right) & \\ & \text{3 - point} \end{cases}$$

Note that

$$f_{\bar{\alpha}}\left(\mathrm{IP}, t+1\right) = \tilde{f}_{\alpha}\left(\vec{x}_f, t\right)$$

$$f_{\bar{\alpha}}\left(\vec{x}_{ff}, t+1\right) = \tilde{f}_{\bar{\alpha}}\left(\vec{x}_f, t\right)$$

$$f_{\bar{\alpha}}\left(\vec{x}_{fff}, t+1\right) = \tilde{f}_{\bar{\alpha}}\left(\vec{x}_{ff}, t\right)$$

Note again that the coefficient add up to one.

And reduces to simple bounce back when $q = 0.5$.

Force and torque acting on a particle

$$\text{Force on solid particle} \times \delta t = \text{loss of mementum of fluid}$$

$$= \text{momentum before - momemtum after}$$

$$= \sum_{\text{all f lattice nodes}} \sum_{\text{all boundary links}} \tilde{f}_\alpha\left(\vec{x}_f, t\right)\vec{e}_\alpha - f_{\bar{\alpha}}\left(\vec{x}_f, t+\delta t\right)\vec{e}_{\bar{\alpha}}$$

$$= \sum_{\text{all f lattice nodes}} \sum_{\text{all boundary links}} \left[\tilde{f}_\alpha\left(\vec{x}_f, t\right) + f_{\bar{\alpha}}\left(\vec{x}_f, t+\delta t\right)\right]\vec{e}_\alpha$$

Precise momentum conservation of the whole system!

Mesoscopic, no spatial gradients!

$$\text{Force on solid particle} \times \delta t = \text{loss of mementum of fluid}$$

$$= \text{momentum before - momemtum after}$$

$$m_p \frac{\mathrm{d}\vec{\mathrm{V}}^{(\mathrm{i})}}{\mathrm{dt}} = \sum_{\substack{\text{all boundary links} \\ \text{on the i-th particle}}} \left[\tilde{f}_\alpha\left(\vec{x}_f, t\right)\vec{e}_\alpha - f_{\bar{\alpha}}\left(\vec{x}_f, t+\delta t\right)\vec{e}_{\bar{\alpha}}\right] + m_p\vec{g} + \sum_j \vec{F}_{ij}$$

$$I_p \frac{\mathrm{d}\vec{\Omega}}{\mathrm{dt}} = \frac{2}{5} m_p a_p^2 \frac{\mathrm{d}\vec{\Omega}}{\mathrm{dt}} = a_p \sum_{\substack{\text{all boundary links} \\ \text{on the i-th particle}}} \vec{n} \times \left[\tilde{f}_\alpha\left(\vec{x}_f, t\right)\vec{e}_\alpha - f_{\bar{\alpha}}\left(\vec{x}_f, t+\delta t\right)\vec{e}_{\bar{\alpha}}\right]$$

Updated by C-N scheme

Methodology

- Short range particle-particle interactions
  - stiffness-based elastic model (Glowinski *et al*.,2001; Feng and Michaelides, 2005)

$$\mathbf{F}_{ij} = \begin{cases} 0, & r_{ij} > R_{ij} + \varsigma \\ \dfrac{c_{ij}}{\varepsilon_p}\left(\dfrac{r_{ij} - R_{ij} - \varsigma}{\varsigma}\right)^2 \left(\dfrac{\mathbf{r}_{ij}}{r_{ij}}\right), & r_{ij} \le R_{ij} + \varsigma \end{cases}$$

- Or exact lubrication force corrections (as in Tony Ladd's work)

Methodology

- Refill problem for new fluid nodes:
  Minimize force fluctuations on moving particles
  - ✧ equilibrium + non-equilibrium refill (Caiazzo, 2008)

$$f_i(\mathbf{r}) = f_i^{(eq)}(\mathbf{r};\mathbf{u}_w,\overline{\rho}) + f_i^{(neq)}(\mathbf{r}+\mathbf{e}_\alpha)$$

MPI implementation

- One-dimensional domain decomposition in z
- Particles assigned to a local process according to their location
- Comprehensive and efficient handling of finite-size particles crossing the domain boundary (e.g., a particle close to a corner)
- Optimal use of local and global variables
- Efficient updating of changing boundary links
- Efficient data communication near domain boundaries

A validation case

➢ Single steel sphere settling in a tank

✧ physical parameters (Mordant and Pinton, 2000)

$$d = 0.8 \text{ mm}, \qquad \nu = 0.9\times10^{-6} \text{ m}^2/\text{s},$$
$$\rho_p = 7710 \text{ kg/m}^3, \quad \rho_f = 1000 \text{ kg/m}^3,$$
$$V_t = 0.316 \text{ m/s}, \quad \mathrm{Re}_p = 280.8$$

✧ numerical setup (Lucci *et al.*, 2010)

triply periodic BC

$$\mathrm{Lx} = \mathrm{Ly} = 12.5d, \ \ \mathrm{Lz} = 125d$$

$$V_t = 0.315 \text{ m/s}$$

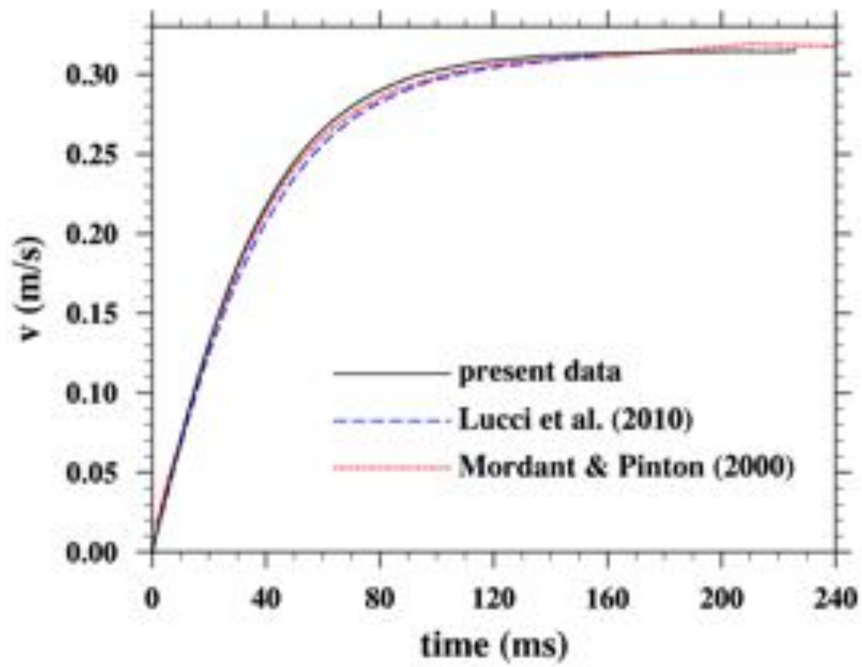

Drafting, kissing and tumbling in 3D: $Re_p \sim 27$

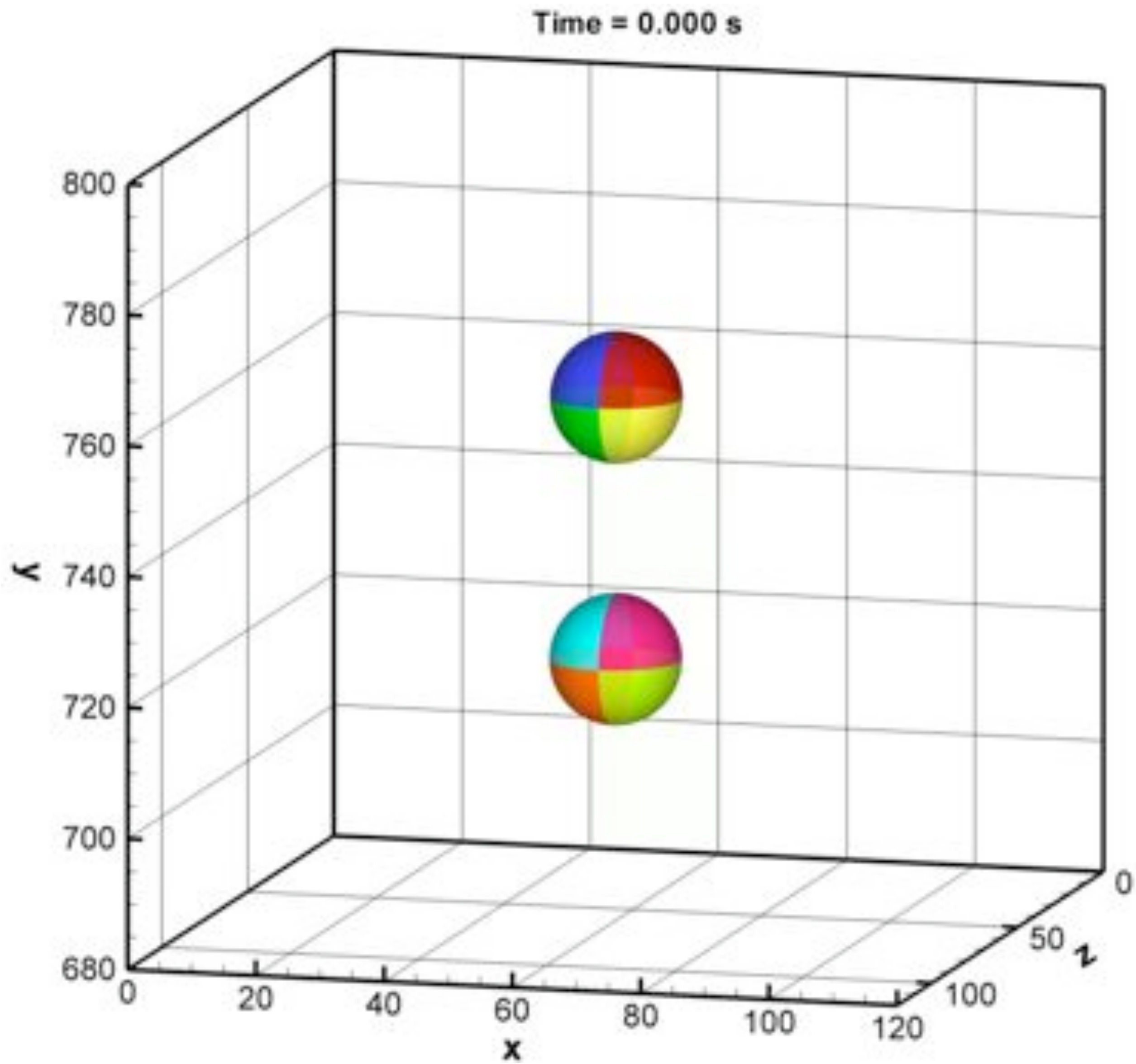

Sedimentation of a random suspension

- numerical setup (Clement and Maxey, 2003)
  domain size: 128^3, triply periodic BC, $a_p = 5$, $N_p = 1, 40, 120, 240, 480$
  $Re_p = 4.1, 11.2$

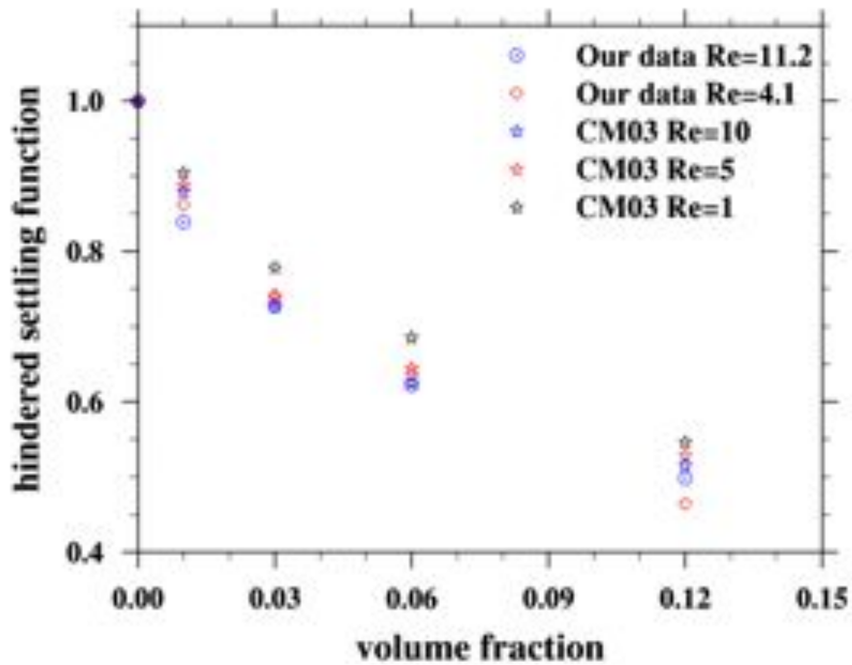

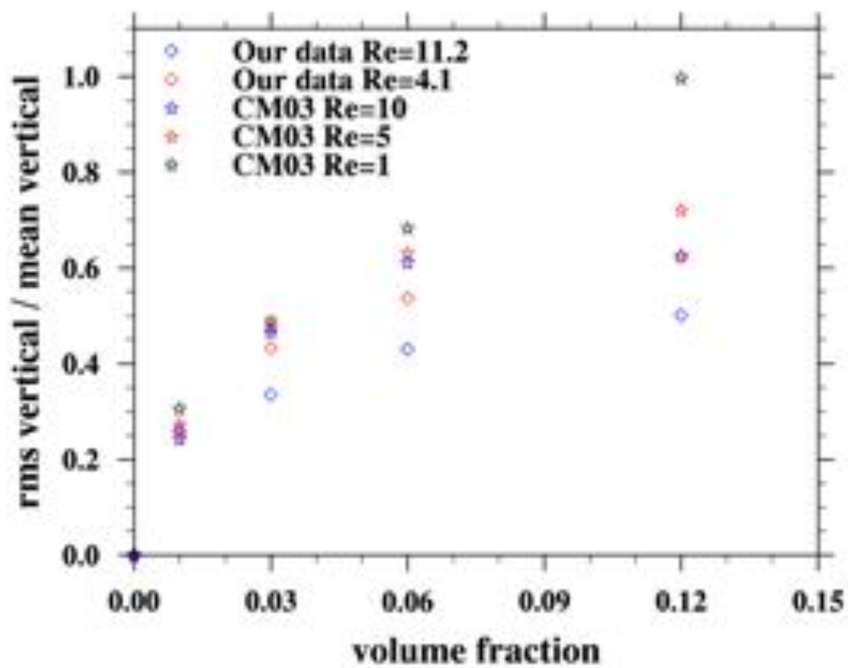

Decaying turbulence laden with finite-size particles

- consider several cases simulated by **Lucci *et al.*, 2010**
  - initial kinetic energy spectrum

$$E(k) = \left(\frac{3u_0^2}{2}\right)\left(\frac{k}{k_p^2}\right)\exp\left(-\frac{k}{k_p}\right)$$

  - 256^3 periodic domain, $\mathrm{Re}_{\lambda 0} = 78$
  - initialization of velocity field → density field evolution → skewness development → particle release

Case 2,3,4 are Case A, D, E, G in Lucci et al. (2010).

Table 1: Particles parameters at release time.

Case	d	ρ_p/ρ_f	N_p	d/η	d/λ	ϕ_v	ϕ_m	τ_p/τ_k
1	–	–	0	–	–	0	0	–
2	8.0	2.56	6400	16.1	1.2	0.1023	0.226	36.8
3	8.0	5.0	6400	16.1	1.2	0.1023	0.363	71.9
4	11.0	2.56	2304	22.1	1.5	0.0957	0.213	69.6
5	8.0	5.0	51200	8.08	0.559	0.1023	0.363	18.1

  - simulation duration: 2.12 eddy turnovers (5000 lattice time steps)

Wall-clock time for 256^3 runs with 32 processors on NCAR Bluefire

Case	d	N_p	Φ_v	Wall clock	Additional time
1 (flow only)	-	-	-	3.11 s / step	-
2 (case D)	8.0	6,400	0.102	3.84 s / step	23%
3 (case E)	8.0	6,400	0.102	3.85 s / step	24%
4 (case G)	11.0	2,304	0.096	3.74 s / step	20%

Wall-clock time for 512^3 runs with 128 processors on NCAR Bluefire

Case	d	N_p	Φ_v	Wall clock	Additional time
1(flow only)	-	-	-	7.01 s / step	-
3(case E)	16.0	6,400	0.102	8.84 s / step	26%
5	8.0	51,200	0.102	10.1 s / step	44%

The CPU time is comparable to single-phase turbulence simulation.

Parameters for the undisturbed (background) turbulence

$\varepsilon,\ u',\ L_f,\ \nu,\ L_{Box}$

or derived three independent dimensionless parameters

$$R_\lambda = (u')^2\sqrt{\frac{15}{\nu\varepsilon}},\qquad \frac{\varepsilon L_f}{(u')^3},\qquad \frac{L_{Box}}{L_f}$$

But the last two will approach asymptotic values when R_λ is large enough.

Parameters for the dispersed phase

$$\theta,\quad \frac{d_p}{\eta},\quad St = \frac{\tau_p}{\tau_k} = \frac{1}{18}\frac{\rho_p}{\rho_f}\left(\frac{d_p}{\eta}\right)^2,\quad S_v = \frac{W}{\mathrm{v}_k}\qquad \text{or}\qquad \theta,\quad \frac{d_p}{\eta},\quad \frac{\rho_\mathrm{p}}{\rho_\mathrm{f}},\quad S_v$$

3D visualization of vorticity and particle distribution

Vorticity contour at 3,000 time step ($1.27T_{e,0}$) for case 4

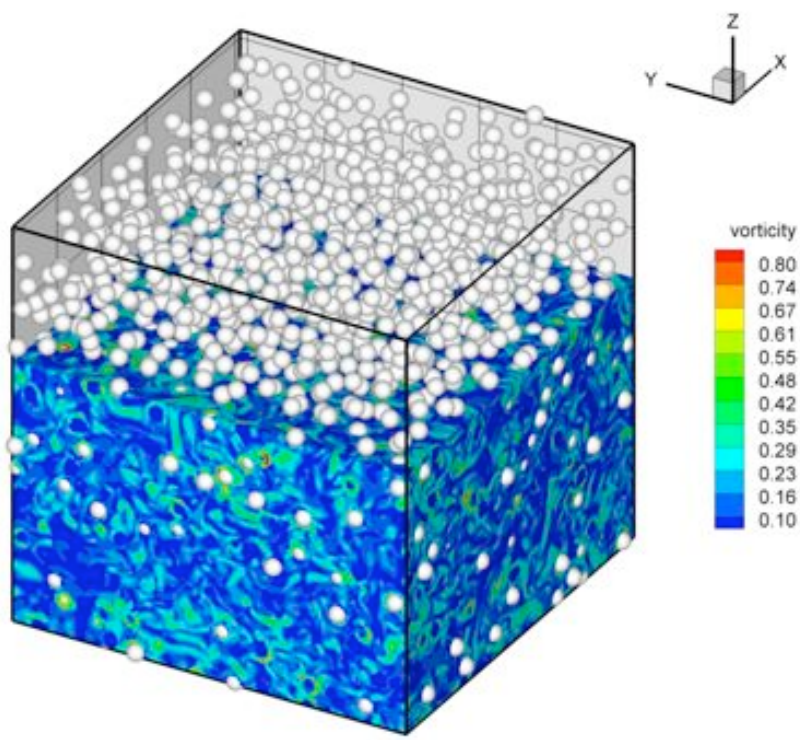

Vorticity contour at 5,000 time step ($2.12T_{e,0}$) for case 4

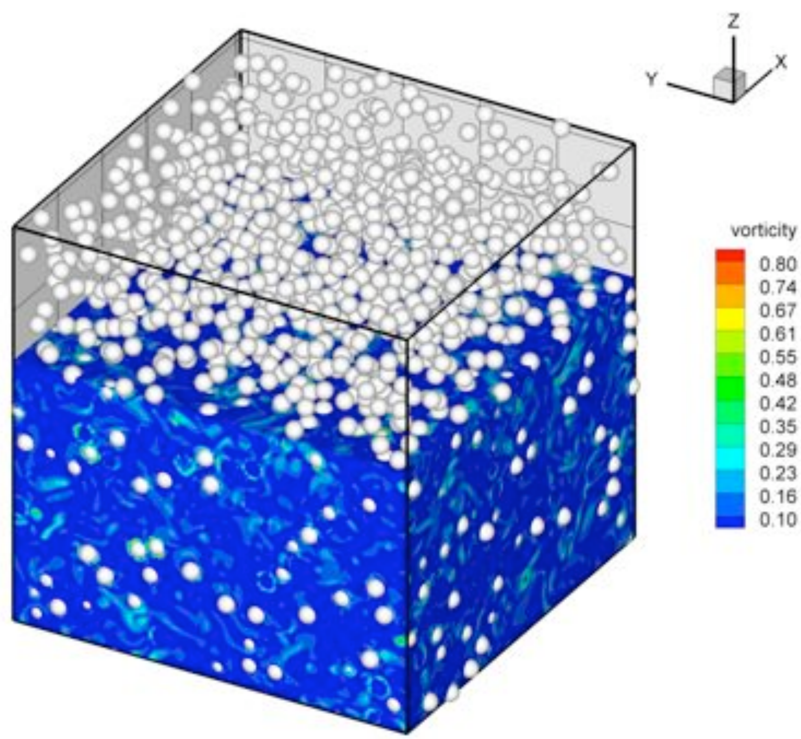

$$Re_\lambda = 78 \sim 22$$

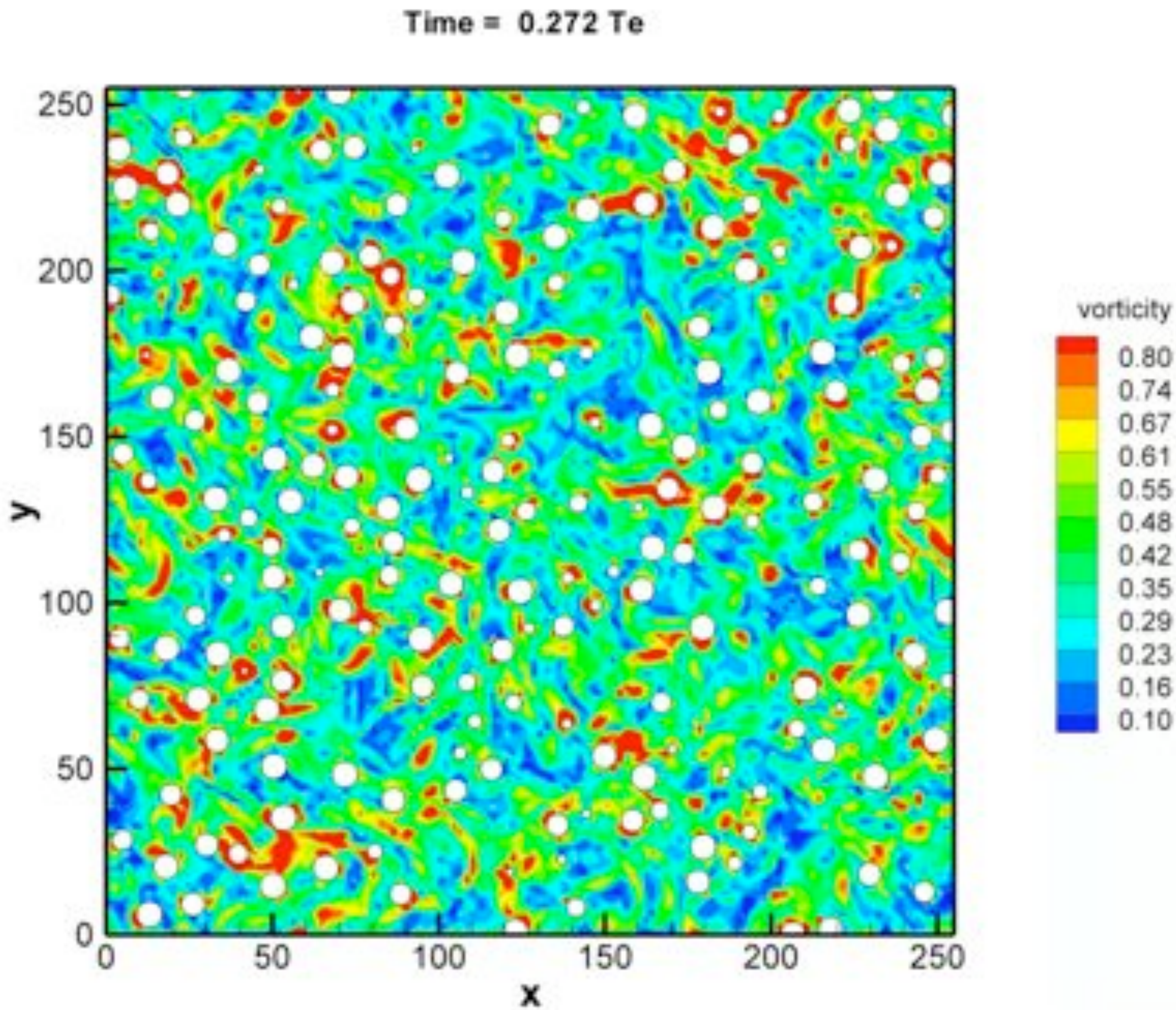

For case E with D_p=8.

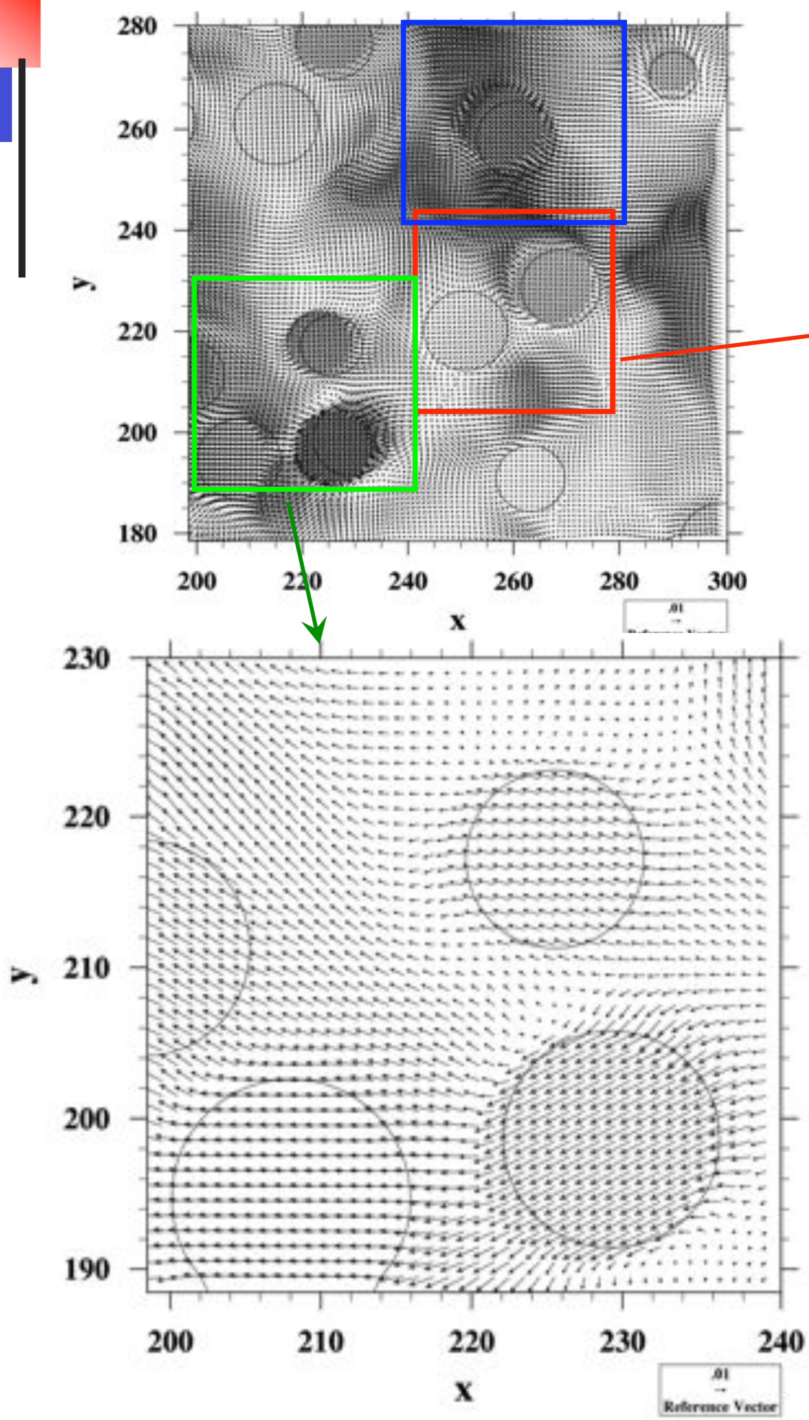

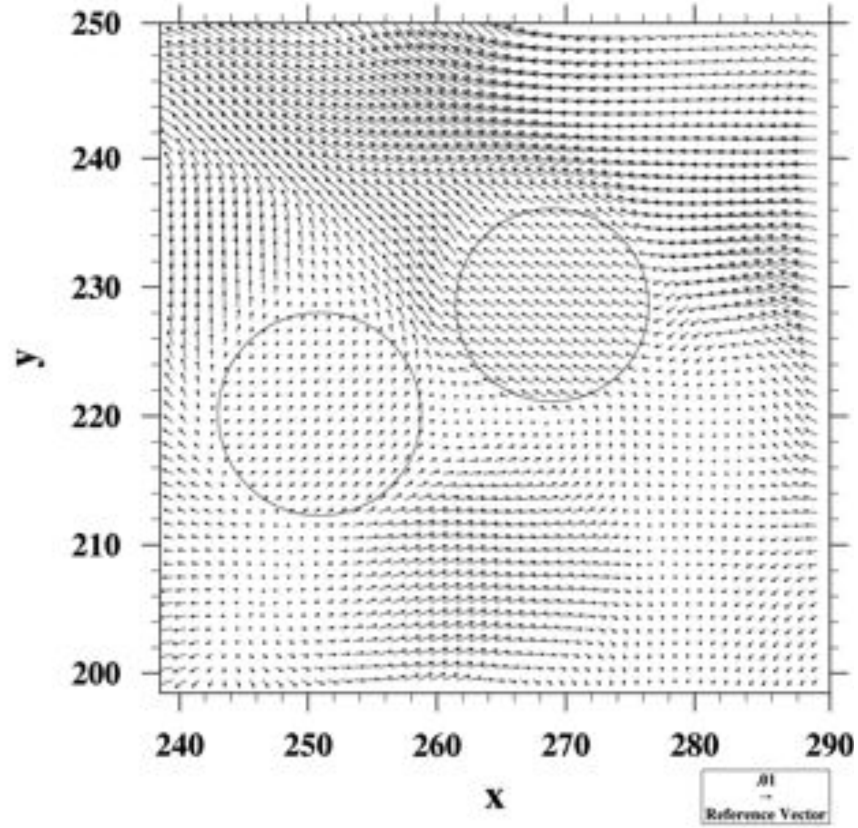

Velocity snapshot at time = 1.06Te on the plane of z=256.5 near the center of the computational domain for case E at 512^3 grid resolution

Kinetic energy spectrum

TKE at 5,000 time step ($2.12T_{e,0}$)

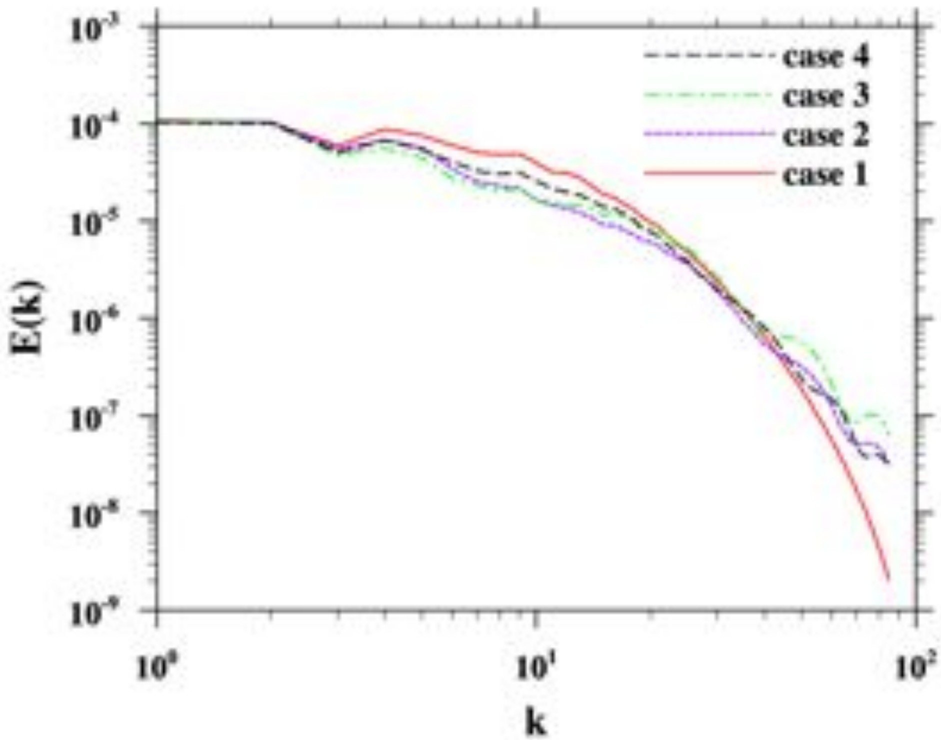

Case	St	a/η	pivoting
2	22.5	16.1	$k_p \approx 1.25 k_D$
3	57.6	16.1	$k_p \approx 0.94 k_D$
4	42.5	22.1	$k_p \approx 1.28 k_D$

$[k_D \equiv 2\pi / d]$

Lucci et al. (2010) :

$k_p \approx k_D$ for $a/\eta \approx 16$

Ten Cate et al. (2004) :

$k_p \approx 0.72 k_D$ for $a/\eta \sim 4$

Yeo et al. (2010) :

$k_p \approx 0.67 k_D$ for $a/\eta \sim 5$

Normalized pivot wavenumber

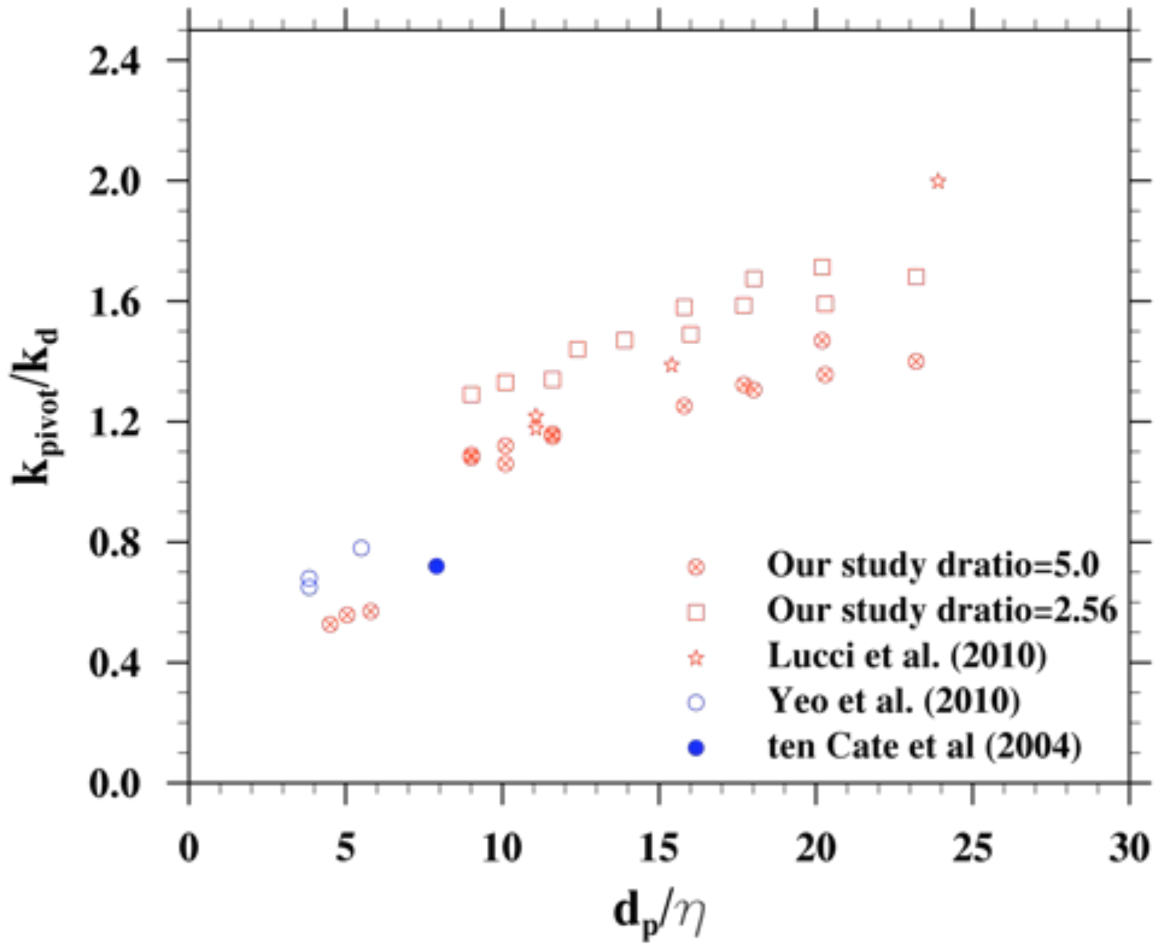

Blue: forced simulation; Red: decaying simulation.
Dependence on particle-to-fluid density ratio.

Decreased thickness of viscous boundary layer as particle Reynolds number is increased.
The nature of Faxen corrections changes as particle size is increased.

Normalized pivot wavenumber

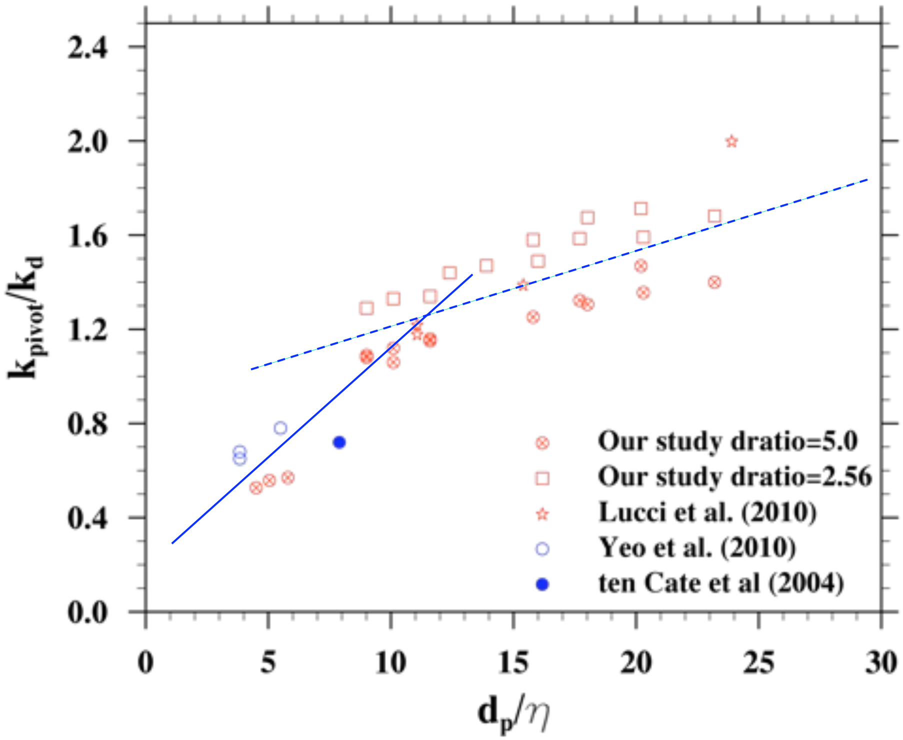

Kolmogorov length

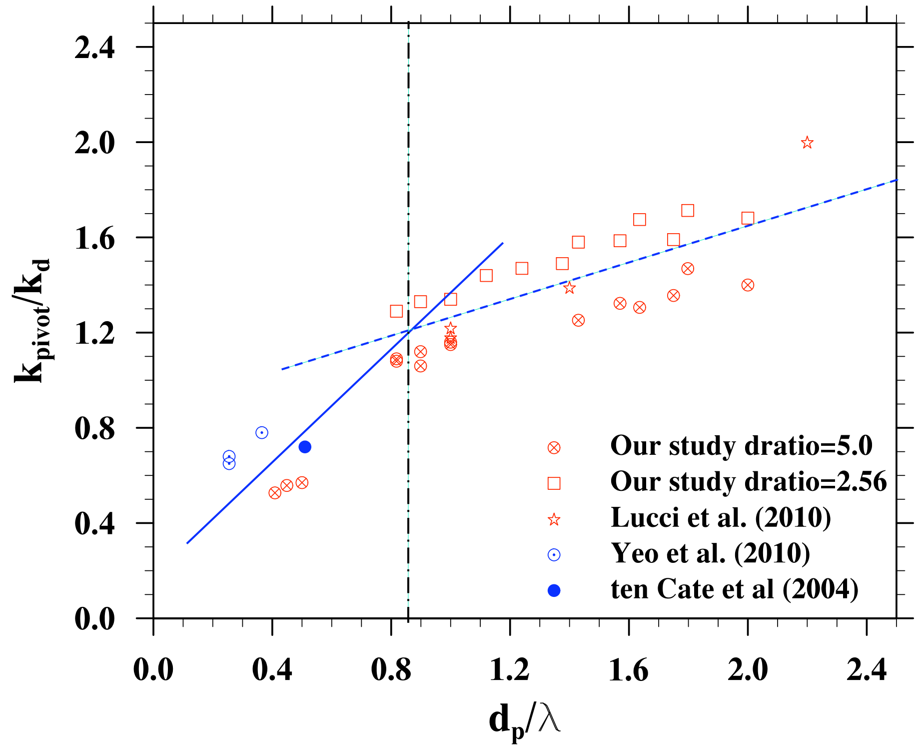

Taylor microscale

Locally averaged dissipation rate relative to particle surface

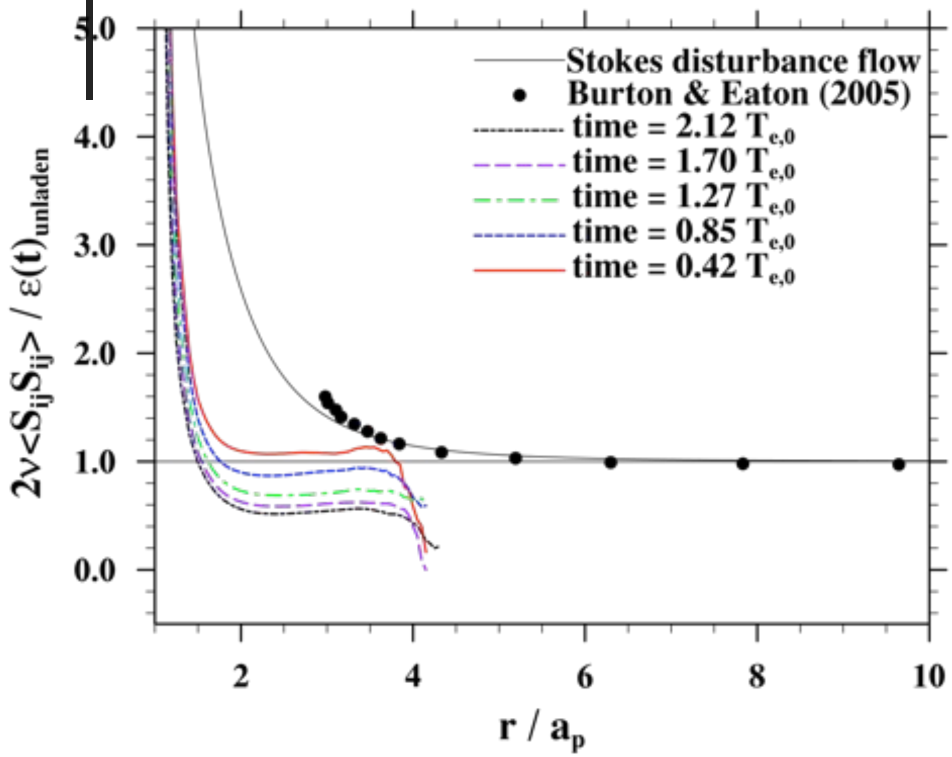

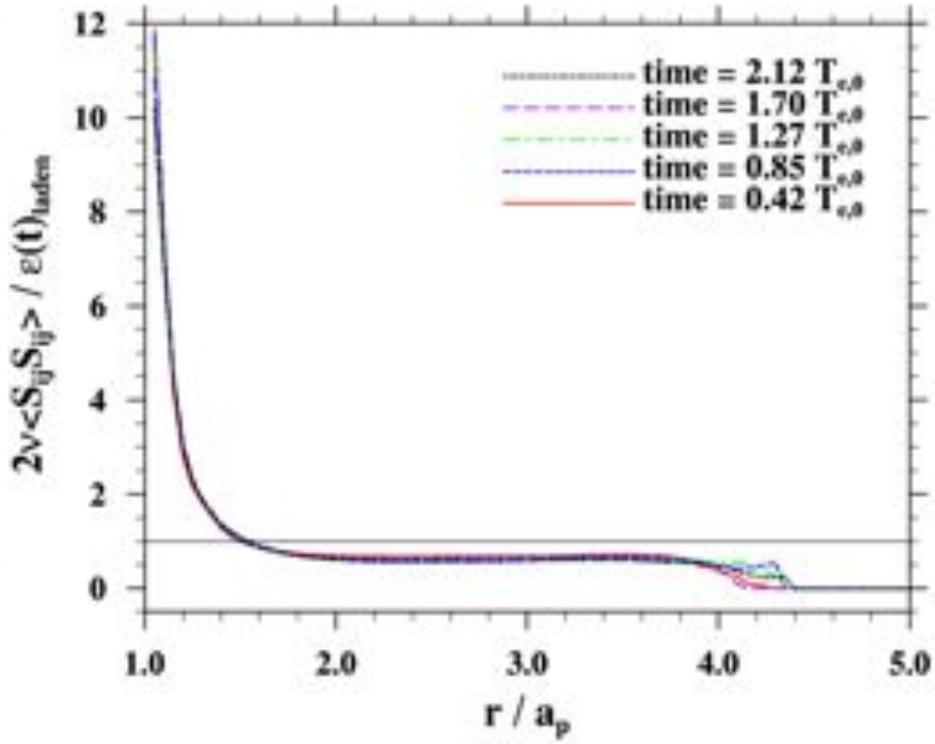

Based on case E, 512^3

The Burton & Eaton data are from Fig. 17 of their paper, representing an average of their profiles for t-ti=6,9,12,15.

Normalized by transient dissipation rate of the whole domain, including both solid and fluid region.

Bin size = $0.05a_p$. Case E. 512^3, $a_p = 8$.

Comparing various methods

	Point-particle based DNS	Hybrid DNS	Particle-resolved DNS
Capability and limitations	Turbulent Geometric collision rate only	Turbulent collision efficiency, but Stokes disturbance flow only	Most accurate and could handle finite droplet Reynolds number. But limited to low flow Re or simple setup.
Complexity (coding / numerics)	less	→	more
Accuracy	Least accurate	→	Most accurate
Efficiency	Most efficient	←	Least efficient

✧ Matching the turbulent cloud conditions is difficult
✧ Could at least be used to study gravitational collision efficiency at finite particle Re number

The dream simulations of the future

1 m box = 1000η, dx~1 μm
1,000,000 grid points in each direction
Maybe for the next generation

10 cm box = 100η, dx~1 μm
100,000 grid points in each direction
Resolved dissipation range
Likely before my retirement

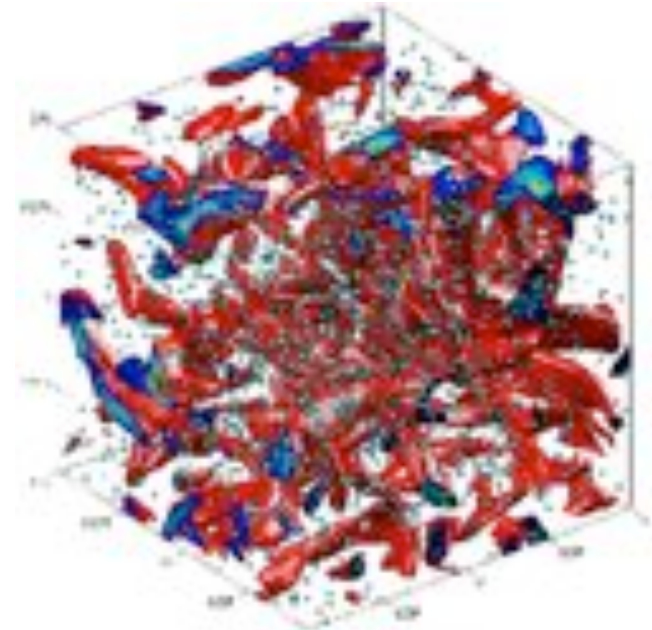

More realistic

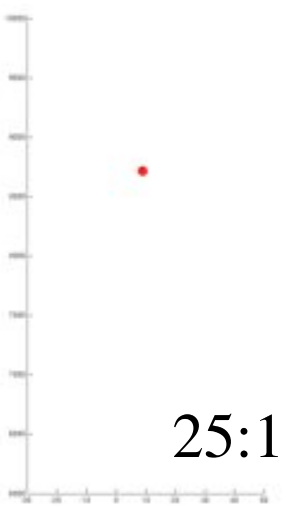

N	R_λ	Re	$\langle\varepsilon\rangle$ DNS	Domain size (cm) (400 cm^2/s^3)	Domain size (cm) (100 cm^2/s^3)	u′
32	23.5	40.6	3646	4.2	6.0	7.08
64	43.3	90.6	3529	8.4	11.9	9.61
128	74.6	212	3589	16.9	23.9	12.61
256	123.	532.	3690	34.0	48.1	16.18
512	204.	1,373	3900	68.9	97.5	20.84
1024	324.	3,806	3777	137.	193.	26.29

Summary

- LBM with MPI has been developed to perform particle-resolved simulations

- The method was validated with single particle settling and random particle suspension

- Results were obtained for decaying turbulence laden with finite-size particles
  - Confirm previous results related to turbulence modulation
  - The normalized pivot wavenumber depends on size and density ratio (Particle Re #)
  - Strong modulation occurs near particle surface, within half particle radius
  - Local profiles are self similar with proper normalization
  - Requires < 50% additional computational effort even for over 50,000 particles

- Ongoing work: Many important issues may be explored and studied
  - Gravitational collision efficiency at finite droplet Reynolds number
  - Particle velocity, acceleration, angular velocity, angular acceleration statistics
  - Particle-pair statistics, i.e., radial / transverse relative velocities, particle RDF, particle collision rates
  - Improve representation of short-range particle-particle interactions
  - Sensitivity on resolution, short-range interaction representation, etc.

Some overall messages

- It makes sense to use DNS to study turbulent collision of cloud droplets using the state-of-the-art computing techniques. DNS can be an independent research tool when carefully conducted.

- The atmospheric community has now been convinced that the effect of air turbulence is *important to cloud microphysics*

- A turbulent collision kernel has been developed, providing a first *conservative* estimate due to low flow Re an a limited range of flow scales

- There are certain advantages in computational approach, but also a lot of challenges

- Numerical results are challenging the state-of-the-art experimental techniques